Determining the contribution of utrophin A versus other components of the slow, oxidative phenotype in the beneficial adaptations of dystrophic muscle fibers following AMPK activation

By

Hasanen Al-Rewashdy

A thesis submitted to the Faculty of Graduate and Postdoctral Studies

University of Ottawa

In partial fulfilment of the requirements for the degree of Master of Science in Cellular and Molecular Medicine

Department of Cellular and Molecular Medicine

Faculty of Medicine

University of Ottawa

ABSTRACT

Duchenne Muscular Dystrophy (DMD) results from the absence of a functional dystrophin protein. Among its possible therapeutic options is the upregulation of dystrophin's autosomal analogue, utrophin A. This can be achieved by a pharmacologically induced shift towards a slower, more oxidative skeletal muscle phenotype, which has been shown to confer morphological and functional improvements on models of DMD. Whether these improvements are a result of the utrophin A upregulation or other beneficial adaptations associated with the slow, oxidative phenotype, such as improved autophagy, has not been determined. To understand the importance of utrophin A to the therapeutic value of the slow, oxidative phenotype, we used the utrophin/dystrophin double knockout (dKO) model of DMD. We found the dKO mouse to have a similar skeletal muscle signaling capacity and phenotype to mdx mice. When treated with the adenosine monophosphate activated protein kinase (AMPK) agonist 5-aminoimidazole-4-carboxamide-1-β-D-ribofuranoside (AICAR), both dKO and mdx mice expressed a shift towards a slower, more oxidative phenotype. In the mdx mice, this shift caused improvements in muscle fiber central nucleation, IgM penetration, damage from eccentric contractions, and forelimb grip strength. These morphological and functional benefits were not seen in the AICAR treated dKO mice. This study highlights the importance of utrophin A upregulation to the benefits of the slow, oxidative myogenic program to dystrophic mice. It confirms utrophin A as a therapeutic target in DMD and the slow, oxidative myogenic program as clinically relevant avenue towards treatment of the disease.

CONTENTS

LIST OF FIGURES AND TABLES

LIST OF ABBREVIATIONS

AAV- adeno-associated viral
AICAR- 5-amino-4-imidazolecarboxamide riboside
AIF- Apoptosis-inducing factor
AO- antisense oligonucleotide
ARE- AU-rich element
Ca2+- calcium
COX- cytochrome c oxidase
DAPC- dystrophin-associated protein complex
DMD- Duchenne muscular dystrophy
ECM- extracellular matrix
EDL- extensor digitorum longus
FOXO- forkhead box class O
GAPB- GA binding protein
GLUT4- glucose transporter type 4
GRMD- golden retriever muscular dystrophy
IgM- immunoglobin M
mdx- X-linked muscular dystrophy
MHC – myosin heavy chain
NFAT- nuclear factor of activated T cells
NF-κB- nuclear factor kappa-light-chain-enhancer of activated B cells
NMJ- neuromuscular junction
NO- nitric oxide
NOS- nitric oxide synthase
PGC-1α- peroxisome proliferator-activated receptor ϒ coactivator 1α
PPAR- peroxisome proliferator-activated receptor
PPRE- PPAR- response element
RT-PCR- reverse transcription polymerase reaction
SIRT- sirtuin (silent mating type information regulation 2 homolog)
TA- tibialis anterior
TGFβ- transforming growth factor-β
β-DG- β-dystroglycan

ACKNOWLEDGEMENTS

My sincere gratitude and appreciation goes to my supervisor, Dr. Bernard Jasmin. I extend my thanks to all members of the Jasmin lab, past and present, who have all had a positive impact on my studies. I would not have been able to accomplish this without them. A special thank you to Vladimir Ljubicic for his guidance throughout my project. Thank you to Tara, Guy, and Christine who helped me surmount some of the obstacles in my research. I appreciate the prompt and ever present assistance of John Lunde. Thank you to Aymeric and Olivier for their feedback and pleasant company. My fellow MSc student, Aatika, has been a great comrade and I thank her for that. The undergraduates, Amanda and Jonathan, have been a pleasure to work with. I also will not forget the contributions of Adel and Lucas.

I would like to thank the administrative and technical staff, particularly Kim Wong and the ACVS technicians, for their significant contributions to this work. I extend my thanks to my committee members, Dr. Renaud and Dr. Korneluk, for their valuable advice and feedback. Thank you to the Renaud lab for their assistance in some of the experiments I had to perform. This work would also have not been possible without the generous funding of The Canadian Institutes of Health Research, the Muscular Dystrophy Association, and Jesse's Journey.

My friends, who know themselves, are as good as friends can get. Their support, belief, and friendship are and will always be indispensable to me.

Finally, my gratitude and appreciation for my family and their support cannot be summed in words. My parents are unmatched in their strength, in their faith in me, and in the support they provided me. Ali is a legend. Noor and Yasamin are all anyone can ask for in siblings. Zahraa and Mohammed-Reza are the greatest source of joy. Hissan and Balgees are an amazing addition to the family.

1: INTRODUCTION

Muscular dystrophies are inherited progressive muscle wasting disorders whose pathology also includes varying muscle weakness. The most common of these disorders is Duchenne muscular dystrophy (DMD), which affects 1 in 3500 new born males (114). DMD was first described by the English physician Edward Meryon in 1851, but was named after French neurologist Guillaume Duchenne, who gave a comprehensive account of the disease in the following decade (114). Dr. Meryon described the basic symptoms of the disease and demonstrated that it is familial, only affects boys, and that it is not a result of abnormalitites of the spinal cord, indicating that it is myogenic (114,115).

1.1 DMD is a devastating disease caused by the absence of a functional dystrophin protein

DMD manifests in early childhood, beginning with symptoms like difficulty running and climbing stairs at 3-5 years of age. The children display the Gower's maneuver, having to climb up on and push on their thighs to stand up due to weakness in their knee and hip extensors. Pseudohypertrophy is also common, as patients have enlarged calves like in other forms of muscular dystrophy. Weakening of muscles progressively worsens, and is mostly seen proximally. The muscle wasting results in wheelchair dependence by the early teens and cardiopulmonary complications arise by the early 20s, usually resulting in death within a few years (116). Mental impairment is also a common manifestation of DMD, with around one fifth of affected boys having IQ scores below 70 (117).

In addition to detailing the symptoms above, Edward Meryon importantly noted, through his histological studies, that the muscle membrane (sarcolemma) of DMD patients was often damaged. This observation was particularly important since we now know that DMD is caused by mutations in the gene that encodes dystrophin, a large and vital protein found on the cytoplasmic face of the sarcolemma (118,119). The dystrophin gene is found on the X-chromosome, at the Xp21 locus (116). Dystrophin is a 427 kDa protein and has four domains: the N-terminal, the rod domain, the cysteine-rich domain, and the C-terminal (120). In skeletal muscles, dystrophin is found at the cytoplasmic face of the sarcolemms, where it binds to cytoskeletal filamentous (F)-actin via its N-terminus and part of its rod domain, and to an important group of proteins called the dystrophin associated protein complex (DAPC) via its cysteine rich domain and c-terminal domain (121). The various DMD mutations cause the production of a non-functional dystrophin protein, which disperses the DAPC and leads to dystrophy (116).

1.2 Dystrophin and the DAPC play important roles in muscle fibers

The DAPC is made of three multiprotein complexes (123). The dystroglycan complex binds dystrophin at the cytoplasmic face of the sarcolemma and crosses the membrane to bind laminin in the extracellular matrix. Making up the core of DAPC, the dystroglycan complex is made of α and β dystroglycan, and is indispensable for survival as its deletion in mice is embryonic lethal (122). The sarcoglycan complex consists of four transmembrane glycoproteins (α–δ sarcoglycan) and sarcospan. While only one of the sarcoglycans binds directly to dystrophin, abolishing any one of them causes the rest to dissociate from the sarcolemma, and that causes the

limb girdle dystrophies (124,125). Sarcospan is a 25 kDa transmembrane protein whose absence from the DAPC has yet to be linked to any dystrophies in humans or animal models (126,127).

The last major complex of the DAPC contains the syntrophins and dystrobrevin. The syntrophins may serve to recruit signalling proteins to the sarcolemma and DAPC, as they show binding interactions with skeletal muscle sodium channels, neuronal nitric oxide synthase (nNOS) and other proteins, but no disease has been linked to syntrophin mutations other than the downregulation of nNOS in their absence (119,128,129). Loss of dystrobrevin, on the other hand, results in a DMD-like phenotype in mice (130). This is thought to be because dystrobrevin mediates a link between the DAPC and desmin intermediate filaments, so the loss of that link contributes to dystrophy (130). Besides these major complexes, there are other members of the DAPC such as nNOS, which is important in regulating local blood flow to match muscle metabolic load during contraction. nNOS is thought to counter the vasoconstrictive response of the muscle, especially during exercise (131,132). Perhaps it is not surprising, then, that DMD patients show abnormal blood vessel constriction and ischemic stress has been linked to their muscle degeneration (133).

Judging by these defects associated with the loss of members of the DAPC, it is obvious that this complex plays an important role in myofibers. In fact, dystrophin and the DAPC have been hypothesized to play a dual role, protecting the sarcolemma from contraction induced stress, and contributing to muscle signaling pathways. Through the dystrophin-dystroglycan bonds, the DAPC forms a mechanically strong link between the sarcolemma, the internal cytoskeleton, and the extra cellular matrix (134). Since dystrophin has multiple spectrin repeats in its rod domain, it has been proposed to dampen or resist the mechanical strain imposed on the sarcolemma by repeated contraction and relaxation (135,136). The dystrophin-DAPC link between the

sarcolemma and the cytoskeleton has been compared to the spectrin network, which supports the cell membrane of red blood cells (137). This view is further supported by the links found between the DAPC and desmin intermediate filaments through syncoilin and dysbindin and by transgenic studies which verify the importance of the physical link between actin, the sarcolemma, and the extracellular matrix (138,139). However, the role of the DAPC and dystrophin goes beyond structural support, as newer evidence suggests they play a significant role in signal transduction (119). Members of the DAPC are expressed in almost all tissues, suggesting they play at least some universal, non-muscle specific functions (119). Altered cell signaling has been reported in *C. elegans,* when mutations in genes homologous to dystrophin and dystrobrevin are induced (140). In addition, there is a large and growing list of signaling molecules that have been shown to associate with the DAPC, such as mitogen activated protein kinase (MAPK), G proteins, G protein coupled receptors, and ion channels (141). Finally, the similarities of the complex to the integrin and caveolin-3 protein complexes also supports the role of the DAPC in signaling, since these complexes are known to be involved in signaling and cause muscular dystrophies when mutated (142,143).

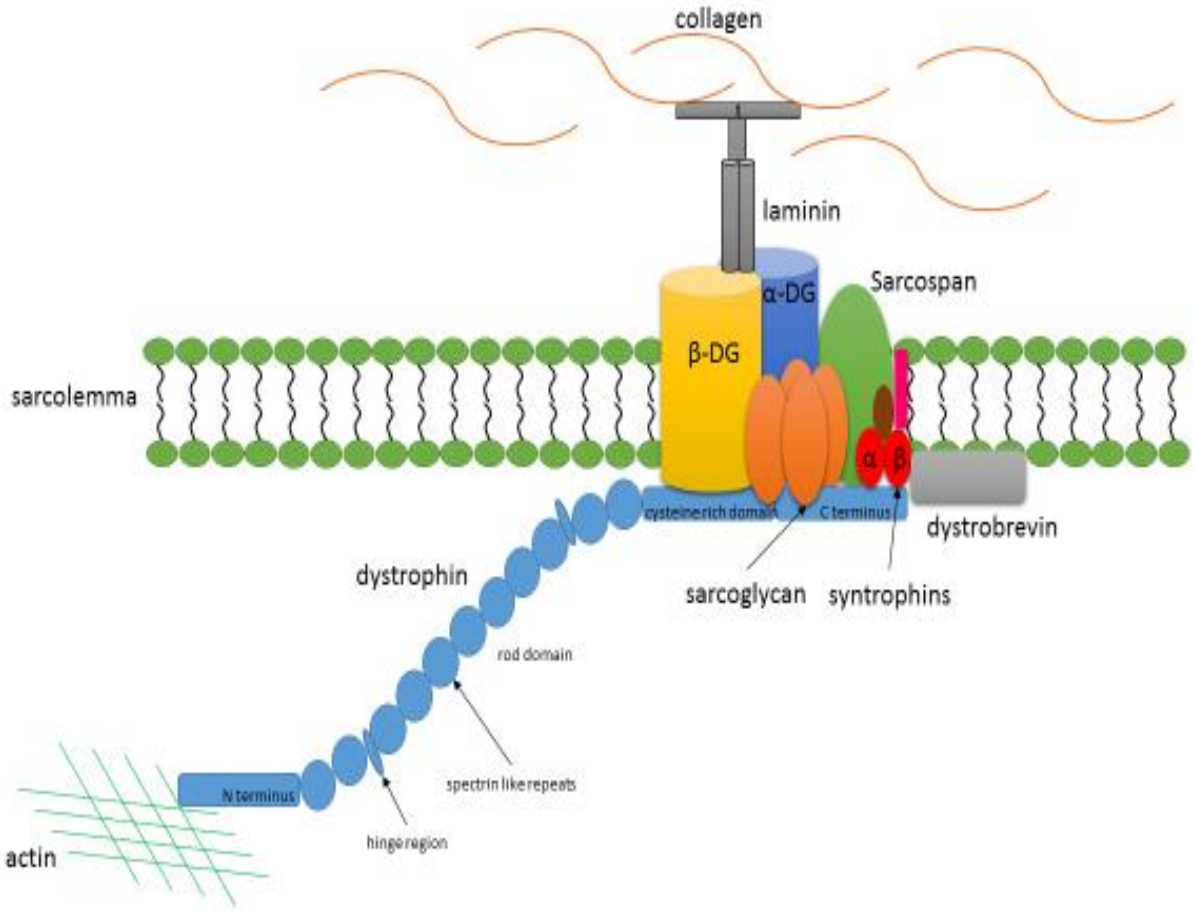

Figure 1.1: The interactions of dystrophin with members of the dystrophin-associated protein complex (DAPC) in healthy adult skeletal muscle fibers.

Through its association with the DAPC, dystrophin provides a structural link between intracellular actin and the extracellular matrix, supporting the sarcolemma and protecting it from contraction induced damage. Dystrophin also helps recruit important signaling molecules, like nNOS, to the DAPC. Interactions of dystrophin with the DAPC in healthy adult skeletal muscle are shown.

1.3 Loss of dystrophin and the DAPC leads to muscle degeneration

The absence of dystrophin and the DAPC in DMD renders the sarcolemma susceptible to physical damage, which only increases as the organism's size, the load on its muscles, as well as their force generation increases (144). The resulting damage to the unprotected sarcolemma allows unregulated influx of Ca^{2+} ions into the sarcoplasm (148). This has been shown to have toxic and damaging effects on the muscles as Ca^{2+} influences mitochondrial genes involved in apoptosis and activates calcium-dependent proteases (145,146). Stresses such as this cause the muscle fibers of DMD patients to continuously degenerate and regenerate, until the regenerative capacity of the muscles is exhausted, exposing them to fibrosis, the replacement of muscle tissue by fibrotic proteins such as collagen (147). This fibrosis is thought to play an important role in the progression of DMD (109). The lack of dystrophin, which inhibits the localization of the syntrophins to the sarcolemma, results in the downregulation nNOS (149). The absence of nNOS causes dysregulation of blood flow and results in functional ischemia (150). In addition, the absence of dystrophin has been suggested to result in downregulation of members of the non-specific serine/threonine-protein kinase family, Akt, which normally inhibits E3 ubiquitin ligases involved in muscle atrophy (151). These deleterious changes, among others, are believed to cause the muscle wasting that is the hallmark of DMD, and they have been characterized, at least in part, through the popular mdx mouse model of DMD.

1.4 The mdx mouse is an important animal model of DMD

The mdx mouse has been used extensively to help characterize DMD and search for potential therapies. The mdx mouse cannot produce a functional dystrophin protein because of a similar genetic disorder to the one found in humans (153,154). However, the resultant myopathology is much less severe compared to what is seen in humans, possibly due to improved muscle regeneration compared to humans or enhanced expression of a dystrophin analogue, which we will discuss later (176,177). Histologically, mdx mouse muscles appear normal until 3 weeks of age, when muscle necrosis develops and muscle weakness is observed. The mice display elevated serum creatine kinase and pyruvate kinase levels, and accumulation of macrophages in skeletal muscles, indicating muscle degeneration. In response to this degeneration and necrosis, muscle satellite cells activate a regenerative response and result in hypertrophy, just like what is seen in some human muscles. Regenerating fibers are easily identified by having a small diameter and central nucleation (152). As it would be expected, the muscles of the mdx mice are also more susceptible to activity induced injury (24).

1.5 There is no cure for DMD, but multiple therapeutic options are being researched

Despite the relative prevalence and the detailed characterization of DMD and its causes in human patients and animal models, there remains no cure or effective treatment for the disease. The main therapy currently is the use of glucocorticoids (GCs), including prednisone, prednisolone, and deflazacort, for symptom management. These treatments slow the decline in muscle strength and pulmonary function, prolong patients' ability to move, and delay the onset of cardiomyopathy and scoliosis (155,156). However, GCs have many deleterious side effects, including obesity, immune suppression, bone demineralization, and behavioral changes. They also do little more than slow down the inevitable collapse of patients. As a result, several other therapeutic options for DMD are actively being researched. These approaches include exon-skipping, stop codon readthrough, cell therapy, and viral vector-mediated gene delivery (157-159).

Exon skipping is an RNA-based therapy that uses antisense oligonucleotides (AONs) that are carried into the cell using a range of different chemical backbones (183). Antisense oligonucleotides alter splicing either by sterically blocking splice enhancer sequences or by altering secondary mRNA structure folding. Some of the AONs used include peptide nucleic acids like 2′-O-methyl-phosphorothiate-AONs, phosphorodiamidate morpholino oligomer (PMO) and cell-penetrating peptide-conjugated PMO (PPMO) (78). This technique has been used to relieve the DMD pathology in multiple mouse models of DMD (161,162). The most popular exon skipping target is exon 51, which is the location of the most common DMD mutation. Several clinical trials that target exon 51 with various AONs are ongoing and are at different stages (184,185). Though it is a promising technique which could target up to 83% of DMD patients with

deletions, there are still challenges like poor cellular uptake of AONs and their rapid clearing from circulation, in addition to variable efficiency of the technique in different muscles (168). Other hurdles include the need of very high dosages of AONs for effective treatment, which makes this an unrealistic therapeutic options for most DMD patients due to costs. However, there is research into developing PPMOs that can be used at low doses (186,187). A drawback that will always remain with exon skipping is that it can only target certain patients of DMD, and that specific AON sequences need to be developed and applied for each individual exon that needs to be skipped (160-162).

Stop codon readthrough is a technique that relies on interfering with the ability of the ribosome to recognize premature stop signals, which are the result of non-sense mutations in the dytrophin gene (163). This can be done through the use of aminoglycoside antibiotics, such as gentamicin, a trial of which lead to a significant increase in dystrophin expression and reduced damage in DMD patients' muscles. The use of gentamicin, though, is faced by hurdles such as its lack of potency and the toxic effects it caused in one of the patients (164). Another option to induce read through of premature stop codons is PTC124. Treatment of mdx mice with this synthetic drug resulted in a significant increase in dystrophin protein expression and a reduction of the DMD pathology (164). However, as with the exon skipping technique, stop codon read through can only be used to treat patients a specific subset of DMD patients, those with a non-sense mutation, who represent about 13% of the total number of DMD patients (78).

Cell therapy is based on delivering myoblasts or other stem cells to damaged muscles to regenerate them. Myoblasts are muscle precursor cells. They can differentiate to form myofibers, and can be derived from healthy host muscles to be grown in culture and transplanted into the muscles of DMD patients (78). This results in gene complementation, with the muscles that receive

myoblast transplantation expressing genes from both the host and the donor (188). This technique has provided positive results in animal models of DMD, significantly increasing dystrophin expression and ameliorating the DMD pathology in mdx mice, but these results could not be transferred to humans (189-191). The lack of efficacy of this technique in humans can be a result of the patients' immune response to the transplanted cells and the dystrophin they express, in addition to an insufficient number of cells being transplanted or insufficient distribution of these cells (192-194). Transplantation of tissue splice grafts has been shown to be more effective than transplantion of cells, but the clinical application of this technique is rather limited (195). To avoid the immune response of patients, researchers are currently assessing the effectiveness of implanting genetically modified host cells into DMD patients (196,197). Since injection of cells into the blood or intraperitonealy is ineffective at treating dystrophy, a major setback to this therapeutic option is that the cells have to be injected directly into the muscles to regenerate them (165). As a result, the injected cells fuse with and regenerate only the zones near the site of injection, and treatment of less accessible muscles, such as the diaphragm, becomes nigh impossible (166,167).

There has also been research to directly reverse the cause of DMD, through direct gene replacement approaches. The dystrophin gene is very large (2.4 Mb), so its incorporation into vectors for delivery is unrealisitic. Despite this, mini- and micro-dystrophin genes with large sections of the rod domain removed have enabled researchers to clone the gene into adeno-associated virus (AAV) vectors (168). These mini-dystrophin genes have been very effective at reversing the DMD phenotype when delivered in mice and dogs with the AAV9 vector (169). However, a recent clinical trial in DMD patients did not yield promising results after delivery of dystrophin via the AAV2 vector. Since DMD patients do not express the dystrophin protein, its

sudden appearance after delivery by the AAV2 vector might have elicited an immune response, which prevented the efficacy of the treatment (170). This therapeutic technique also faces other challenges, such as the inability of the shortened dystrophin proteins to reinstate all of the interactions with the DAPC. For example, nNOS reqruitement to the DAPC is dependent on spectrin like repeat sections 16 and 17 of the rod domain, so the dystrophin proteins with a shortened rod domain might not be able to recruit nNOS properly (132). Alternatively, some researchers have used delivery of microgenes encoding the dystrophin-related protein, utrophin A, to circumvent the immune response and other problems associated with dystrophin replacement (85,95).

Table 1.1: Summary of potential treatments being researched for DMD.

Treatment target	Treatment method	Effect
Symptom management	Glucocorticoids	Slow DMD progression
Restoration of dystrophin	Exon skipping	Avoid mutation sights during translation
	Stop codon readthrough	Avoid premature stop signals during translation
	Cell therapy	Restore dystrophin via muscle precursor transplants
	Viral vector gene delivery	Restore functional dystrophin gene in muscle genome
Utrophin A upregulation	Viral vector gene delivery	Add utrophin A gene with a promoter active in all muscles
	Protein therapy	Deliver utrophin A protein to muscles
	Recruitment	Increase the localization of utrophin A to extrasynaptic regions of the sarcolemma
	Pharmacologic	Increase utrophin A transcription
	Slow, oxidative myogenic program	Increase utrophin A expression through a change in muscle phenotype

1.6 Utrophin A may be able to substitute dystrophin in DMD patients

Utrophin A is the autosomal analogue of dystrophin. Located on chromosome 6q24, it has a molecular mass of 395 kDa, and a very similar structure to dystrophin, with 3 of their domains being 80 % identical (198-200,171). There is significant evidence that utrophin A and dystrophin have functional redundancy, and they bind the same proteins of the DAPC, so utrophin A may be able to serve as a replacement for dystrophin (118,172). Like dystrophin, utrophin A binds members of the DAPC like α-dystrobrevin-1 and β-dystroglycan via its C-terminus (79,80). Utrophin A also binds F-actin via its N-terminus (201,202). The rod domain, while showing the greatest disparity between the proteins with 35% sequence identity, shares largely the same function in both: to provide support for membrane flexibility through the force induced folding of spectrin repeats and hinge regions (203). The similarities between the domains and the binding of the proteins certainly point to them playing similar roles.

However, while full-length dystrophin is expressed only in the muscles and the brain, utrophin A is expressed universally in the body (118,199). The two promoters of utrophin A transcription, A and B, encode the two utrohpin isoforms: utrophin A A and utrophin A B (118). Utrophin A A is found in peripheral nerves and muscular tissues, while utrophin A B is found in vascular endothelial cells (204). Within skeletal muscle, dystrophin and utrophin A can have different expression patterns. While dystrophin is normally expressed throughout the sarcolemma, utrophin A is only expressed throughout the sarcolemma early in development, and is confined to the myotendinous and the neuromuscular junctions in adult skeletal muscle (173,174). Despite the differences in expression pattern, the similarities between the structures of dystrophin and utrophin A and the proteins they bind, give utrophin A the potential to substitute dystrophin in dystrophic

fibers. The expression of utrophin A has been found to be negatively correlated with the DMD pathology, and the fact that it is already expressed in the muscles of DMD patients will prevent an immune response to it (205). However, in order for a utrophin A-based therapy to be successful, utrophin A expression must be stimulated throughout the sarcolemma.

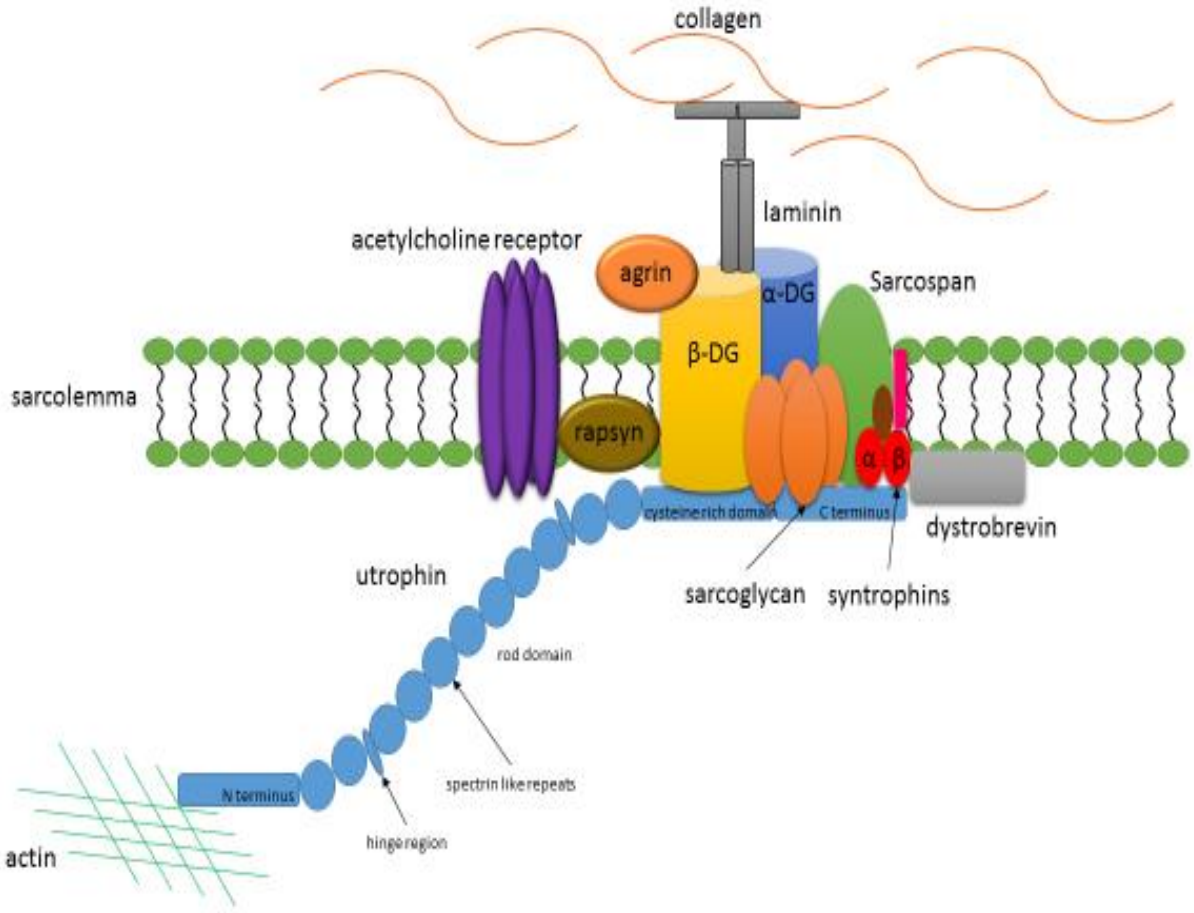

Figure 1.2: Utrophin A and its interaction with members of the dystrophin-associated protein complex (DAPC) in healthy adult skeletal muscle fibers.

Utrophin A provides a structural link between intracellular actin and the extracellular matrix through its association with the DAPC. This protects the muscle from contraction-induced damage. It also helps recruit other members of this complex, including β-DG. In addition to binding proteins of the DAPC, utrophin A, binds neuromuscular junction proteins like the acetylcholine receptor. It can be found at the crests of the neuromuscular junction.

1.7 Upregulating utrophin A expression in models of DMD

While utrophin A A expression is up-regulated in the skeletal muscle of DMD patients and mdx mice, likely as a compensatory mechanism, this upregulation is not enough to substitute for the absence of dystrophin (205-207). However, increased utrohpin expression throughout the sarcolemma has been accomplished by several studies that show that transgenically increased utrophin A expression can substitute dystrophin and alleviate the DMD pathology (88,95,96). Utrophin A expression can upregulated through other means, such as adenoviral utrophin A A gene transfer (208-210), protein therapy (211-213), and pharmacological interventions (214,215).

AAV vectors have been used to deliver full-length and micro-utrophin A transgenes to treat multiple mouse models of DMD (208,209). This treatment caused expression of utrophin A throughout the sarcolemma, restored the DAPC, and improved the DMD pathology (208,209). However, since the AAV vectors do not persist for very long, multiple injections of the vector need to be made, increasing the cost and reducing the practicality of this treatment in human patients of DMD (208).

On the other hand, protein therapy involves delivery of actual proteins, like full length or "micro" utrophin A, to the muscles of DMD patients (211-213). TAT-mediated utrophin A protein delivery to mdx mice showed signs of ameliorating the DMD pathology (211,212). The protein delivered to the muscles does not have to be utrophin A, however, as delivery of biglycan has also been shown to improve muscle function and reduce the DMD pathology. This is because biglycan is an extracellular matrix protein that binds members of the DAPC, and recruits utrophin A to the sarcolemma, without changing its expression (213).

Delivery of biglycan is not the only way to recruit utrophin A to the sarcolemma. One of the pharmacological interventions aimed at substituting utrophin A with dystrophin, uses L-arginine to recruit utrohpin to the sarcolemma (214). L-arginine is a precursor, necessary for nNOS-induced NO synthesis (214), which is thought to play a role in utrophin A A maintenance (216). L-arginine treatment increases utrophin A levels throughout the sarcolemma and significantly improves the DMD pathology in mdx mice (214,217,218). Other pharmacological interventions, such as SMTC1100, target utrophin A transcription directly (215). SMTC1100 was recently identified by a high throughput utrophin A transcription screen and is currently proceeding to phase II clinical trials after pre-clinical success in ameliorating DMD (215).

1.8 Slow, oxidative muscles express greater amounts of utrophin A than fast, glycolytic muscles

Our laboratory was the first to observe that slow, oxidative muscles express significantly more utrophin A than fast, glycolytic muscles (47). While utrophin A expression is restricted to the neuromuscular junction in fast, glycolytic muscle, immunofluorescence indicates that it can be found elsewhere along the sarcolemma in slow, oxidative muscles (47). This is because the expression of mRNA transcripts encoding synaptic proteins, like utrophin A, is higher in and found beyond synaptic regions in slow, oxidative muscle fibers (47). This higher presence of utrophin A A mRNA transcripts is partly due to the effects of calcineurin/NFAT signaling, which drives utrophin A transcription, promotes the slow, oxidative phenotype, and has a higher presence in slow muscles (43-46). Our lab has also shown that the increased presence of utrophin A mRNA in slow muscles is due to its improved stability, as slow, oxidative muscles fibers have less destabilizing factors that bind to the AU-rich element (ARE) of the utrophin A mRNA 3' untranslated region, which was shown to mediate mRNA decay (219). Of clinical importance, it is also known that these slow, oxidative muscles are more resistant to the DMD pathology, exhibiting reduced necrosis and contraction induced damage, in human patients and animal models of the disease, like the mdx mouse (41,42).

1.9 The slow, oxidative myogenic program is a therapeutic option for DMD

Several years ago, our laboratory hypothesized that that inducing the slow, oxidative myogenic program benefits models of DMD morphologically and functionally, which has since been echoed and confirmed by other laboratories (24, 43-61). This hypothesis has been supported by multiple studies that show significant improvements in mdx mice following triggering of the slow, oxidative myogenic program. Beneficial adaptations were seen at the level of the mitochondria and contractile apparatus and were accompanied by augmented utrophin A and β-DG expression throughout the sarcolemma. Sarcolemmal structural integrity during damaging muscle contractions in fast, glycolytic skeletal muscle was also improved (75, 24). Other possible benefits of the oxidative or slow, oxidative phenotype include reduced muscle atrophy from mitochondrially mediated apoptosis, reduced damage from reactive oxygen species, and an increase in expression of proautophagic markers, indicating improved autophagy (101-104).

1.10 Several muscle signaling pathways control the expression of the slow, oxidative myogenic program

Stimulating the slow oxidative myogenic program in the mdx and dKO mice can be done via multiple signaling pathways. Three important signaling elements are known to elicit the slow, oxidative myogenic program. These are (i) calcineurin (CN)/nuclear factor of activated T-cells (NFAT) (4,178), (ii) PPARδ (179,180), and (iii) peroxisome proliferator-activated receptor (PPAR) γ co-activator-1α (PGC-1α) (14,15).

The CN-NFAT pathway is an activity-dependent signaling pathway that maintains the phenotype of adult slow muscles and induces it in regenerating slow muscle (4,220). When CN-NFAT signaling is increased transgenically, it promotes expression of the slow, oxidative phenotype in mdx mouse muscles. This brings with it increased utrophin A expression and a significant improvement of the dystrophic pathology (44,220,221). When CN-NFAT signaling was reduced, the opposite effects were achieved in dystrophic mice, verifying the role of the pathway in controlling expression of the slow, oxidative muscle phenotype and utrophin A (45).

PPARs are part of a large group of nuclear transcription factors (222). PPARβ/δ are the most abundant PPAR isoform in skeletal muscle, and they upregulate genes involved in lipid metabolism and oxidative respiration by binding to PPAR-response elements in their promoter regions (223,224). PPARβ/δ overexpression leads to a more oxidative muscle phenotype with increased mitochondrial DNA, upregulation of some slow contractile protein genes, and increased resistance to fatigue (179,180). Hence, when PPARβ/δ expression is increased through treatment with the PPARβ/δ agonist GW501516, there is a significant increase in skeletal muscle utrophin A expression and an attenuation of the dystrophic pathology in mdx mice (50,231).

PGC-1α is a transcriptional co-activator that regulates gene transcription through interactions with transcription factors (181). It stimulates an oxidative phenotype by increasing mitochondrial biogenesis and oxidative enzymes through nuclear respiratory factors (NRF)-1 and 2, which control the transcription of many mitochondrial genes. When PGC-1α expression is increased transgenically in mice, a fast to slow skeletal muscle fiber type conversion is observed along with an increase in oxidative capacity (14). Also, our lab showed that overexpression of PGC-1α through transfection activates the utrophin A A promoter (43). When mdx mice were crossed with mice that overexpressed PGC-1α in muscles, the offspring showed a significant improvement in pathology (56). PGC-1α can also be induced by pharmacologic means to elicit the slow, oxidative myogenic program and increase utrophin A expression in muscles.

There are other molecules that have been identified to evoke the slow, oxidative myogenic program. These include the transcriptional repressor E2F transcription factor 1 (5). E2F1 participates in the control of the cell cycle by regulating expression of genes involved in cell proliferation, but has been recently described to have a role in metabolic control (229,230). E2F1 deletion elevates utrophin A expression and leads to increased mitochondrial number and function, and improved fatigue resistance, and reduces the DMD pathology in mdx mice (228). It has yet to be determined, however, if E2F1 cross talks with any of the pathways mentioned above, and whether it is affected by the same slow, oxidative myogenic program elicitors that influence the signaling molecules above (5,228).

1.11 Adenosine monophosphate-activated protein kinase (AMPK) is a potent elicitor of the slow, oxidative myogenic program

As mentioned in the previous section, there are multiple ways to activate the signaling molecules and pathways that promote the slow, oxidative phenotype. AMPK is one of the most potent factors that induce skeletal muscle plasticity and can be targeted by specific agonists, making it an ideal avenue of inducing a more oxidative, possibly slower myogenic program in our mice (48). It integrates multiple cell signaling pathways to regulate energy metabolism and promote muscle plasticity, and its influence on PGC-1α expression and activity is particularly interesting for our aims (9-11,24,69). When AMPK is activated by phosphorylation, it elicits a strong shift towards a more oxidative, possibly slower muscle phenotype, which includes a fast to slow myosin ATPase shift, mitochondrial biogenesis, increased glycogen storage, augmented PGC-1a, PPARb/d and glucose transporter type 4 expression, enhanced insulin sensitivity, and improved exercise performance (62-65). This is accompanied, in dystrophic mice, by reduced myofiber necrosis, reduced serum creatine kinase levels, improved muscle function, and increased resistance to contraction induced damage (24,69,93,94).

As an energy sensor, AMPK is sensitive to the AMP/ATP ratio, and increased intracellular AMP concentrations result in its activation (10). As a result, one of the potent pharmacological activators of AMPK is 5-aminoimidazole-4-carboxamide-1-β-D-ribofuranoside (AICAR). In muscle cells, AICAR is phosphorylated to AICA-ribotide (ZMP), which is an analogue of AMP, to activate AMPK (182). Our lab (24) and others (57,238) have shown that AMPK activation via chronic AICAR treatment induces a more oxidative, possibly slower phenotype in mdx mouse muscles and confers morphological and functional benefits on them.

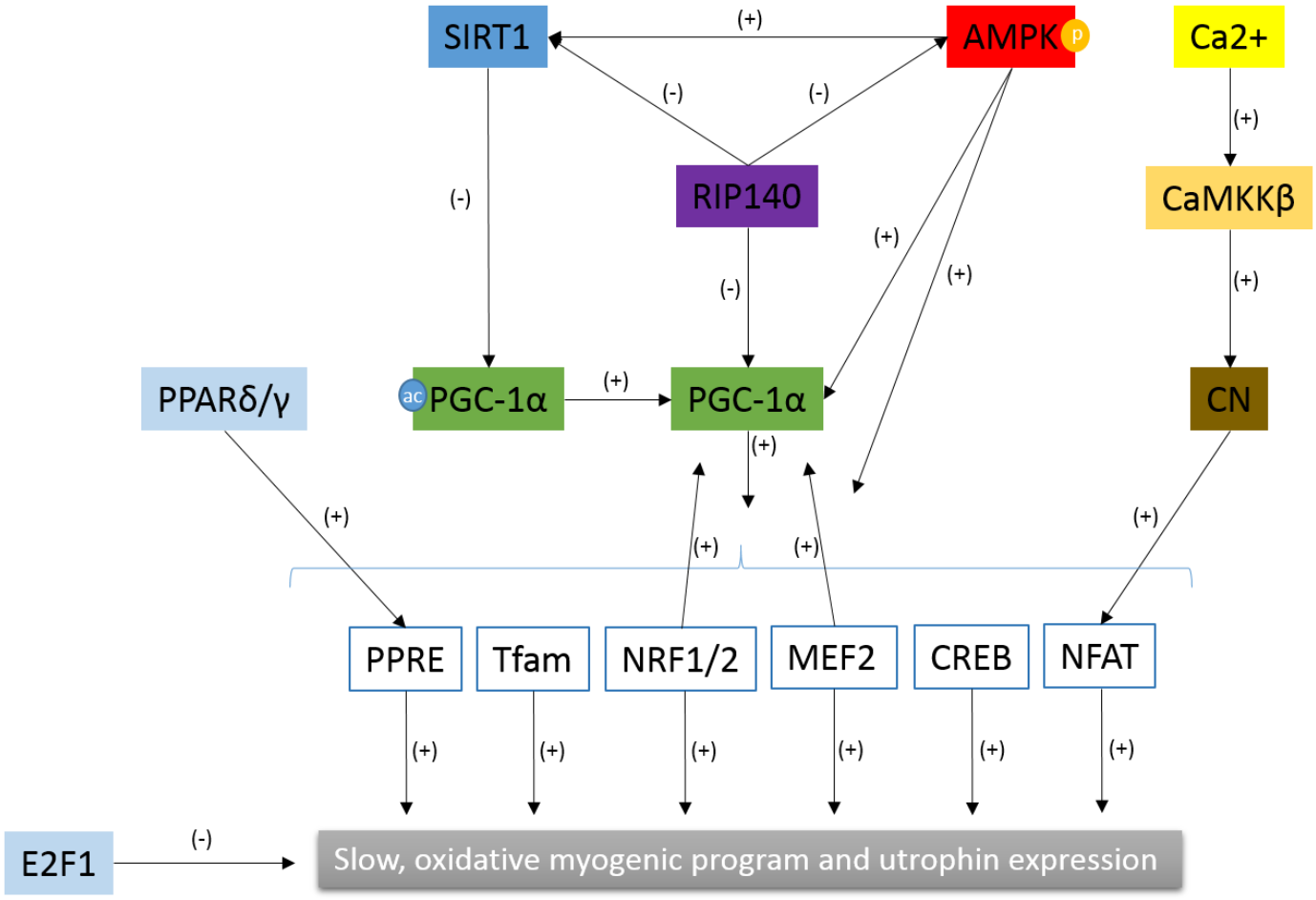

Figure 1.3: Signaling cascades that trigger the slow, oxidative myogenic program and increased utrophin A expression.

The transcription factor PPARδ binds PPREs in upstream regions of slow, oxidative genes. Phosphorylated AMPK activates the deacetylase SIRT1 and the transcriptional co-activator, PGC-1α. SIRT1 also induces PGC-1α activity through deacetylation. PGC-1α interacts with transcription factors like MEF2 and PPARδ to induce slow, oxidative gene expression. Calcium ion influx as a result of activity increases CN activity, which influences gene expression via its interaction with NFAT. These pathways have been shown to induce the slow, oxidative myogenic program, increase utrophin A expression, and provide benefits to dystrophic muscles.

1.12 Statement of the problem

DMD is a devastating degenerative disease that results in severe obstruction of patients' lives and death (114-117). There is currently no cure or effective treatment for DMD, but multiple therapeutic avenues are being researched (155-159). Among those, is the induction of the slow, oxidative myogenic program. Slow, oxidative muscles are more resistant to the dystrophic pathology than fast, glycolytic ones and induction of the slow oxidative, myogenic program has been shown to improve the dystrophic pathology of mdx mice (5,24,41,42). This can be due to the multiple beneficial adaptations to dystrophic fibers that are associated with the slow, oxidative phenotype, including improvements in mitochondrial function and autophagy, reductions in mitochondrially mediated apoptosis, and increased expression of the autosomal dystrophin analog, utrophin A. The purpose of this study is to determine the role of utrophin A versus the other benefits of the slow, oxidative phenotype in the improved pathology seen in mdx mice after induction of the slow, oxidative myogenic program.

To pursue this, we will need to trigger the program in utrophin A expressing mdx mice and utrophin A null dystrophin/utrophin A double knockout (dKO) mice. Thus, we will be able to compare the morphological and functional improvements that the program may or may not confer in the presence and absence of utrophin A. dKO mice are created by interbreeding utrophin A-null mice (*utrn*$^{-/-}$) with *mdx* mice, and have a much more severe DMD pathology than mdx mice, suggesting that there is indeed a role for utrophin A in preventing some of the damage from the disease. (176,177).

1.13 Hypothesis and predictions

Our hypothesis is that the benefits conferred by the slow, oxidative myogenic program on mdx mice are directly linked to the upregulation of utrophin A protein expression. We therefore predict that while both dKO and mdx mice will express a slower, more oxidative phenotype after chronic AICAR treatment, only the mdx mice will show morphological and functional muscle improvements.

1.14 Objectives

In order to assess the importance of utrophin A to the benefits of the slow oxidative myogenic program, we will:

In order to assess the importance of utrophin A to the benefits of the slow oxidative myogenic program, we will:

(1)- Characterize the signaling capacity and muscle phenotype of the dKO in comparison to mdx mice.
(2)- Treat both strains of mice with AICAR and measure indicators of muscle signaling and phenotype to ensure that the drug is working as expected and inducing a shift towards a slower, more oxidative phenotype.
(3)- Perform histological and functional analyses to determine the benefits that the chronic AICAR treatment confers on the two strains of mice.

2: MATERIALS AND METHODS

2.1 Animal care and breeding

All experimental protocols were approved by the University of Ottawa Institutional Animal Care Committee and were in accordance with Canadian Council of Animal Care guidelines. Female mice that are heterozygous for the *Utrn*^{tm1Ked} allele and homozygous for the *Dmd*^{mdx} allele and male mice that are heterozygous for the *Utrn*^{tm1Ked} allele and hemizygous for the *Dmd*^{mdx} allele were ordered from The Jackson Laboratory (Bar Harbor, USA). They were housed in the Animal Care and Veterinary Service of the University of Ottawa, under a constant 12 h light/dark cycle and given free access to food and water. They were bred to produce Utrn^{tm1Ked} Dmd^{mdx}/J mice, which are the utrophin/dystrophin double knockout (dKO) mice, and mdx mice.

2.2 Genotyping

2.2.1 Tissue collection

After breeding, the offspring mice were weaned at 3 weeks of age. During weaning, the mice were tagged and ear notch samples were taken.

2.2.2 Tissue digestion

The ear notch samples were digested in tissue lysis buffer (50 mM KCl, 10 mM TrisHCl pH 8.3, 2.5 mM MgCl2.6H2O, 0.1 mg/mL gelatin, 0.45% v/v NP40 (Thermo Scientific, Rockford, USA), 0.45% v/v Tween 20) overnight at 65 C. Prior to use, 1X pronase was added to the tissue lysis

buffer from a 40X stock (20 mg/mL Pronase in 10 mM Tris HCl pH 7.5, 10 mM NaCl). The next day, the samples were briefly vortexed, then centrifuged at 2000 RPM for 10 minutes. The supernatant was collected and the concentration of DNA in it was quantified using a Synergy H1 Hybrid Reader (Biotek, Winooski, USA).

2.2.3 PCR

Two polymerase chain reactions were run for each animal. Both reactions used 12.5 uL 2X KAPA 2G Fast HS Genotyping Mix (KM5606, KAPA Biosystems, Wilmington, USA), 1.25 uL forward primer (10 uM), 1.25 uL reverse primer (10 uM), 0.5 uL MgCl2 (25 mM), 8.5 uL H2O, and 100 ng of the DNA extracted from the animals tissue. For a total volume of 25 uL. One reaction used the mutant forward primer (CGC TTC CTC GTG CTT TAC GGT AT), while the other used the wild type forward primer (TGT CAT TCT CTG AGG CCT TTC). Both reactions used the common reverse primer (AAG ATT TGC AGA CCG GAA GA). The reactions were run according to the protocol in Table 2.1 in a T100 Thermal Cycler (Bio-Rad, Mississauga, Canada).

Table 2.1: Thermal cycling procedure for the genotyping PCR reaction.

Step	Temperature	Time
1	94 C	2 min
2	94 C	20 sec
3	65 C	15 sec (-0.5 C per cycle)
4	68 C	10 sec
5	Repeat steps 2-4 10X	
6	94 C	15 sec
7	60 C	15 sec
8	72 C	10 sec
9	Repeat steps 6-8 28X	
10	72 C	2 min
11	10 C	hold

2.2.4 Gel running

A 2% agarose gel was prepared as the PCR ran. To make the gel, 3 g of agarose were added to 150 mL of TBE (89 mM Tris, 89 mM boric acid, 2 mM EDTA pH 8.0) and microwaved for 2.5-3 minutes. Then, 6 uL of ethidium bromide were added and the gel was cast with a comb for the appropriate number of wells. After completion of the PCR, 10 uL from each sample as well as DNA ladder were loaded into the wells and the gel was run for 2 hours at 100 V in a TBE filled chamber.

2.3 *In vivo* AICAR treatment

After approval by the University of Ottawa Animal Care Committee in accordance with Canadian Council of Animal Care guidelines, we performed the *in vivo* AICAR treatment according to protocol and dosage used by Ljubicic et al. in 2011, which has been shown to induce the slow, oxidative myogenic program in murine models (24,57,238,242,243). AICAR (TRC, Toronto, Canada) was dissolved in sterile saline at 50 mg/ml daily prior to treatments. Three to four week old dKO and mdx mice were treated daily with vehicle or AICAR (500 mg/kg/day) by subcutaneous interscapular injections for 28 days.

2.4 Western blot

2.4.1 Protein extraction

The tissue of interest was dissected and snap frozen in liquid nitrogen and stored at -80 C. The tissue was ground with a mortar and pestle on dry ice until it is a powder. 300-500 uL of lysis buffer (7 M urea, 2 M thiourea, 4 M CHAPS, 100 mM DTT, 125 mM Tris-HCl pH 6.8, cOmplete mini protease inhibitor (Roche, Laval, Canada), PhosSTOP phosphatase inhibitor (Roche, Laval Canada)) was added to the tissue in a 1.5 mL Eppendorf tube depending on its size. Constant agitation was maintained on a vortex for 30 minutes at room temperature. The samples were centrifuged at 16000 g for 15 minutes. The supernatant was transferred to a fresh tube and stored at -20 C.

2.4.2 Protein quantification

1 mL of -20 C CB-X (G-Biosciences, St. Louis, USA) was added to 5 uL of protein solution. The mixture was centrifuged at 16000 g for 5 minutes and the supernatant discarded. 50 uL of CB-X Solubilisation Buffer I (G-Biosciences, St. Louis, USA) and 50 uL of CB-X Solubilisation Buffer II (G-Biosciences, St. Louis, USA) were added to the protein pellet. The pellet was allowed to dissolve in the solubilisation buffers. In a 96 well plate, 100 uL of CB-X assay was added to 5 uL of dissolved protein from each sample and incubated at room temperature for 5 minutes. The absorbance was read at 595 nm using a Synergy H1 Hybrid Reader (Biotek, Winooski, USA).

2.4.3 Gel preparation

The gel plate sandwich was prepared with a 1.5 mm plate and aligned in the gel plate clamp. The resolving gel was either a 5% (5.75 mL H_2O, 2.5 mL 4X Tris-SDS pH 8.8, 1.65 mL 30% acrylamide, 200 uL 10% APS, 10 uL TEMED) or a 10% (4 mL H_2O, 2.5 mL 4X Tris-SDS pH 8.8, 3.33 mL 30% acrylamide, 100 uL 10% APS, 10 uL TEMED), based on the protein of interest's size. The solutions were combined in a beaker on a stir plate stirring at a low-medium frequency. The liquid gel mixture was poured into the gel sandwich, leaving 3-5 cm of space at the top. The gel was overlaid with 100 uL of 100 % butanol and allowed to polymerize for 30 minutes. Meanwhile, the stacking gel was prepared with 4.67ml water, 2ml 4X Tris-SDS (pH=6.8), 1.33ml 30% Acrylamide, 65µl 10% APS, and 10µl TEMED. The butanol was washed away from on top of the resolving gel with water. 1 mL of the stacking gel mixture was added and a comb was placed in it. The gel was allowed to polymerize for 30 minutes.

2.4.4 Protein preparation

The protein samples were thawed and an aliquot containing 20 ug of protein from each sample was placed in a fresh microfuge tube. Add an equal volume of 2X Laemmli buffer (4% SDS, 10% 2-mercaptoethanol, 20% glycerol, 0.004% bromophenol blue, 0.125 M Tris-HCl, pH 6.8). Heat the samples for 5 minutes at 75 C (except when using the OXPHOS cocktail antibody).

2.4.5 Gel run

The gel plate sandwich was removed from the clamp and placed in the gel core unit. The gel core unit was filled with 1X running buffer (25 mM Tris base, 190 mM glycine, 0.1% SDS, pH 8.3). The protein/lammeli buffer mixture as well as prestained protein marker were loaded into the gel wells. The gel was run at 120 V for 1-2 hours using a Power Pac 300 (Bio-Rad, Mississauga, Canada).

2.4.6 Transfer

While the gel is running, 1 piece of Nitrocellulose membrane and 4 pieces of filter paper matching the size of the gel were cut out. When the gel run was complete, the nitrocellulose membrane was soacked in ddH2O and the filter paper was soacked in transfer buffer (25 mM Tris base, 190 mM glycine, 20% methanol, pH 8.3) along with the transfer sponges. The gel was removed from the gel plate sandwich and soacked in transfer buffer for 1 minute. A wet transfer sandwich was placed on the table with the black facing down. A sponge was placed, followed by two pieces of filter paper, the gel, the membrane, two pieces of filter paper, and the second sponge. The sandwich was closed and placed in gel core unit along with a pack of ice. The gel core unit was filled with transfer buffer. The transfer was run at 30 V overnight at 4 C, then at 100 V for 2 hours (3 hours for utrophin A) at 4 C using a Power Pac 300 (Bio-Rad, Mississauga, Canada). The ice pack was replaced every hour during the 100 V transfer.

2.4.7 Detection with antibodies

The membrane was taken out of the transfer sandwich and rinsed with ddH2O. It was placed in a container, covered in Ponceau S solution (0.1% Ponceau S in 1% acetic acid) and placed on a shaker for 5 minutes. The Ponceau S solution was removed and the membrane was observed to ensure that there are proteins on it. A picture of the membrane was acquired. The membrane was placed in a container and washed with TBST (137 mM NaCl, 2.7 mM KCl, 19 mM Tris base, 0.1% Tween 20) on a shaker until the staining was removed. The membrane was blocked with blocking solution (5% milk in TBST) for 1 hour at room temperature. The appropriate dilution of primary antibody was applied to the membrane in blocking solution or 5% BSA in TBST (for AMPK antibodies) overnight at 4 C. The antibodies used were: AMPKα (Cell Signaling 2532, Whitby, Canada), Phospho-AMPKα (Cell signaling 2531, Whitby, Canada), utrophin A (Novocastra, Concord, Canada), PGC-1α (Abcam ab72230, Toronto, Canada), RIP140 (Abcam ab342, Toronto, Canada), SIRT1 (Millipore 09-844, Billerica, USA), GAPDH (Advanced ImmunoChemical 2-RGM2 6C5, Long Beach, USA), Troponin (Santa Cruz sc8119, Dallas, USA), OXPHOS complexes (Mitosciences MS604, Eugene, USA) and cytochrome c (from Dr David A. Hood, Muscle Health Research Centre, York University, Toronto, Canada) The primary antibody was removed and the membrane was washed 3X5 minutes in TBST. The appropriate dilution of secondary antibody coupled to horseradish peroxidase was applied to the membrane in blocking solution for 1 hour at room temperature. The membrane was washed 3X5 minutes in TBST. Sit the membrane on a clean sheet of saran wrap and cover in a 1:1 mixture of the Pierce ECL Western Blotting Substrate (Thermo Scientific, Rockford, USA) reagents for 1 minute. Tap the membrane dry on a Kim wipe (Kimberley Clark). Cover the membrane in transparent plastic and place face

up in the development cassette. The blot was developed in a darkroom and the films (CL-X Posure, Thermo Scientific, Rockford, USA) were scanned and analyzed using ImageJ (NIH).

2.5 Immunohistochemistry

2.5.1 Sectioning

After animal euthanasia, the desired tissues were embedded in Tissue-Tek OCT Compound (Sakura Finetek, Torrace, USA) and frozen in isopentane dipped in liquid nitrogen, then stored at -80 C until use. The tissues were sectioned at 10 um using a Microm HM 500 M microtome (Microm) and the sections were placed on glass microscope slides.

2.5.2 Detection with antobodies

The tissue sections were fixed with 5% PFA (5% PFA in 1X PBS, pH 7.4) for 10 minutes, then washed with buffer A (0.5% BSA, 0.15% glycine in 1X PBS). They were incubated in buffer A for 1 hour at room temperature. The primary antibody was diluted to the recommended concentration in buffer A and applied to the tissue sections overnight at 4 C. The primary antibodies used include utrophin A (Novocastra NCL-DRP2, Concord, Canada), Laminin (Sigma Aldrich, Oakville, Canada), and MHC I and MHC II A (from Dr. Renaud, University of Ottawa, Canada). The next day, the sections were washed 3X10 minutes with PBS. The appropriate fluorescently labelled secondary antibody was diluted to the recommended concentration in buffer A and applied in a dark room for 1 h at room temperature. For IgM staining, a fluorescein-conjugated IgM anti-mouse secondary antibody (Sigma-Aldrich, Oakville, Canada) was used. The

secondary antibody was removed by washing 3X10 minutes with PBS, then the slide was mounted using Vectashield mounting medium (Vector Laboratories, Burlington, Canada) and a cover slip. The slides were visualized with a fluorescent microscope and images were acquired.

2.5.3 Haematoxylin and Eosin

The slides were heated on a 37 C plate for 10 minutes. They were immersed in filtered Harris Hematoxylin for 1 minute, then rinsed in running tap water. The tap water was exchanged until it became clear. The slides were immersed in Eosin for 1 minute, then rinsed with tap water, which was exchanged until it became clear. The tissue sections were dehydrated through ascending, graded 1 minute ethanol washes (50%, 70%, 80%, 95%, 100%) followed by a 1 minute wash with xylene. The slides were mounted with Permount and a coverslip. They were visualized with a fluorescence microscope and images were acquired.

2.6 Ex vivo eccentric contractions

After 4 weeks of AICAR treatment, the animals were euthanized and their EDL muscles dissected. One tendon of the EDL muscle was attached to a Cambridge ergometer (model 6350*358, Aurora Scientific, Aurora, Canada), while the other was attached to a metal pin. The muscle was continouosly bathed in saline containing 0.1% trypan blue (Sigma-Aldrich, Oakville, Canada), with a flow rate of 15 mL/min at room temperature. The muscle length was adjusted to ensure maximal force output, and the force output at that length was monitored for consistency for 30 minutes. The muscle was subjected to 5 maximal twitch contractions (400 ms train duration, 10

V, 0.3 ms square pulse, 200 Hz) at 100 s intervals to determine muscle contractile kinetics, followed by 12 eccentric contractions at 120 s intervals (700 ms train duration, 10 V, 0.3 ms square pulse, 200 Hz) (model S88, Grass Technologies, West Warwick, USA). During the last 200 ms of the eccentric contractions, 10% lengthening at a velocity of 0.5 Le/s was applied. Throughout the experiment, force was recorded using a Keithley data acquisition board (model KPCI-3104, Cleveland, USA) at a sample rate of 5 KHz. After, the eccentric contractions, the muscle was embedded in Tissue-Tek OCT Compound (Sakura Finetek, Torrace, USA) and frozen in isopentane dipped in liquid nitrogen, then stored at -80 C until use. The muscle was sectioned at 10 um using a Microm HM 500 M microtome (Microm) and the sections were placed on glass microscope slides and observed for red fluorescence, which indicates trypan blue infiltration of the muscle fibres. The peripheral fibers of the muscle sections were omitted from the analysis due to their possible damage during the dissection or the experimental setup.

2.7 Grip test

The same animals that were used for the *ex vivo* eccentric contractions were used for the grip test. Starting at three days before the AICAR treatment was completed, the mice were handled two to three times daily to get them used to handling. One day prior to testing, the mice were marked with a sharpie marker on their tails for easy identification. Their cages were identified to prevent them from being disturbed. After the final AICAR injection was administered, the mice were moved to the testing room 1 h before the test began and left there to habituate. The triangular grid of the Chantillion DFE II (Columbus Instruments, Columbus, USA) grip strength meter was attached and the meter turned on. The meter was set to tension peak mode (T-PK). A mouse was picked out

of the cage and held by the base of its tail. It was allowed to acclimatize near the grip strength meter for 60 sec. The mosue was then moved closer to the meter until it grabbed the bar. Once it had a firm grip, the mouse was pulled horizontally away from the bar at a speed of approximately 2.5 cm/sec, until it released the bar. The value of the maximal peak force was displayed by the meter and recorded. This was repeated 5 times for each animal, with a waiting time of 10-15 sec between each measurement. When testing was completed, the mice were returned to their cages and taken back to their housing.

2.8 Statistical Analysis

The data was analyzed for statistical significance using paired and unpaired Student's t-tests and analysis of variance (ANOVA) procedures and post hoc tests, as appropriate (StatPlus, Vancouver, Canada). In the graphs depicted as fold differences, statistical anaylsis was conducted using the raw data prior to conversion to the fold difference values. Significance was accepted at $P < 0.05$.

3: RESULTS

As mentioned in the introduction, the aim of this study is to assess the importance of utrophin A to the benefits conferred by the slow, oxidative phenotype on dystrophic muscle fibers. To do this, we compared the improvements that are seen in dKO and mdx mice upon induction the slow, oxidative myogenic program. However, besides their pathology, dKO mice have not been characterized to the same extent as mdx mice. It is known that dKO mice have a much more severe DMD pathology than mdx mice, which live largely unhindered lives. The onset of dystrophy is earlier in dKO mice, and they start to lose weight and display progressively worsening kyphosis shortly after weaning (176,177). Their severe pathology leads to death by 20 weeks of age, with most deaths occurring at 8-12 weeks (176,177). Histologically, the dKO diaphragm shows a great amount of necrosis and fibrosis at an early age, followed by regeneration. In the tibialis anterior (TA), there is extensive irregularity in the muscle fiber diameter as well as signs of necrosis, inflammation, and regeneration (176,177). However, there has not been much detailed examination of signaling pathways or muscle phenotype in the dKO mouse.

Therefore, we first assessed the expression levels of important signaling molecules that are involved in the phenotype shifting signaling cascades mentioned earlier. We also assessed the expression of key indicators of muscle phenotype that can be used to determine the oxidative capacity of a muscle and whether it is fast or slow. These measurements were done in dKO and mdx mice, given the fact that they are both dystrophic and comparing how they benefit from the slow, oxidative myogenic program is a central objective in this study. In addition to providing valuable information on the effects of the loss of utrophin A, this information will allow us to determine whether or not the muscles of dKO and mdx mice have the same signaling and

phenotypic capacity. The assessment of their signaling phenotypic capacity will help us determine if treating the mice with AICAR will illicit the same shift in muscle phenotype in both strains or not.

3.1 Characterization of dKO mice

3.1.1 dKO and mdx mice have similar levels and patterns of expression of muscle signaling proteins

Skeletal muscle phenotype is partly controlled by molecules that influence muscle gene expression, including transcription factors, transcriptional co-activators and co-repressors and histone modifying proteins (43,15,56,23,232,21,22). We investigated the content and/or activation levels of some of these phenotype modifying molecules, including AMPK, PGC-1α, receptor-interacting protein 140 (RIP140), and silent information regulator two ortholog 1 (SIRT1) in the EDL and soleus muscles of dKO and mdx animals. These signaling molecules can control muscle plasticity, so the ability of both mice to express them influences their ability to express the slow, oxidative myogenic program (5).

Since AICAR elicits the slow, oxidative myogenic program through AMPK, we measured the activation of AMPK, as denoted by phosphorylation levels. AMPK phosphorylation was higher in the soleus than the EDL in both mice, and there were no differences in activation between the dKO and mdx mice ($P < 0.05$) (Figure 3.1). The expression of PGC-1α, a target of AMPK, was also the same in the dKO and mdx mice and was higher in the soleus compared to the EDL in both strains ($P < 0.05$) (Figure 3.2). RIP140, which opposes the effects PGC-1α, had the same expression levels in dKO and mdx mice, which were significantly lower in the soleus compared to the EDL ($P <$

0.05) (Figure 3.3). Finally, the histone de-acetylase SIRT1 had significantly greater expression in the soleus compared to the EDL in both dKO and mdx mice, and was also expressed at the same level in both strains ($P < 0.05$) (Figure 3.4). Considering the consistency between the dKO and mdx mice, our results indicate that the signaling pathways that we intend to use to trigger the slow, oxidative myogenic program are intact and functional in dKO mice.

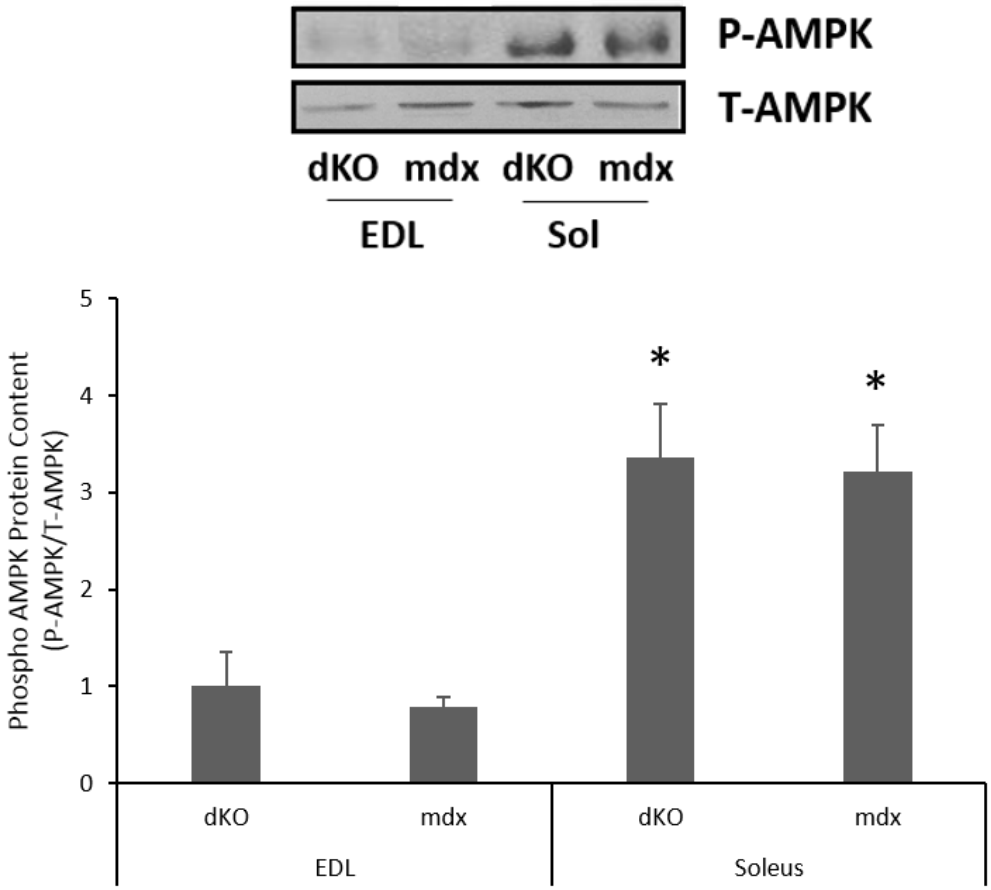

Figure 3.1: Phosphorylation levels of AMPK in fast, glycolytic and slow, oxidative muscles of dKO and mdx mice. Representative western blots of phosphorylated AMPK and total AMPK and graphical summary of the ratio of phosphorylated AMPK to total AMPK in the EDL and soleus muscle of dKO and mdx mice. $n = 6–7$; * indicates significant difference compared to expression in EDL muscles ($P < 0.05$).

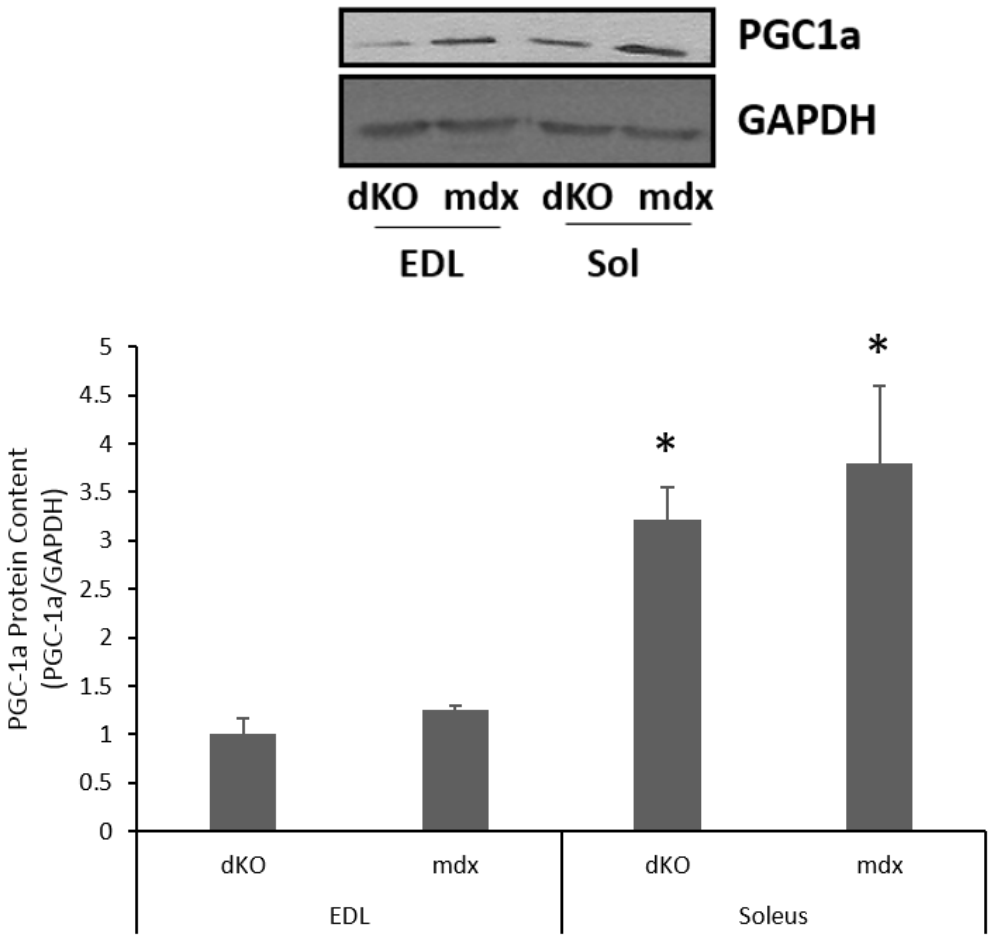

Figure 3.2: Expression of PGC-1a in fast, glycolytic and slow, oxidative muscles of dKO and mdx mice. Representative western blots of PGC-1a and GAPDH, representative Ponceau S stain and graphical summary of PGC-1a protein content in the EDL and soleus muscle of dKO and mdx mice. n = 6–7; * indicates significant difference compared to expression in EDL muscles (P < 0.05).

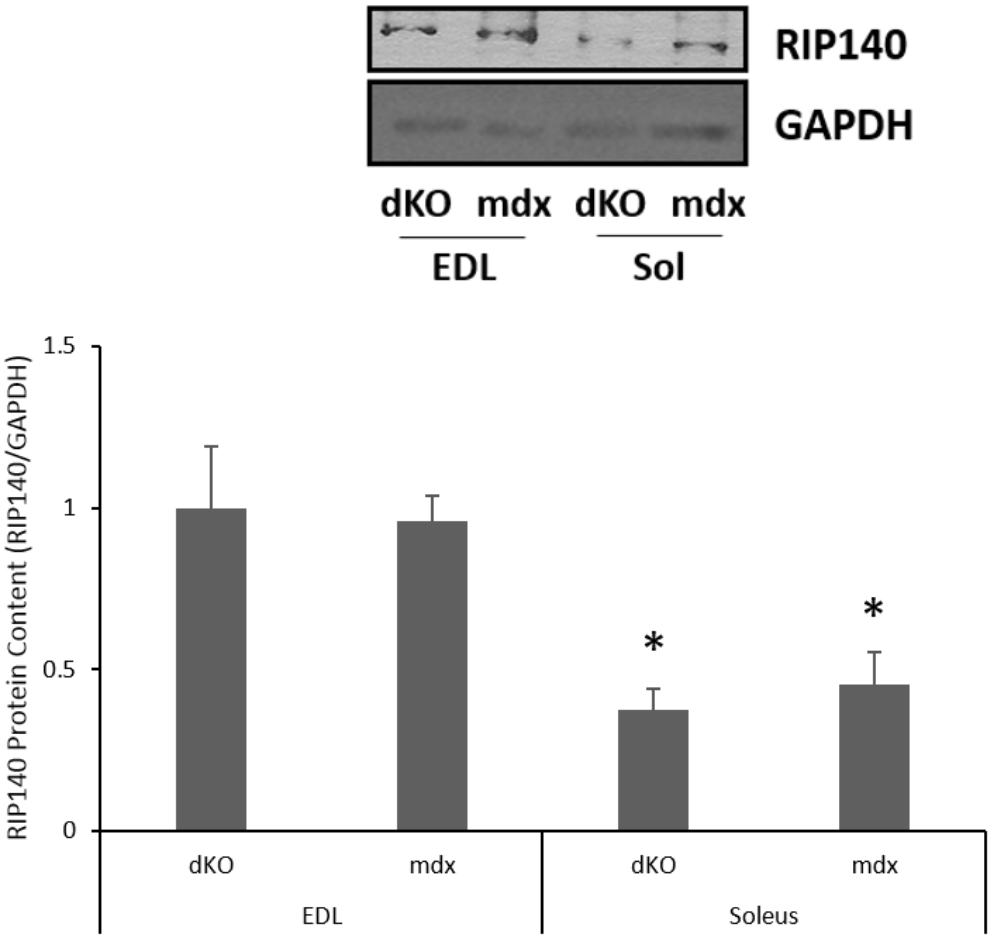

Figure 3.3: Expression of RIP140 in fast, glycolytic and slow, oxidative muscles of dKO and mdx mice. Representative western blots of RIP140 and GAPDH, representative Ponceau S stain and graphical summary of RIP140 protein content in the EDL and soleus muscle of dKO and mdx mice. n = 6–7; * indicates significant difference compared to expression in EDL muscles ($P <$ 0.05).

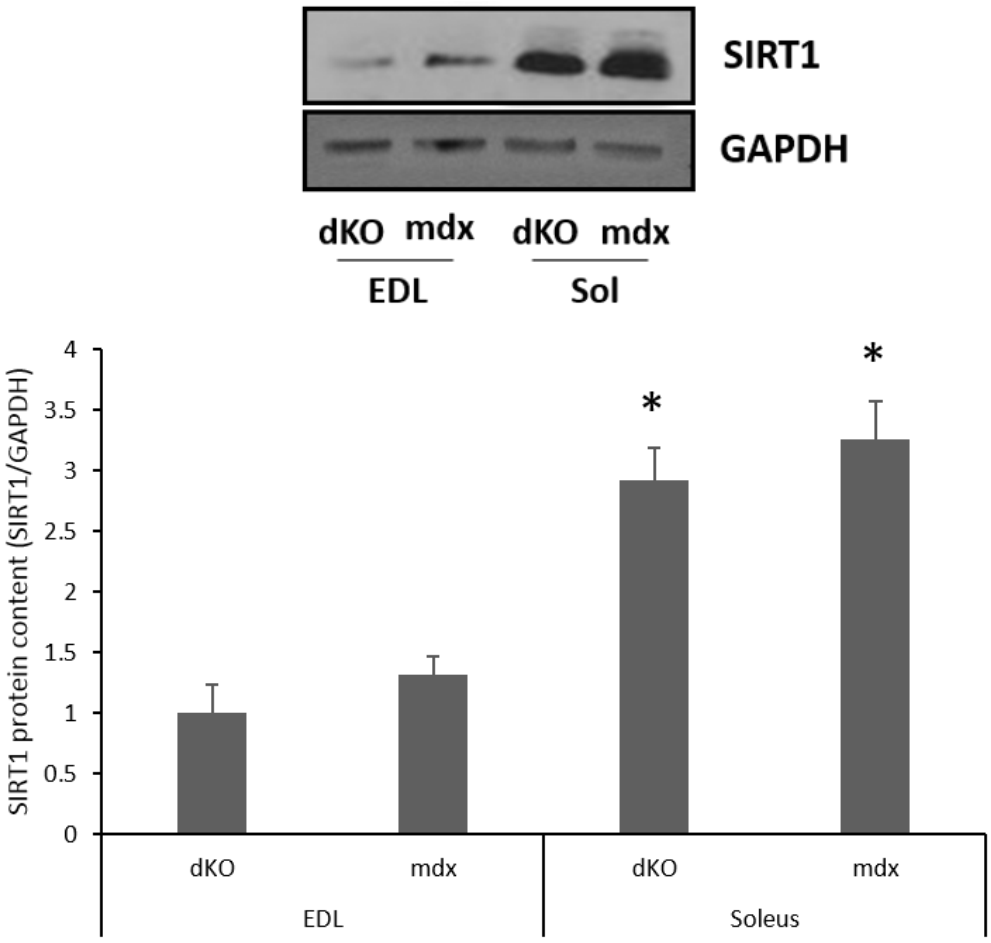

Figure 3.4: Expression of SIRT1 in fast, glycolytic and slow, oxidative muscles of dKO and mdx mice. Representative western blots of SIRT1 and GAPDH, representative Ponceau S stain and graphical summary of SIRT1 protein content in the EDL and soleus muscle of dKO and mdx mice. $n = 6–7$; * indicates significant difference compared to expression in EDL muscles ($P < 0.05$).

3.1.2 dKO and mdx mice have similar levels and patterns of expression of indicators of muscle phenotype

Some proteins have distinct expression patterns between fast, glycolytic and slow, oxidative muscles, and they can be used as markers of muscle phenotype (63,65,233-235). We analyzed some markers of the slow, oxidative phenotype, including cytochrome c, a slow isoform of troponin c, myosin heavy chain I, and myosin heavy chain II A in both dKO and mdx mice. Since the phenotype of a muscle influences its response to pharmacological induction of the slow, oxidative myogenic program, the expression of these phenotype indicators gives an indication of the extent to which dKO and mdx mice respond to the slow, oxidative myogenic program (49).

Cytochrome C expression in the soleus compared to the EDL was greater in dKO and mdx mice ($P < 0.05$) (Figure 3.5). Slow troponin expression was also greater in the soleus compared to the EDL in both strains of mice ($P < 0.05$) (Figure 3.6). Finally, the ratio of fibers expressing MHC I and MHC II A was higher in the soleus compared to the EDL in both dKO and mdx mice (Figure 3.7 and Figure 3.8). Importantly, there were no significant differences in the levels of expression of these markers between dKO and mdx mice. This consistency between dKO and mdx mice indicates that they have the same muscle phenotypes, which gives confidence that they will respond in the same way when the slow, oxidative myogenic program is pharmacologically activated.

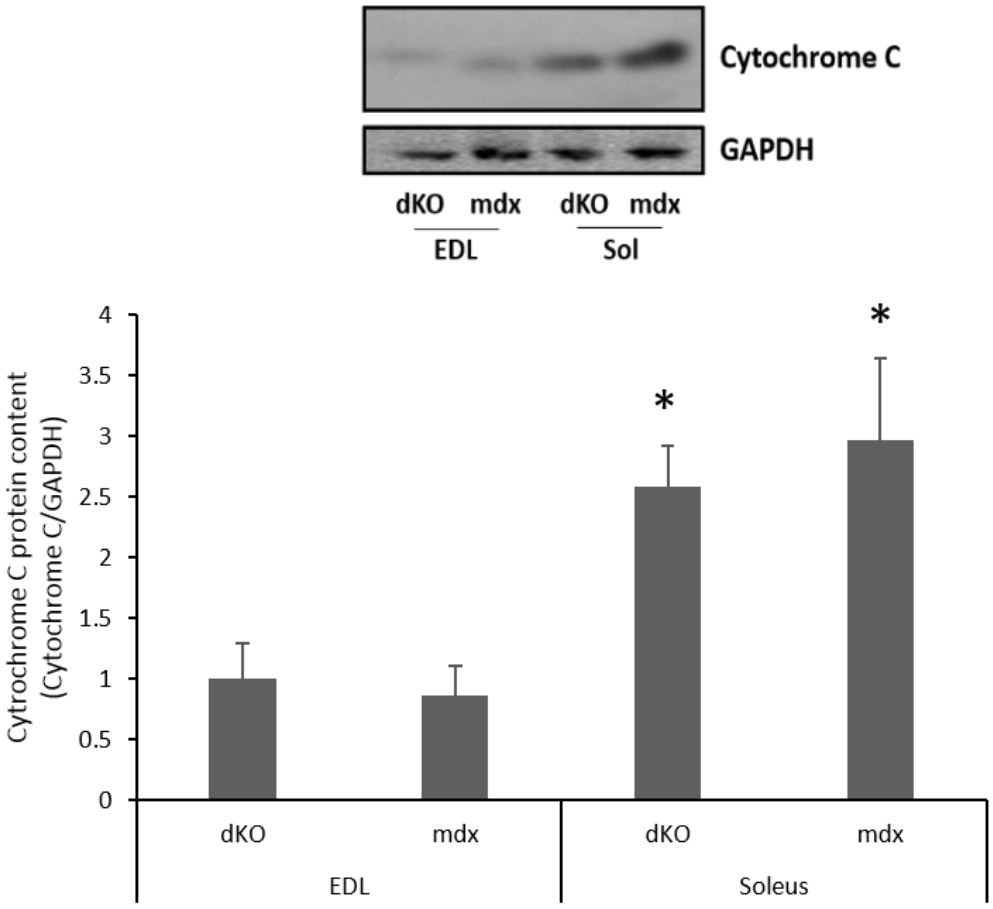

Figure 3.5: Expression of cytochrome c in fast, glycolytic and slow, oxidative muscles of dKO and mdx mice. Representative western blots of cytochrome c and GAPDH, representative Ponceau S stain and graphical summary of cytochrome c protein content in the EDL and soleus muscle of dKO and mdx mice. n = 6–7; * indicates significant difference compared to expression in EDL muscles ($P < 0.05$).

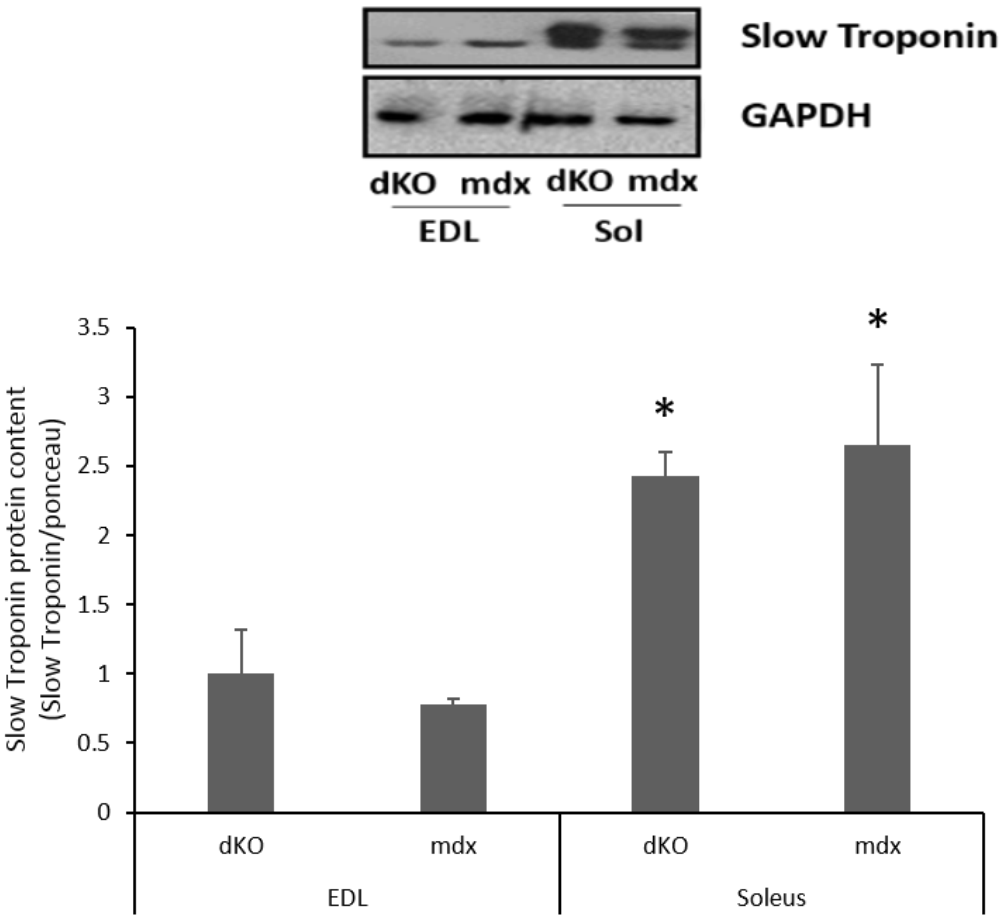

Figure 3.6: Expression of the slow isoform of troponin in fast, glycolytic and slow, oxidative muscles of dKO and mdx mice. Representative western blots of troponin and GAPDH, representative Ponceau S stain and graphical summary of troponin protein content in the EDL and soleus muscle of dKO and mdx mice. n = 6–7; * indicates significant difference compared to expression in EDL muscles ($P < 0.05$).

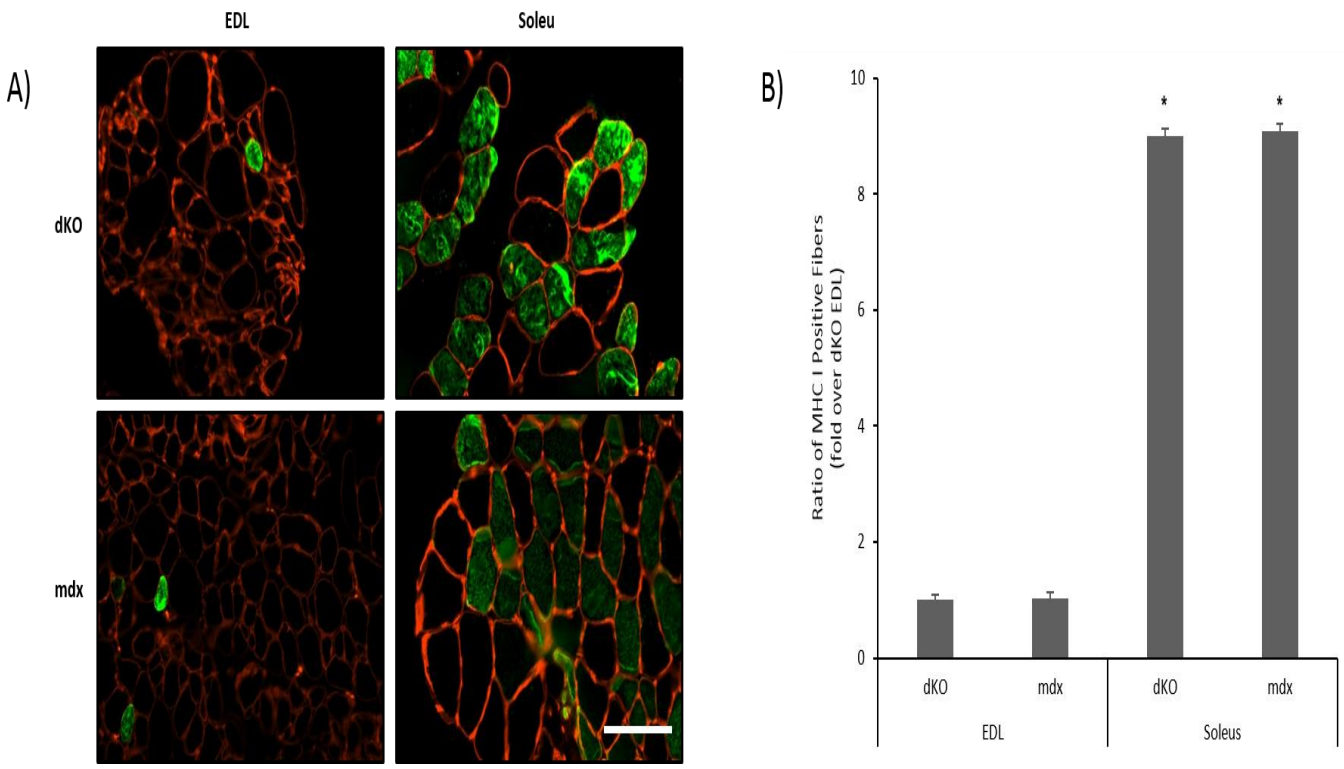

Figure 3.7: Expression of the slow myosin ATPase MHC I in fast, glycolytic and slow, oxidative muscles of dKO and mdx mice. Representative micrographs of MHC I immunofluorescence (A) and graphical summary of MHC I positive fibers (B) in the EDL and soleus muscles of dKO mdx mice. n = 6–7; * indicates significant difference compared to expression in EDL muscles (P < 0.05). Scale bar = 80 μm.

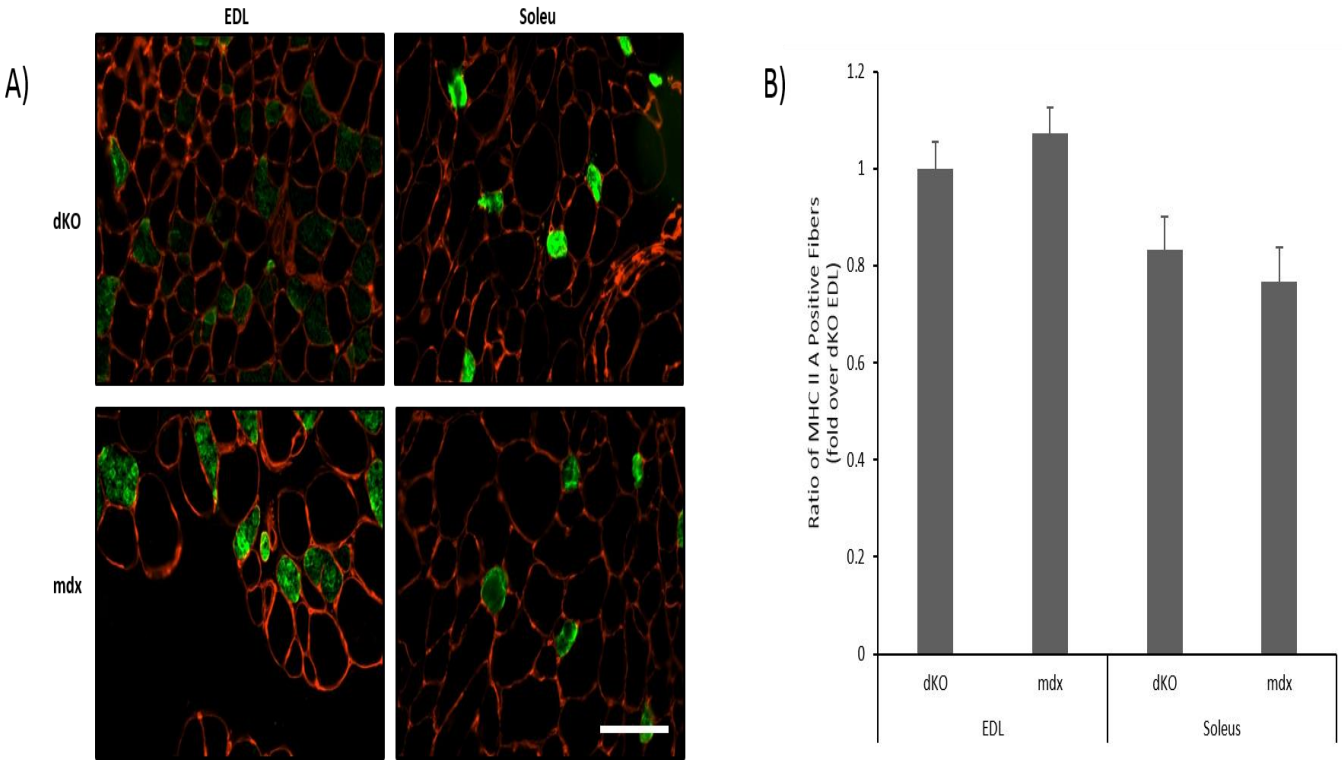

Figure 3.8: Expression of the slowest MHC II isoform, MHC II A, in fast, glycolytic and slow, oxidative muscles of dKO and mdx mice. Representative micrographs of MHC II A immunofluorescence (A) and graphical summary of MHC I positive fibers (B) in the EDL and soleus muscles of dKO mdx mice. n = 6–7. Scale bar = 80 μm.

3.2 AICAR Treatment

In order to activate the slow, oxidative myogenic program in our mice, we treated them for 4 weeks with the AMP analogue AICAR. This drug has been used to elicit the slow, oxidative myogenic program in mdx mice before (24,57,231). Its effects have also been documented in wt mice, so we included a wt control in our experiments (239,240). Since the wt mice do not suffer from DMD related muscle damage, they can also be used the as a baseline to gauge the extent of the morphological and functional improvements seen in the muscles of AICAR treated dKO and mdx mice, which we expected to show increased expression of proteins and signaling molecules of the slow, oxidative phenotype.

3.2.1 AICAR treatment alters the expression of skeletal muscle signaling proteins in dKO and mdx mice

After AICAR treatment, we measured the expression and/or activation levels of the phenotypic modifiers, mentioned earlier, partly through which AICAR can trigger a slower, more oxidative phenotype in the fast, glycolytic muscles of treated mice (43,15,56,23,232,21,22). We investigated the activation and/or protein content of AMPK, PGC-1α, RIP140, SIRT1 in the EDL muscle of wt, AICAR treated, and control dKO and mdx mice.

AMPK phosphorylation was not increased as a result of chronic AICAR treatment in both dKO and mdx mice (Figure 3.9). The expression of one of the targets of AMPK, the transcriptional co-activator PGC-1α, was approximately 1.5-fold higher in AICAR treated dKO and mdx mice compared to their control counterparts ($P < 0.05$) (Figure 3.10). AICAR treatment resulted in a reduction of transcriptional co-repressor RIP140 expression by at least 70 % in both AICAR

treated dKO and mdx mice compared to control dKO and mdx mice ($P < 0.05$) (Figure 3.11). Finally, SIRT1 expression was significantly higher in AICAR treated mice compared to control mice in both the dKO and mdx strain ($P < 0.05$) (Figure 3.12). Importantly, the expression and/or activation levels of all of these signaling molecules were consistent between dKO and mdx mice, both with and without the AICAR treatment. The changes in expression of the signaling molecules indicate that AICAR treatment was effective in equally promoting a shift towards a more oxidative, possibly slower muscle phenotype in the dKO and mdx mice.

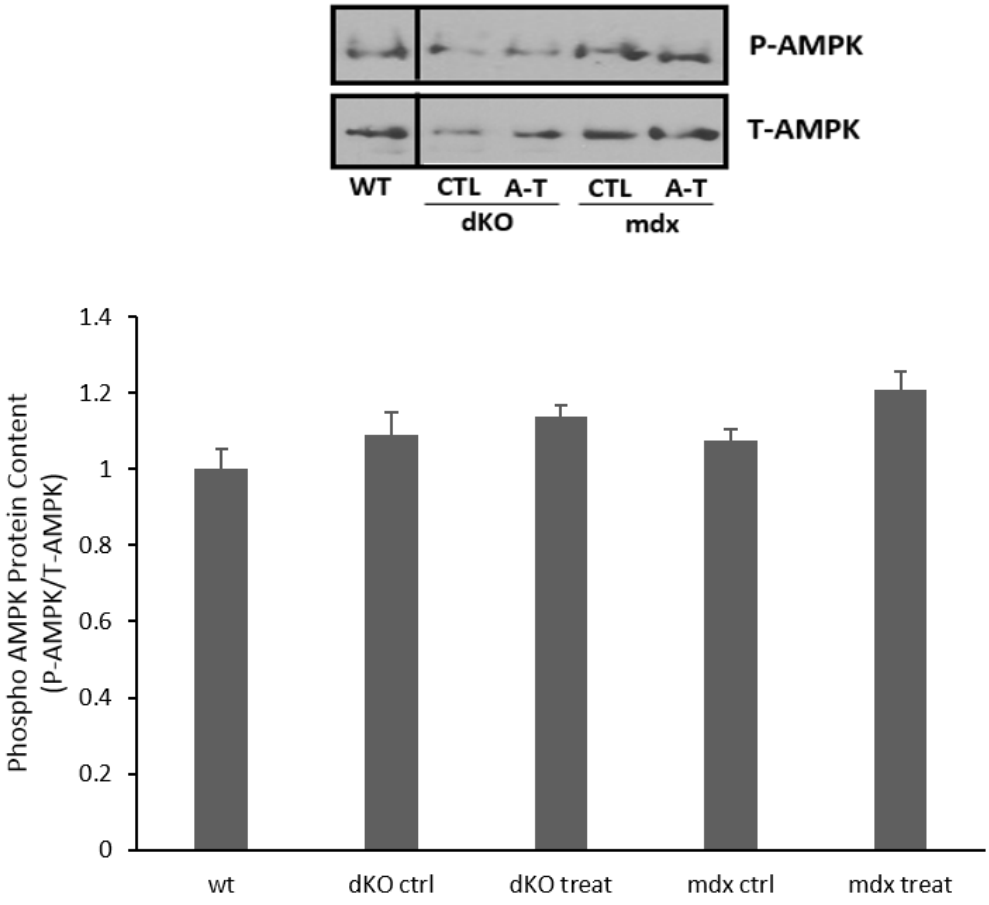

Figure 3.9: Phosphorylation levels of AMPK in the fast, glycolytic muscles of AICAR treated mice. Representative western blots of phosphorylated AMPK and total AMPK and graphical summary of the ratio of phosphorylated AMPK to total AMPK in the EDL muscle of control and AICAR treated dKO mice, and control and AICAR treated mdx mice. *n* = 7 for dKO ctrl, dKO treat, mdx ctrl, and mdx treat; n=3 for wt.

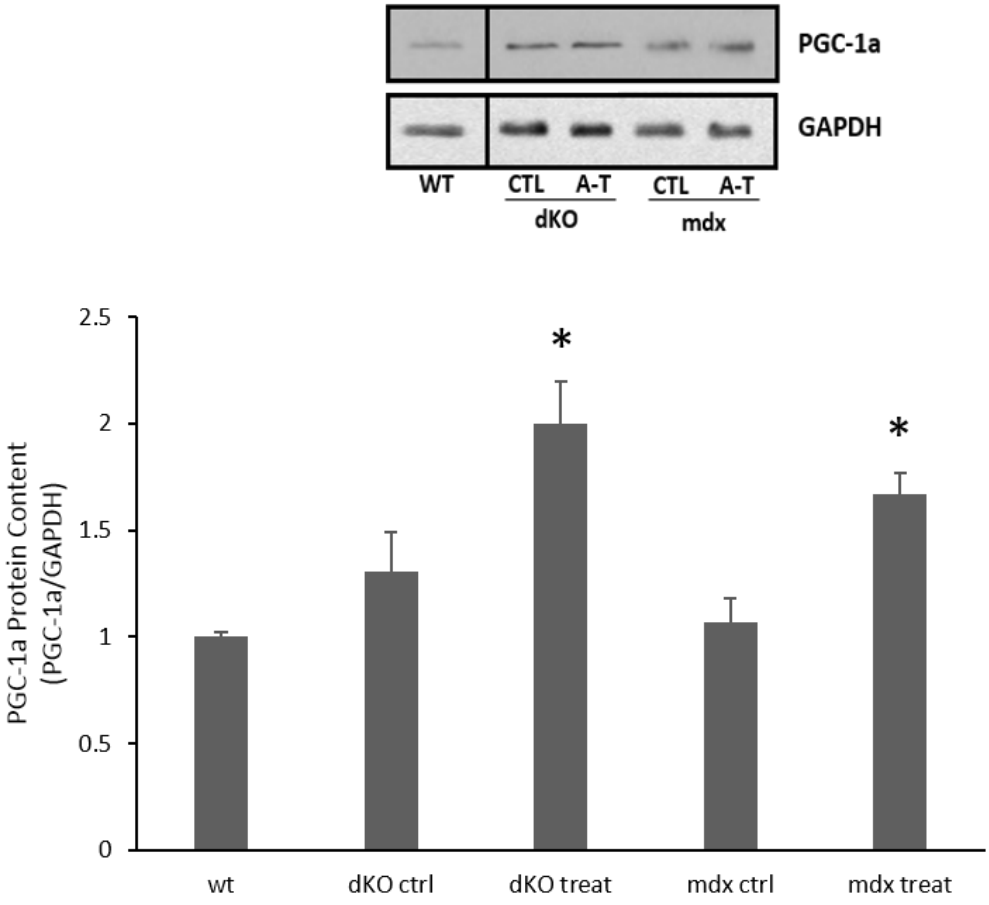

Figure 3.10: Expression of PGC-1a in fast, glycolytic muscles of AICAR treated mice. Representative western blots of PGC-1a and GAPDH, representative Ponceau S stain and graphical summary of PGC-1a protein content in the EDL muscle of control and AICAR treated dKO mice, and control and AICAR treated mdx mice. $n = 7$ for dKO ctrl, dKO treat, mdx ctrl, and mdx treat; n=3 for wt; * indicates significant difference compared to control groups and wt ($P < 0.05$).

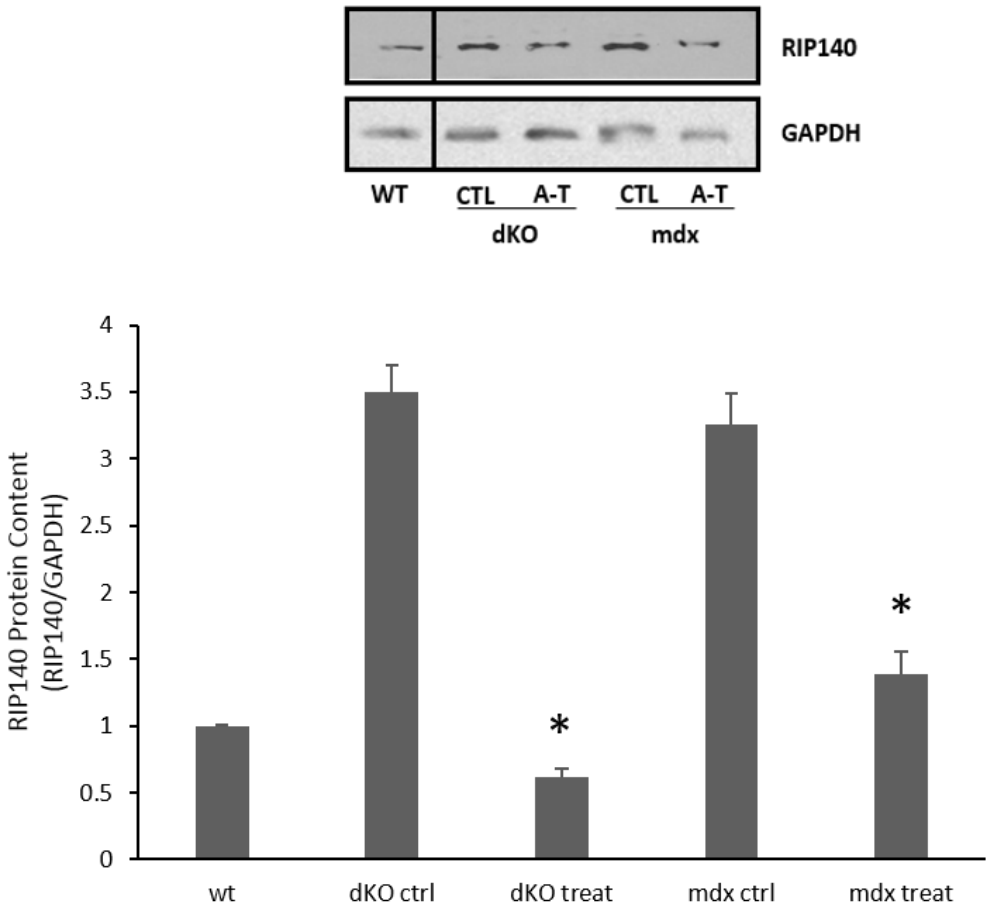

Figure 3.11: Expression of RIP140 in fast, glycolytic muscles of AICAR treated mice. Representative western blots of RIP140 and GAPDH, representative Ponceau S stain and graphical summary of RIP140 protein content in the EDL muscle of control and AICAR treated dKO mice, and control and AICAR treated mdx mice. $n = 7$ for dKO ctrl, dKO treat, mdx ctrl, and mdx treat; n=3 for wt; * indicates significant difference compared to control groups and wt ($P < 0.05$).

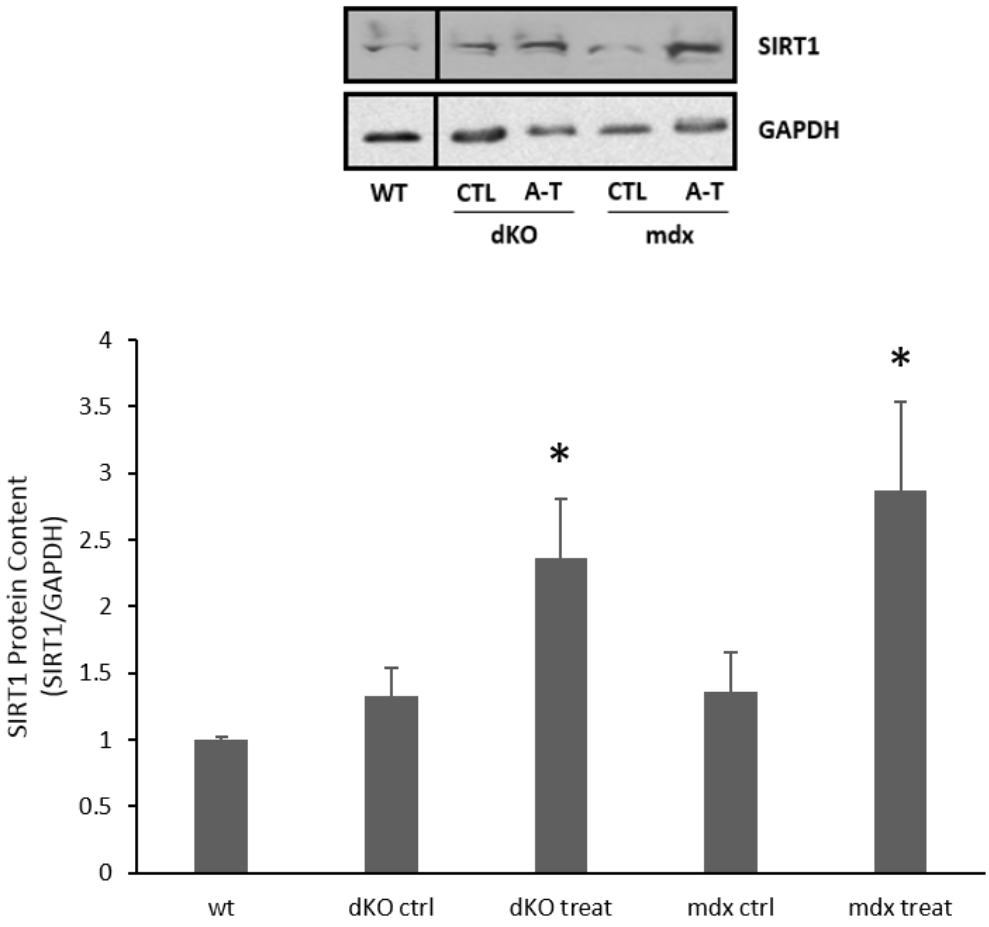

Figure 3.12: Expression of SIRT1 in fast, glycolytic muscles of AICAR treated mice. Representative western blots of SIRT1 and GAPDH, representative Ponceau S stain and graphical summary of SIRT1 protein content in the EDL muscle of control and AICAR treated dKO mice, and control and AICAR treated mdx mice. $n = 7$ for dKO ctrl, dKO treat, mdx ctrl, and mdx treat; n=3 for wt; * indicates significant difference compared to control groups and wt ($P < 0.05$).

3.2.2 AICAR treatment evokes a slower, more oxidative phenotype in the EDL of dKO and mdx mice

To determine whether the AICAR treatment successfully induced the slow, oxidative myogenic program, we analyzed markers of the slow, oxidative phenotype in the EDL muscle of wt, AICAR treated dKO and mdx mice, and control dKO and mdx mice.

The expression of oxidative phosphorylation (OXPHOS) complex proteins is a good marker of skeletal muscle oxidative capacity (100). AICAR treated dKO and mdx mice had significantly higher OXPHOS complex III and complex IV expression relative to control dKO and mdx mice ($P < 0.05$) (Figure 3.13 and Figure 3.14). The expression of cytochrome c, another important protein in oxidative phosphorylation, was significantly increased by 1.7-fold in both treated dKO and mdx mice compared to their control counterparts ($P < 0.05$) (Figure 3.15). There were no significant differences in expression of these molecules between the dKO and mdx mice, indicating that the AICAR treatment equally increased the oxidative capacity of both strains of mice.

We also measured the expression of important contractile proteins to identify and AICAR induced shift towards a slower-fiber type composition. Expression of the slow skeletal muscle isoform of troponin c was also significantly higher in AICAR treated dKO and mdx mice compared to control dKO and mdx mice ($P < 0.05$) (Figure 3.16). Using immunofluorescence, we found the ratio of MHC II A positive muscle fibers to the total number of fibers in the EDL muscle of AICAR treated dKO and mdx mice to be 1.4-fold higher than the same ratio in control dKO and mdx mice ($P < 0.05$) (Figure 3.17). In accordance with the muscle signaling changes seen in the previous section, the changes in expression of the phenotype indicators reported here suggest that the muscles of

both the dKO and mdx mice treated with AICAR shifted towards a more oxidative phenotype with greater expression of slow troponin c and MHC IIA.

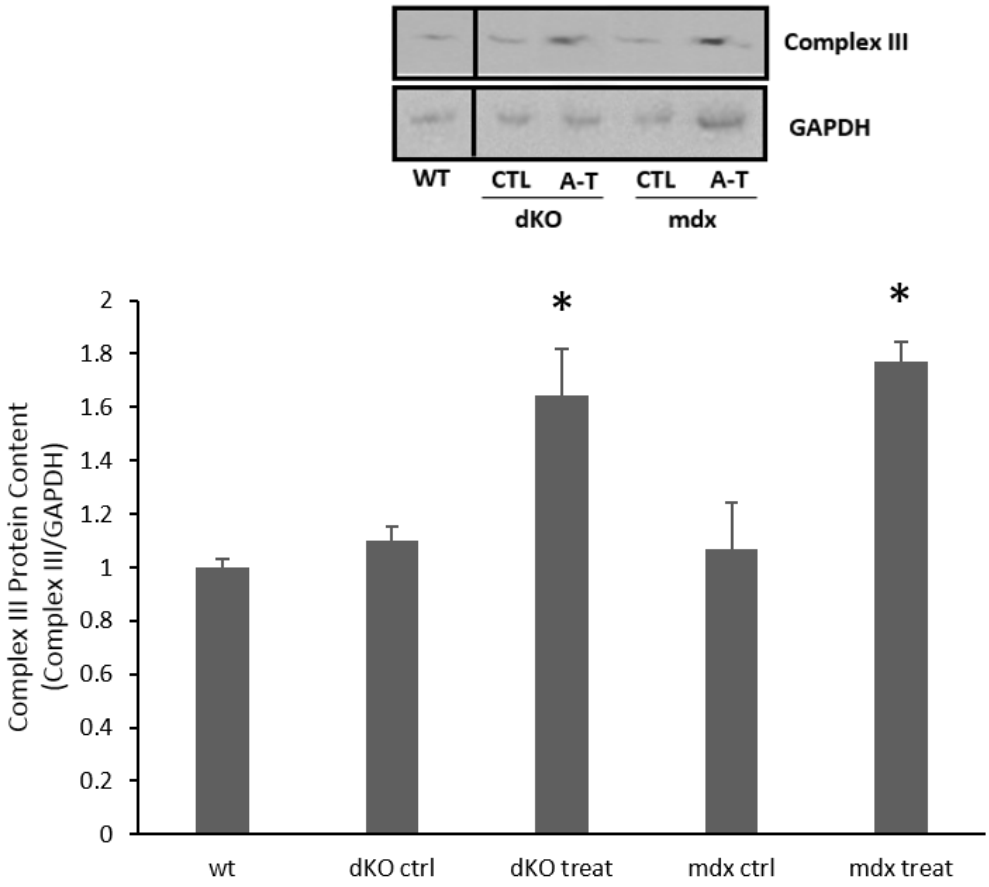

Figure 3.13: Expression of oxidative phosphorylation complex III in fast, glycolytic muscles of AICAR treated mice. Representative western blots of a complex III subunit and GAPDH, representative Ponceau S stain and graphical summary of complex III subunit protein content in the EDL muscle of control and AICAR treated dKO mice, and control and AICAR treated mdx mice. n = 7 for dKO ctrl, dKO treat, mdx ctrl, and mdx treat; n=3 for wt; * indicates significant difference compared to control groups and wt ($P < 0.05$).

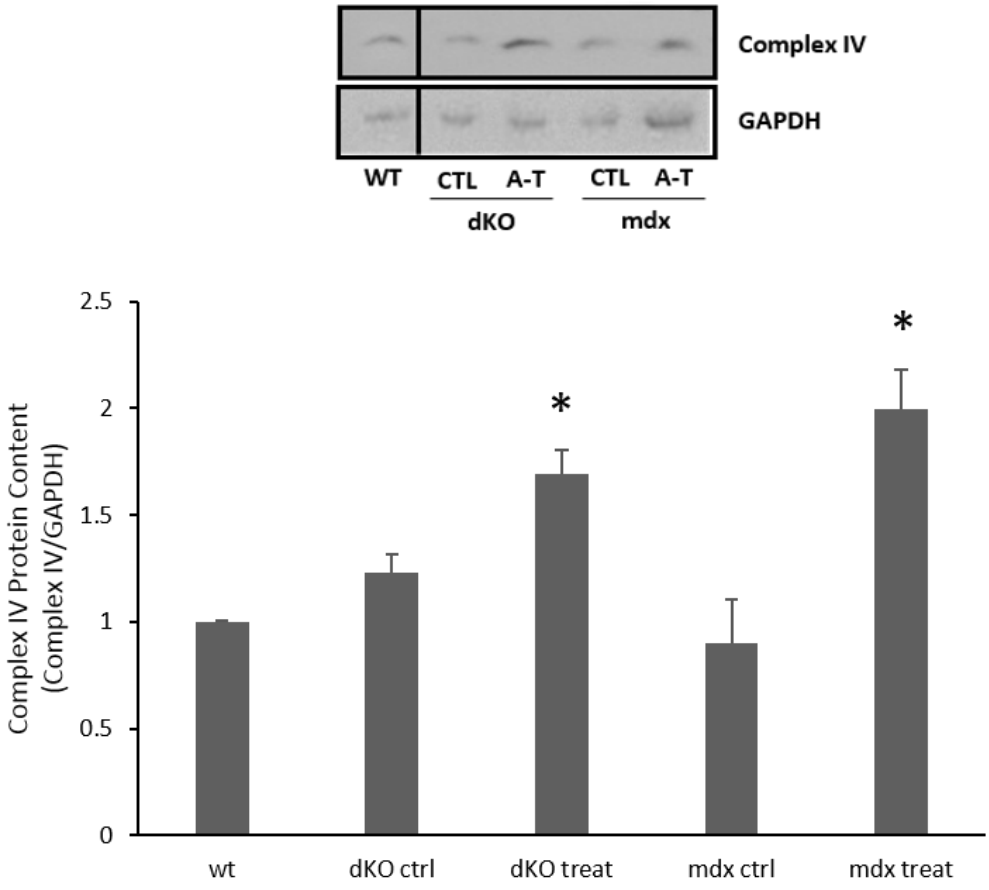

Figure 3.14: Expression of oxidative phosphorylation complex IV in fast, glycolytic muscles of AICAR treated mice. Representative western blots of a complex IV subunit and GAPDH, representative Ponceau S stain and graphical summary of complex IV subunit protein content in the EDL muscle of control and AICAR treated dKO mice, and control and AICAR treated mdx mice. n = 7 for dKO ctrl, dKO treat, mdx ctrl, and mdx treat; n=3 for wt; * indicates significant difference compared to control groups and wt ($P < 0.05$).

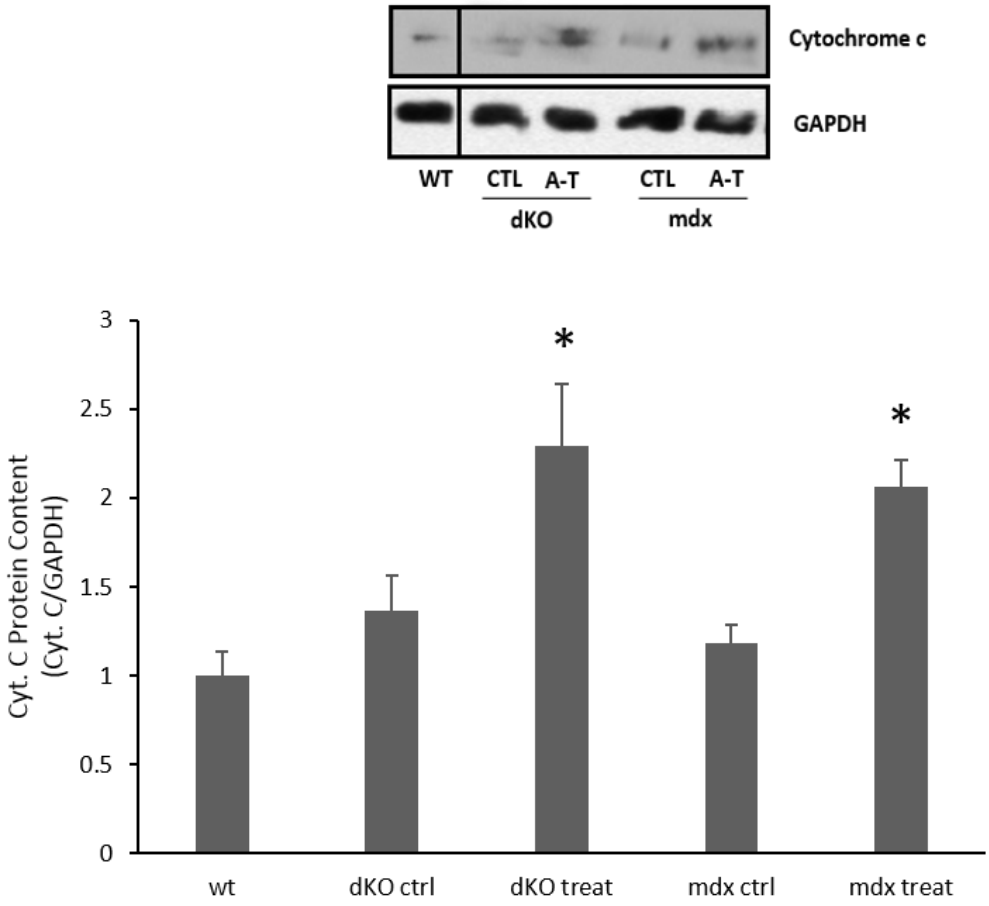

Figure 3.15: Expression of cytochrome c in fast, glycolytic muscles of AICAR treated mice. Representative western blots of cytochrome c and GAPDH, representative Ponceau S stain and graphical summary of cytochrome c protein content in the EDL muscle of control and AICAR treated dKO mice, and control and AICAR treated mdx mice. $n = 7$ for dKO ctrl, dKO treat, mdx ctrl, and mdx treat; n=3 for wt; * indicates significant difference compared to control groups and wt ($P < 0.05$).

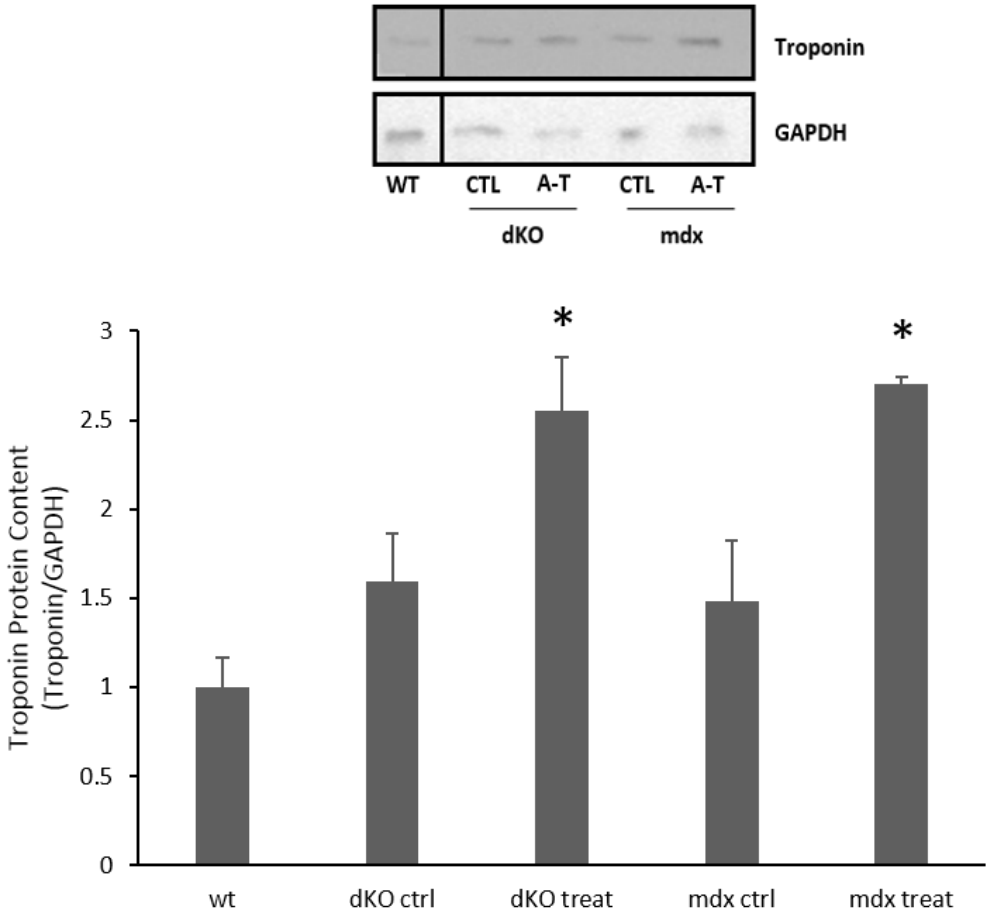

Figure 3.16: Expression of the slow isoform of troponin in fast, glycolytic muscles of AICAR treated mice. Representative western blots of troponin and GAPDH, representative Ponceau S stain and graphical summary of troponin protein content in the EDL muscle of control and AICAR treated dKO mice, and control and AICAR treated mdx mice. $n = 7$ for dKO ctrl, dKO treat, mdx ctrl, and mdx treat; n=3 for wt; * indicates significant difference compared to control groups and wt ($P < 0.05$).

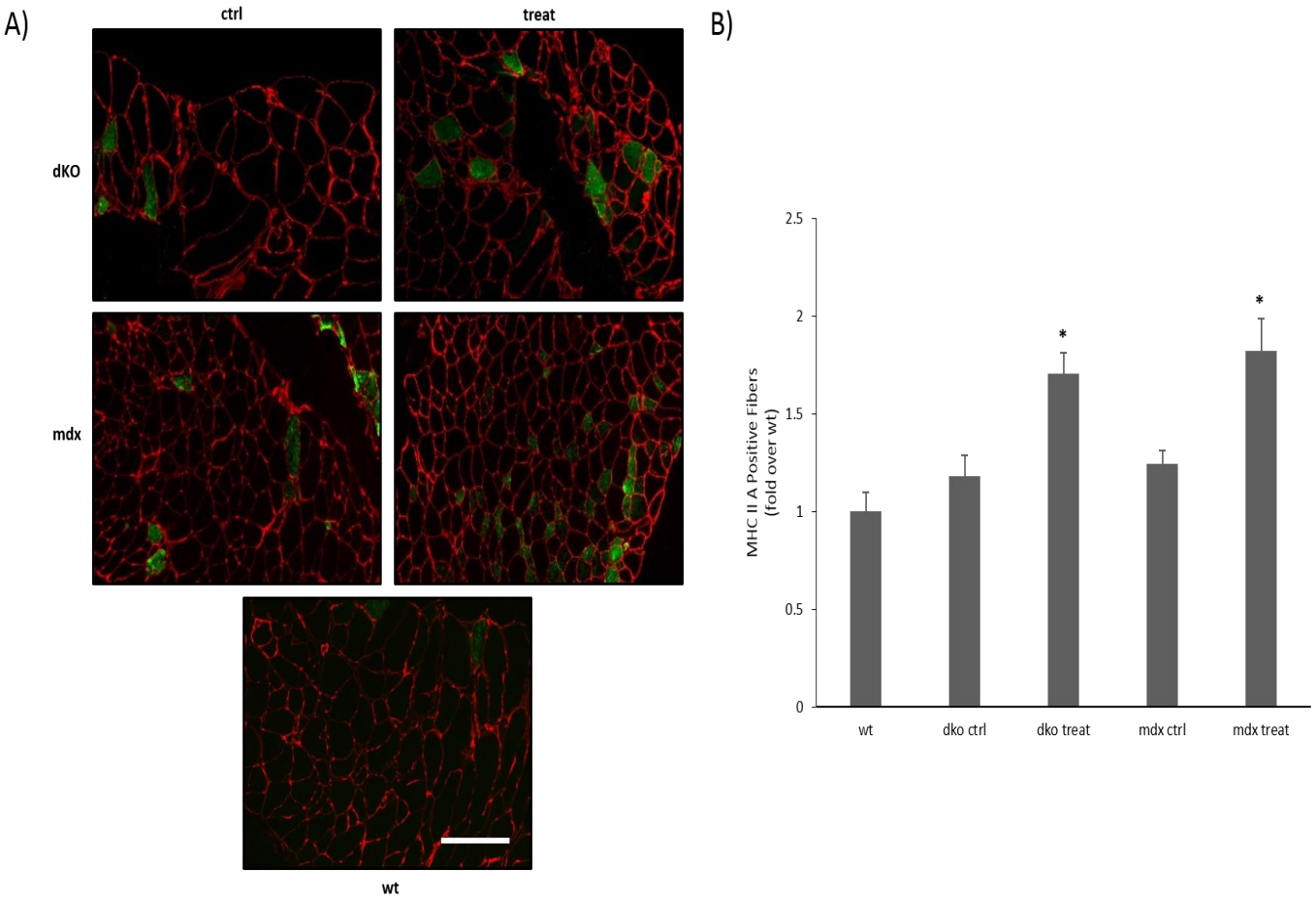

Figure 3.17: Expression of MHC IIa in fast, glycolytic muscles of AICAR treated mice. Representative micrographs of MHC IIa immunofluorescence (A) and graphical summary of MHC IIa positive fibers (B) in the EDL muscle of control and AICAR treated dKO mice, and control and AICAR treated mdx mice. $n = 7$ for dKO ctrl, dKO treat, mdx ctrl, and mdx treat; n=3 for wt; * indicates significant difference compared to control groups and wt ($P < 0.05$). Scale bar = 120 μm.

3.2.3 AICAR treatment increases utrophin And b-DG expression in fast, glycolytic muscle of mdx mice

An important aspect of the slow, oxidative phenotype in relation to DMD is the elevated expression of the dystrophin homolog, utrophin A (47,219). Using western blot analysis, we found that expression of utrophin A was increased by 1.9-fold in the fast, glycolytic TA muscle of AICAR treated mdx mice compared with control mdx mice ($P < 0.05$) (Figure 3.18). This increased expression was also seen with immunofluorescence. As expected, the dKO mice did not show any expression of utrophin A.

Chronic AMPK stimulation has been shown to induce reassembly of the DAPC along the myofiber membrane as a result of the elevated utrophin A expression (24,57,75,231). We evaluated the localization of β-dystroglycan (β-DG), a component of the DAPC, to verify that. We found that AICAR treatment resulted in 1.5-fold increase in β-DG fluorescence intensity in AICAR treated mdx mice compared to control mdx mice ($P < 0.05$), but, as expected, no such increase was seen in dKO mice (Figure 3.19).

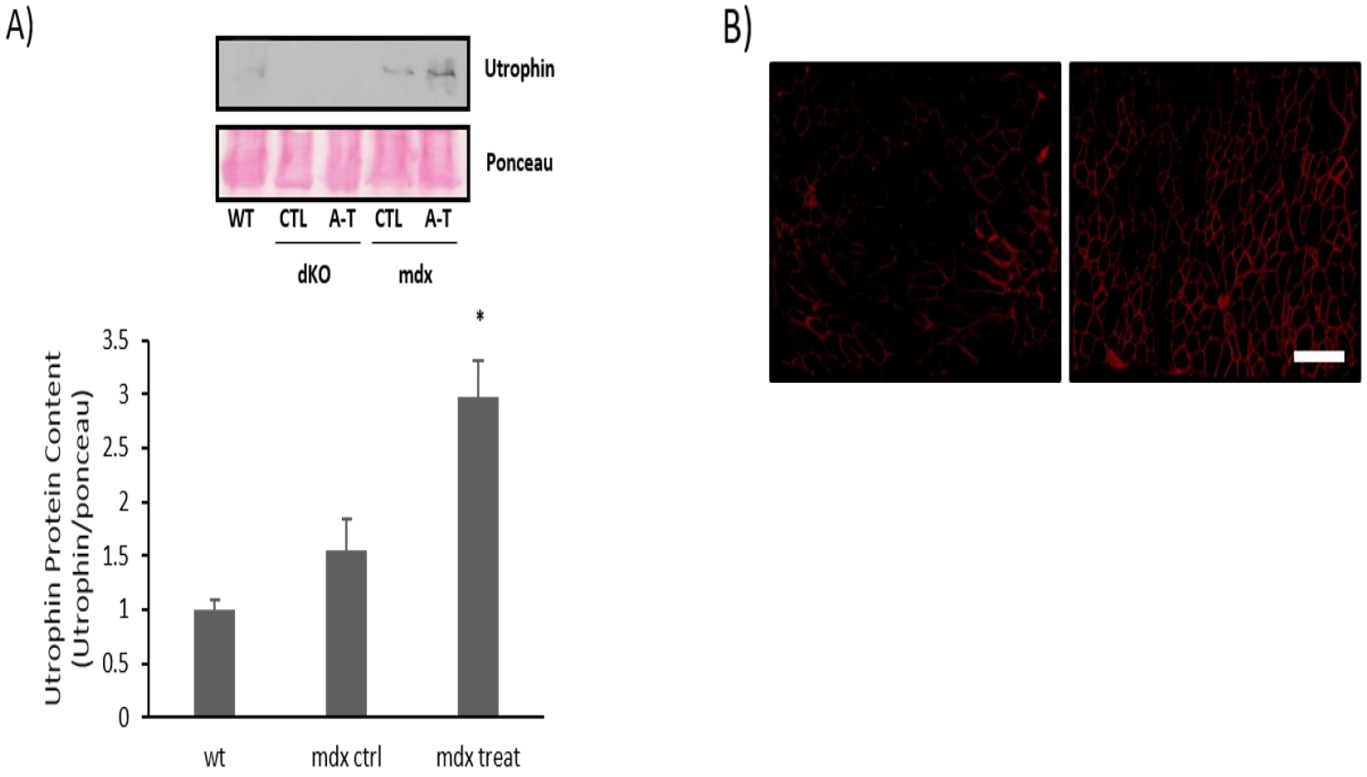

Figure 3.18: Expression of utrophin A in fast, glycolytic muscles of AICAR treated mice. Representative micrographs of utrophin expression (B) and western blots of utrophin A, representative Ponceau S stain, and graphical summary of utrophin A protein content (A) in the EDL muscle of control and AICAR treated mdx mice. $n = 7$ for dKO ctrl, dKO treat, mdx ctrl, and mdx treat; n=3 for wt; * indicates significant difference compared to control groups and wt ($P < 0.05$). Scale bar = 120 µm.

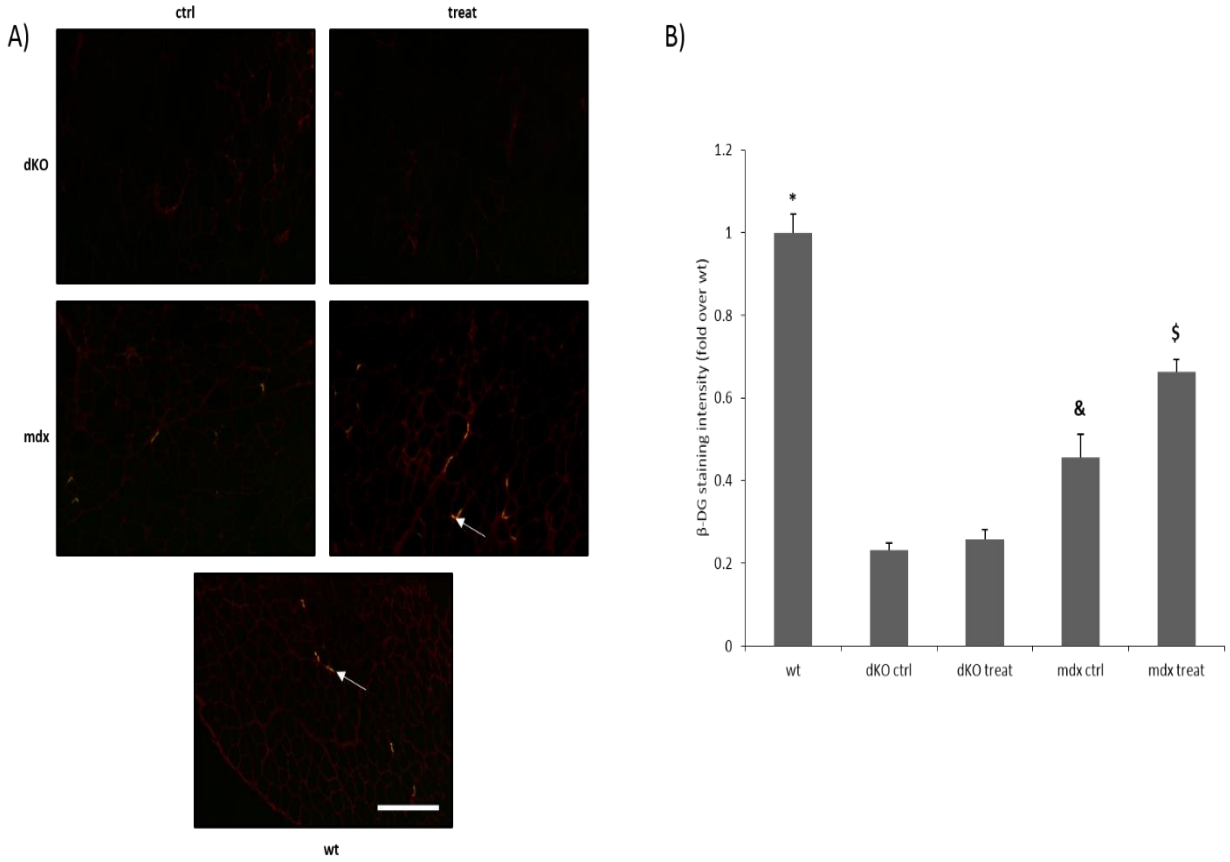

Figure 3.19: β-Dystroglycan expression and localization in fast, glycolytic muscles of AICAR treated mice. Representative micrographs (A) of β-Dystroglycan and α-bungarotoxin (arrows) immunofluorescence, indicating the location of neuromuscular junctions. Graphical summary (B) of the β-Dystroglycan staining intensity in the EDL muscle of control and AICAR treated dKO mice, and control and AICAR treated mdx mice. $n = 7$ for dKO ctrl, dKO treat, mdx ctrl, and mdx treat; n=3 for wt. * indicates significant difference compared to all other groups ($P < 0.05$), & indicates significant difference compared to dKO ctrl and dKO treat ($P < 0.05$), $ indicates significant difference compared to mdx ctrl ($P < 0.05$). Scale bar = 160 μm.

3.2.4 AICAR treatment enhances sarcolemmal integrity of fast, glycolytic muscles in mdx mice, but not dKO mice

To assess the benefits that the more oxidative, possibly slower phenotype bestowed on the dKO and mdx mice, we measured several markers of myofiber integrity and function. We quantified the degree of myofiber central nucleation in the EDL muscle as an indicator of the amount of damage and regeneration occurring in the muscle. The ratio of fibers with centralized nuclei to total number of fibers was significantly lower in wt mice compared to mdx and dKO mice ($P < 0.05$). The ratio was also significantly lower in mdx mice compared to dKO mice, as expected ($P < 0.05$). AICAR treatment did not reduce the ratio of centrally nucleated fibers in dKO mice, but resulted in a 40 % reduction in central nucleation in mdx mice ($P < 0.05$) (Figure 3.20).

To further understand the effect of chronic AICAR treatment on the structural integrity of the sarcolemma, we performed immunoglobulin M (IgM) immunofluorescence on EDL cryosections. While it is normally extracellular, IgM can penetrate and accumulate in muscle fibers that have a damaged sarcolemma (50,236). The ratio of IgM stained fibres to the total number of fibres of the EDL of AICAR treated mdx mice was 28 % lower than control mdx mice ($P < 0.05$), and the wt mice had the lowest ratio of IgM stained fibres at 74 % lower than AICAR treated mdx mice ($P < 0.05$) (Figure 3.21). On the other hand, the ratio of IgM stained fibers in AICAR treated dKO and control dKO mice was unchainged and was significantly higher than all other groups.

3.2.5 AICAR treatment increases forelimb muscle strength in mdx mice, but not dKO mice

To quantify the degree of functional improvement in AICAR-treated mice, as has been done in previous studies, we observed the decline in maximal tetanic tension in the EDL muscles during repetitive electrically stimulated eccentric contractions (ECs) *ex vivo* (50,87,144). The decline in force output is correlated with the amount of damage sustained by the muscles during the ECs (50,87,144). After the 12th EC, the wt mouse force maintenance was significantly higher than the other groups, and the AICAR treatment did not result in an improved force maintenance in either the dKO or mdx mice (Figure 3.23).

During, the EC protocol, the muscles were bathed in 0.1% trypan blue solution, which penetrates into the cytosol of myocytes with a damaged sarcolemma. Observing the extent of trypan blue staining in the muscle fibers allows us to determine the susceptibility of the muscle to sarcolemmal damage caused by the ECs. Following the EC procedure, the trypan blue fluorescence intensity in non-peripheral EDL myofibers of wt mice was lower than in all the other groups, and was 30 % less than the fluorescence in AICAR treated mdx mice ($P < 0.05$) (Figure 3.22). The trypan blue fluorescence in AICAR treated mdx mice was, in turn, 30 % lower than control mdx mice ($P < 0.05$). Finally, the trypan blue fluorescence in AICAR treated and control dKO mice was the same, and was significantly higher than the trypan blue fluorescence in all other groups.

As has been shown in previous studies, the forelimb grip test is a good indicator of forelimb muscle strength. It has been shown that mdx mice have a reduced forelimb muscle strength compared to wt mice, so we wanted to assess whether or not AICAR treatment improves their forelimb muscle strength (237). Wt mouse forelimb grip strength was significantly higher than all of the other groups ($P < 0.05$). AICAR treated mdx mice had a significant increase in grip strength by 16 % compared to controld mdx mice ($P < 0.05$), while AICAR treated dKO mice showed no increase

in forelimb grip strength compared to control dKO mice (Figure 3.24A). Since we found significant differences in bodyweight between wt, mdx, and dKO mice, we normalized the forelimb grip strength to body weight. The results after normalization show that control mdx mice do not have a significantly higher forelimb force production than AICAR treated or control dKO mice, but the AICAR treated mdx mice force production remains significantly higher than that of control mdx mice ($P < 0.05$) (Figure 3.24B).

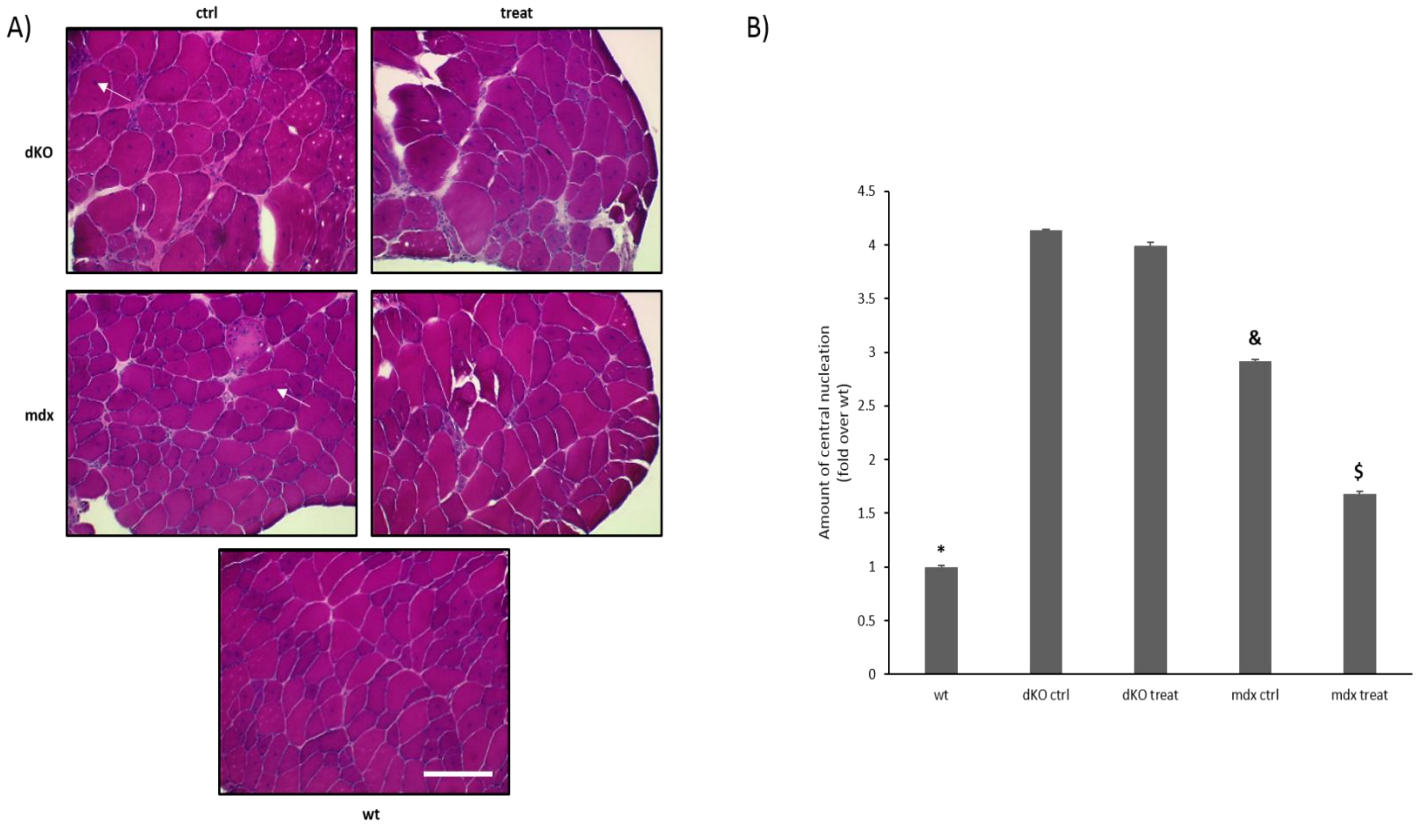

Figure 3.20: The extent of central nucleation in fast, glycolytic muscles of AICAR treated mice. Representative micrographs (A) and graphical summary (B) of the ratio of centrally nucleated (arrows) fibers in the EDL muscle of control and AICAR treated dKO mice, and control and AICAR treated mdx mice. $n = 7$ for dKO ctrl, dKO treat, mdx ctrl, and mdx treat; n=3 for wt. * indicates significant difference compared to all other groups ($P < 0.05$), & indicates significant difference compared to dKO ctrl and dKO treat ($P < 0.05$), $ indicates significant difference compared to mdx ctrl ($P < 0.05$). Scale bar = 120 μm.

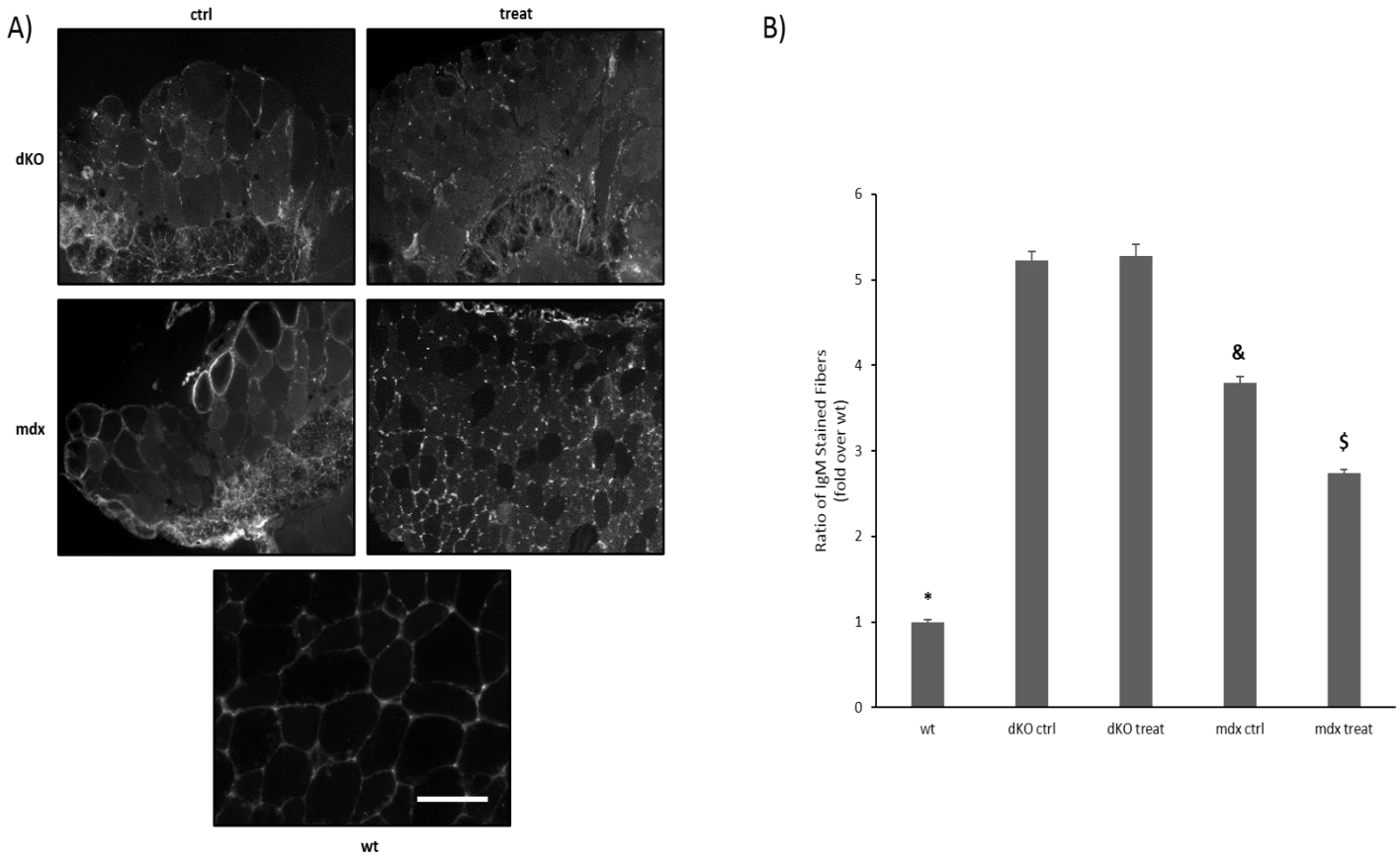

Figure 3.21: IgM intramyocellular protein localization in fast, glycolytic muscles of AICAR treated mice. Representative micrographs (A) and graphical summary (B) of the ratio of IgM stained fibers in the EDL muscle of control and AICAR treated dKO mice, and control and AICAR treated mdx mice. n = 7 for dKO ctrl, dKO treat, mdx ctrl, and mdx treat; n=3 for wt. * indicates significant difference compared to all other groups ($P < 0.05$), & indicates significant difference compared to dKO ctrl and dKO treat ($P < 0.05$), $ indicates significant difference compared to mdx ctrl ($P < 0.05$). Scale bar = 120 μm.

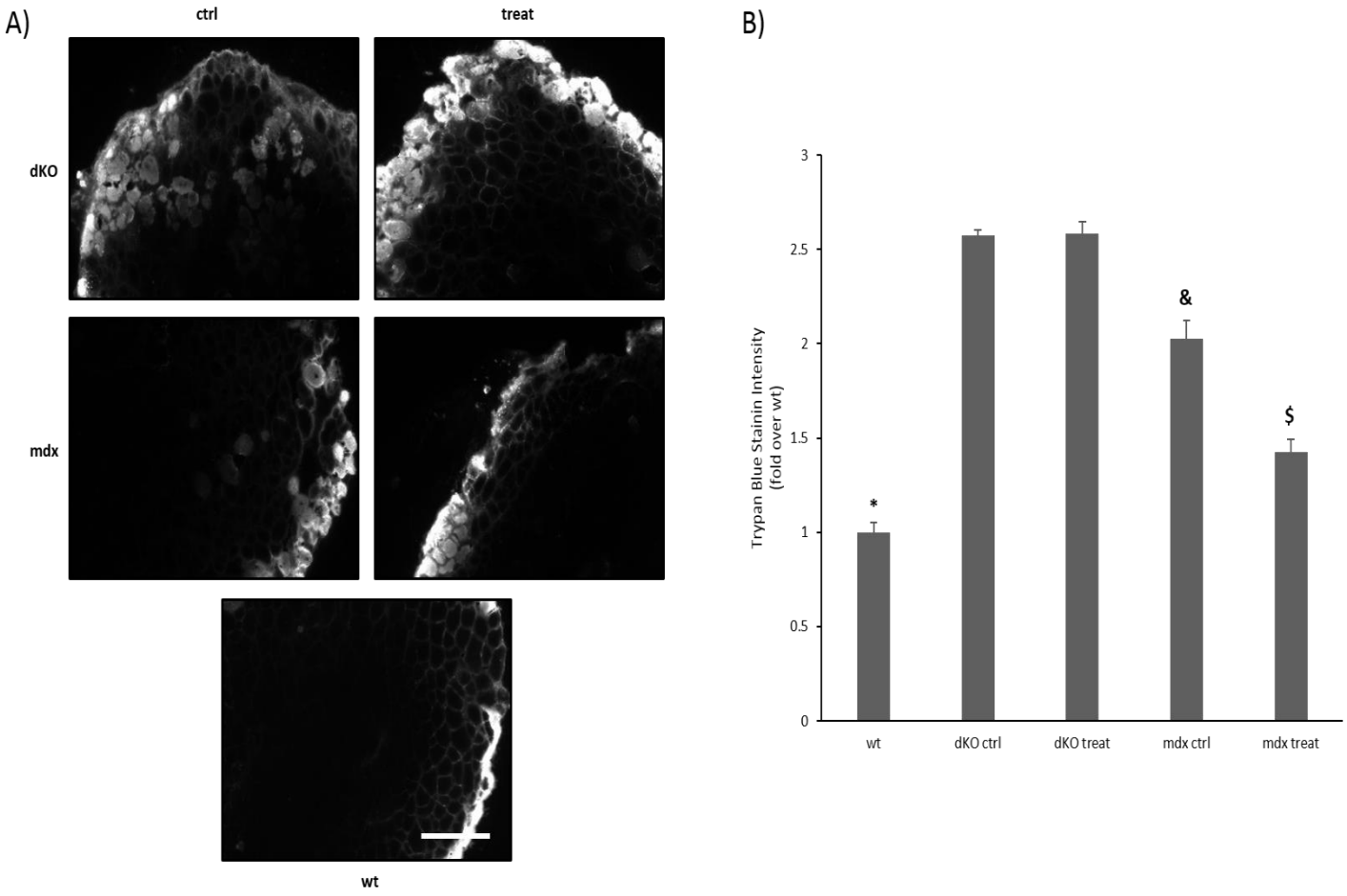

Figure 3.22: Extent of damage from *ex vivo* eccentric contractions in fast, glycolytic muscles of AICAR treated mice. Representative micrographs (A) and graphical summary (B) of the intensity of trypan blue staining in non-peripheral fibers of the EDL muscle of wt, control and AICAR treated dKO mice, and control and AICAR treated mdx mice. n = 3-4. * indicates significant difference compared to all other groups ($P < 0.05$), & indicates significant difference compared to dKO ctrl and dKO treat ($P < 0.05$), $ indicates significant difference compared to mdx ctrl ($P < 0.05$). Scale bar = 160 µm.

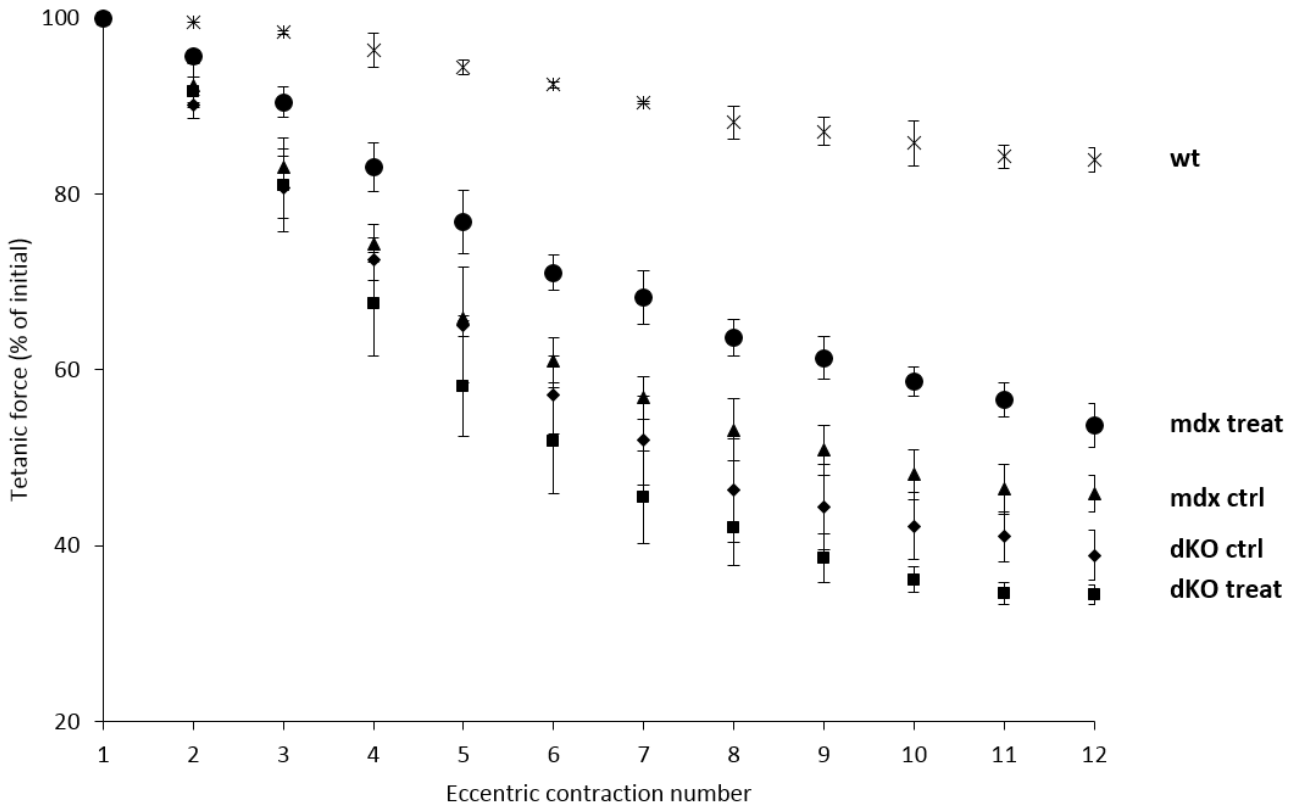

Figure 3.23: *ex vivo* skeletal muscle performance of fast, glycolytic muscles of AICAR treated mice. Graphical representation of maximal tetanic force development, expressed as a percentage of the initial contraction in the EDL muscle of wt, control and AICAR treated dKO mice, and control and AICAR treated mdx mice during twelve electrically stimulated eccentric contractions. n = 3-4; *$P < 0.05$.

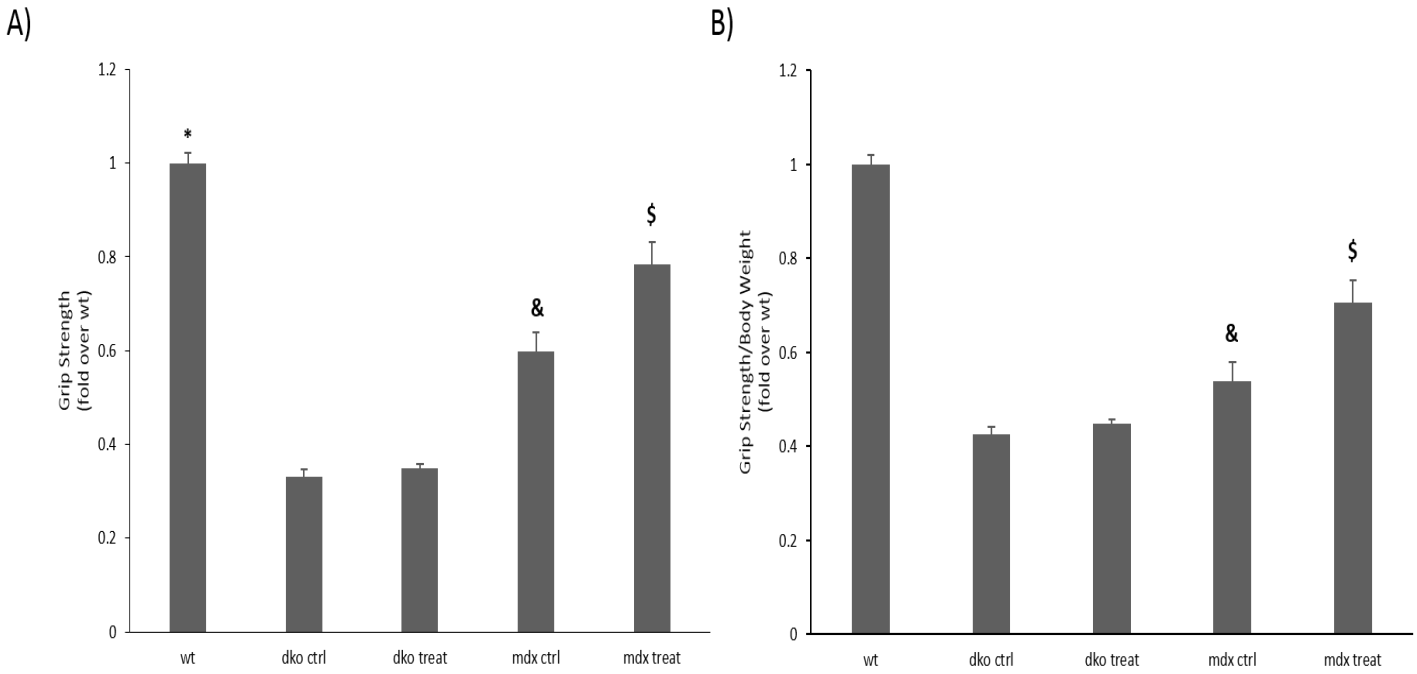

Figure 3.24: Forelimb strength in AICAR treated mice. (A) Graphical summary of the average peak force produced by wt, control and AICAR treated dKO mice, and control and AICAR treated mdx mice in the forelimb grip strength test. (B) Graphical summary of the average peak force normalized to body weight produced by wt, control and AICAR treated dKO mice, and control and AICAR treated mdx mice in the forelimb grip strength test. n = 3-4. * indicates significant difference compared to all other groups ($P < 0.05$), & indicates significant difference compared to dKO ctrl and dKO treat ($P < 0.05$), $ indicates significant difference compared to mdx ctrl ($P < 0.05$).

4: DISCUSSION

At the outset of this project, we hypothesized that the benefits of the slow, oxidative myogenic program to mdx mice are directly related to utrophin A. As a result, we predicted that the slow, oxidative myogenic program would result in improved muscle morphology and function in mdx mice, but not in dKO mice. Our results support our hypothesis. Both the dKO and mdx mouse skeletal muscles showed increased expression of important, phenotype shifting signaling molecules like PGC-1a and SIRT1after AICAR treatment. This was accompanied by an increase in expression of oxidative phosphorylation proteins, slow troponin c, and MHC IIA. However, only the strain that expressed utrophin A showed increased resistance towards dystrophy, as indicated by multiple tests of muscle morphology and function. Clearly, the main point of difference between the two strains, the absence of utrophin A in the dKO mice, plays a role in their different responses to the shift in phenotype. This result confirms utrophin As a valid, and important therapeutic target for DMD.

4.1 Skeletal muscles of dKO and mdx mice have the same signaling capacity

Mammalian skeletal muscle has a variety of fiber types with different contractile and metabolic properties. Under natural conditions, the fiber type profile of skeletal muscles is determined by the type of activity they are needed to perform (4). Different forms of activity are associated with different patterns of neural firing (1-3). Specifically, brief bursts of neural activity between long periods of neuronal quiescence, trigger a fast, glycolytic fiber profile, while extended periods of tonic motor nerve activity trigger a shift towards slow, oxidative fibers. This change in fiber-type is controlled by specific signaling pathways, and research into these signaling pathways has led to the discovery of several signaling proteins that are capable of inducing muscle plasticity and fiber type changes. These proteins include calcineurin (CN), peroxisome proliferator-activated receptor (PPAR) γ coactivator 1α (PGC-1α), PPARβ/δ, AMP-activated protein kinase (AMPK), silent mating type information regulator 2 homologue 1 (SIRT1), receptor-interacting protein 140 (RIP140), and E2F transcription factor 1 (E2F1) (5). Considering the focus of this project on muscle phenotype shifting, it was imperative for us to understand the levels and patterns of expression of some of these important, phenotype modifying signaling proteins in the dKO mice relative to the mdx mice.

Our results show that dKO and mdx mice have a similar pattern of expression of several important muscle signaling proteins. The activation of AMPK was shown to be higher in the slow, oxidative soleus muscle compared to the fast, glycolytic EDL in the mdx mouse. This parallels what has been previously seen in our lab and in the literature (7,8). We also showed this same result in the dKO mouse. AMPK is an important regulator of energy metabolism, exerting control over key systems such as glucose uptake and beta oxidation of fatty acids (9-11). With its involvement in

the upregulation of slow, oxidative functions, the higher AMPK activation in the slow, oxidative soleus muscle compared to the fast, glycolytic EDL was expected (12).

Since AMPK is known to interact with several other molecules to affect muscle phenotype, including PGC-1a and SIRT1, we also measured their expression, and found it to be elevated in the soleus muscle compared to the EDL in both dKO and mdx mice (13). As a promoter of mitochondrial biogenesis (14,15), it was not surprising to see PGC-1a expressed at higher levels in the soleus. Also, PGC-1a has previously been shown to have higher expression in slow, oxidative muscles compared to fast, glycolytic ones (16-18).

Similarly, our data for SIRT1 matches the expression pattern that has been documented in the past in rodents (19,20). SIRT 1 has been implicated in promotion of the oxidative phenotype, so its higher expression in the soleus of dKO and mdx mice is expected (21,22). On the other hand, Rip140 expression was higher in the EDL compared to the soleus in both dKO and mdx mice. This pattern of expression is in agreement with the role of RIP140, which promotes the fast, glycolytic myogenic program and/or repress the slow, oxidative phenotype (23,24). This result has also been shown previously (25,26). To our knowledge, for all of the phenotypic modifiers mentioned above, we were the first to document their expression in dKO mice and compare it to the expression in mdx mice. It was noteworthy that dKO mice had the same expression levels of these molecules as mdx mice, indicating that they have similar signaling capacities and are capable of modifying muscle phenotype to a similar extent. In addition, these results indicate that dystrophin and utrophin have little impact on the expression of these signaling molecules.

4.2 Skeletal muscles of dKO and mdx mice have the same phenotypic capacity

Slow, oxidative and fast, glycolytic skeletal muscles differ from each other in multiple ways including contractile physiology, metabolic capabilities, morphology, and fatigue resistance. It has become common knowledge that this specialization is important, so research has identified ways to distinguish these muscle types including the presence of specific contractile proteins and the level of expression of certain metabolic enzymes (27-29). Fast, glycolytic muscle fibers have low mitochondrial content, ranging from 1 to 3% of the total cellular volume, while oxidative muscle fibers have much greater mitochondrial content, and as a result higher expression of oxidative phosphorylation proteins (30). The contractile physiology of these muscles is also different and is a result of the expression of different contractile apparatus proteins, like different isoforms of troponin c and the myosin ATPase. In addition, fast-twitch fibers can be further classified as they show large variations in mitochondrial content and express a variety of myosin ATPase, including type IIa and IIb, (31-34).

To further characterize the dKO mice and compare their muscle phenotype to that of mdx mice, we measured at the expression of cytochrome c, slow troponin, and myosin heavy chain I and II A in their fast and slow muscles. All of these phenotype indicators, except MHC II A, displayed higher expression in the soleus than the EDL, and showed no differences between the two strains. Cytochromce c plays an important role in oxidative phosphorylation, residing on the inner membrane of the mitochondrion and shuttling electrons between oxidative phosphorylation complexes III and IV (35,36). Since the soleus is an oxidative muscle, cytochrome c expression

was expected to be higher in the soleus compared to the EDL in both strains of mice. In addition, the slow contraction kinetics of the soleus are a manifestation of its contractile apparatus, which includes more of the slower myosin heavy chain, MHC I, and other slow contractile proteins such as slow troponin c type 1 (37,38). Therefore, our results indicating a greater amount of MHC I, MHC II A, and slow troponin in dKO and mdx soleus muscles compared to their EDL muscles were in line with expectations.

This characterization of the dKO mice as having a similar oxidative capacity and contractile apparatus to mdx mice is important. An already slower, more oxidative phenotype in the dKO, would block complementary signaling that activates the slow, oxidative myogenic program (49). Since we showed that dKO mice have a similar muscle signaling capacity and phenotype to mdx mice, it increases the probability that if we treated both strains of mice with AICAR, under the same conditions, they will respond similarly.

4.3 Chronic AICAR treatment activates signaling pathways that are associated with the slow, oxidative myogenic program in dKO and mdx mice

We have already mentioned that slow, oxidative muscle fibers in DMD patients and animal models are more resistant to the dystrophic pathology than the fast, glycolytic fibers (41,42). Therefore, the idea that the slow, oxidative myogenic program provides morphological and functional benefits in muscular dystrophy has been raised by our lab (24, 43-50) and others (51-61). One of the most powerful factors that has been identified to stimulate skeletal muscle plasticity and have specific agonists is AMPK (48). AMPK has been described as an important integrator of cell signaling pathways that mediate phenotypic plasticity within the context of dystrophic skeletal muscle, so we sought to activate the slow, oxidative myogenic program in our dKO and mdx mice through it. Perhaps the most-studied pharmacological stimulator of AMPK is 5-aminoimidazole-4-carboxamide-1-β-D-ribofuranoside (AICAR). Chronic pharmacological AMPK stimulation via systemic AICAR administration elicits robust phenotypic plasticity, such as fast to slow myosin isoform shifts, mitochondrial biogenesis, increased glycogen storage, augmented PGC-1a, PPARb/d and glucose transporter type 4 expression, enhanced insulin sensitivity, and improved exercise performance [62-65].

AICAR induces the slow, oxidative myogenic program by increasing the activity/phosphorylation of AMPK (48). After chronic AICAR treatment, the phosphorylation levels of AMPK were not increased significantly in both dKO and mdx mice, though a trend towards increased phosphorylation was present (Table 4.1). Out lab has previously shown that chronic AICAR treatment increases AMPK phosphorylation in mdx mice (24). The absence of increased phosphorylation in our data can be due to several reasons, including the amount of time elapsed

between the injection of the mice with AICAR and their dissection on the final day of treatment. It is possible that our mice were culled and dissected before the AICAR treatment produced an effect on that day. Also, it has been shown that once a phenotype shift is induced pharmacologically in dystrophic muscles, it prevents subsequent, complementary changes in signaling (49). It is possible that once a slow, oxidative phenotype is expressed, subsequent AICAR injections stopped producing an increase in AMPK phosphorylation. However, since AICAR is known to induce phosphorylation mediated changes in the expression of proteins associated with slower, more oxidative muscle fibers, we measured the expression of these downstream targets to determine the impact of AICAR on our mice (Figure 1.3). We saw increases in PGC-1a and SIRT1 expression, as well as a reduction in RIP140 expression in the EDL muscles of dKO and mdx mice (Table 4.1). These changes indicate that the AICAR treatment was indeed inducing increased activity of AMPK.

The increase in PGC-1a expression after AICAR treatment has been shown before in mdx mice (24). We showed that dKO mice react in a similar manner to AICAR treatment, as their expression of PGC-1a was also increased. AMPK can increase PGC-1a expression through phosphorylation of transcription factors like MEF2, which is known to promote PGC-1a gene expression (17,18,66) (Figure 1.3). In addition, AMPK can phosphorylate PGC-1a directly, increasing its activity, and can indirectly protect it from degradation through its influence on NADH levels, which mediate NADH quinone oxidoreductase 1 (NQO1) inhibition of PGC-1a degradation (66). As mentioned earlier, PGC-1a promotes a slow, oxidative muscle phenotype through coactivation of nuclear receptors and other transcription factors (18,67) (Figure 1.3). PGC-1a is also implicated in direct regulation of the mitochondrial genome through the mitochondrial transcription factor A (Tfam) (68). Increased expression of PGC-1a via AMPK activation has been correlated with upregulation

of various proteins associated with the slow, oxidative phenotype, including utrophin A, cytochrome *c* and COX IV (24). As well, PGC-1α affects itself in a positive autoregulatory fashion, and has been shown to convert fast, glycolytic type II B muscle fibers to mitochondria rich type I and II A fibers (18, 24).

Studies have revealed that AMPK and PGC-1a do not act alone. Rather, they act through a web of intracellular signaling that also involves SIRT1 to evoke a slow, oxidative myogenic program (69) (Figure 1.3). Therefore, the upregulation of SIRT1 concomitantly with increased AMPK activity and increased PGC-1a expression after AICAR treatment is expected. This result is in agreement with what has previously been shown in mdx mice (24). In dKO mice, we saw the same increase in SIRT1 expression, showing that they similarly respond to pharmacological activation of AMPK. SIRT1 uses NAD+ as a cofactor, meaning its activity is modulated by NAD+/NADH, which is directly affected by the activation of AMPK (20). Through deacetylation, SIRT1 regulates a host of transcription factors and co-regulators that influence many cellular functions (20). This includes SIRT1's deacetylation of PGC-1α. Deacetylated PGC-1α is thought to be a more active form, as the deacetylation facilitates its incorporation into protein complexes at promoter regions, increasing transcription of several genes associated with the slow, oxidative myogenic program (69). The effects of the AMPK-PGC-1a-SIRT1 web, however, can be counteracted by RIP140, which has been shown to induce expression of genes associated with the fast, glycolytic phenotype (24).

RIP140 is powerful phenotypic modifier in skeletal muscle (23). By acting as a scaffold protein between nuclear receptors and chromatin remodeling enzymes that promote transcriptional repression, it can reduce mitochondrial enzyme gene expression (70). RIP140 has also been reported to interact directly with and inhibit the activity of PGC-1 (71) (Figure 1.3). Transgenic

RIP140 mice have reduced mitochondrial enzyme activity and significantly lower expression of genes associated with the slow, oxidative phenotype, while RIP140 null mice have increased oxidative capacity and a greater proportion of the slower MHC type II A expressing skeletal muscle fibers (23). Therefore, in order for AICAR to induce a slow, oxidative phenotype, RIP140 expression must be reduced, so our results are in line with expectations. It is also consistent with other studies which showed that chronic AMPK activation by various means significantly down-regulated RIP140 expression in the muscles of rodents, including mdx mice (24,72). In dKO mice, we saw the same decrease in RIP140 expression, which, combined with the increased PGC-1a and SIRT1 expression, indicates that they will, like mdx mice, express the slow, oxidative myogenic program in response to AICAR treatment (24) (Table 4.1).

Table 4.1: The effects of AICAR treatment on the activation and/or expression of important phenotype shifting singaling molecules in the fast, glycolytic muscles of dKO and mdx mice.

Signaling molecule	dKO-AICAR	mdx-AICAR
P-AMPK	unchanged	unchaged
PGC-1a	Up 50%	Up 60%
SIRT1	Up 70%	Up 90%
RIP140	Down 80%	Down 70%

4.4 Chronic AICAR treatment induces a more oxidative, possibly slower phenotype in dKO and mdx mouse skeletal muscles

In the slow, oxidative myogenic program, increased oxidative capacity is brought on mainly through mitochondrial adaptations that are generally referred to as `mitochondrial biogenesis' (68). Mitochondrial biogenesis in muscle can mean either or both of the following changes: increased in mitochondrial content per gram of tissue and/or changed mitochondrial composition, such increased amounts of mitochondrial proteins (73). This increase in mitochondrial biogenesis can be determined through observation of cytochrome c and cytochrome *c* oxidase (COX) subunits (74,75). The slower phenotype that is also part of the slow, oxidative myogenic program can be characterized through observation of members of the contractile apparatus, like troponin c, the myosin ATPase.

With the upregulation of important promoters of the slow, oxidative myogenic program, and the downregulation of the fast, glycolytic phenotype promoter RIP140, we expected to see an increase in indicators of the slow, oxidative phenotype. Indeed, our results showed that there was a significant increase in the oxidative phosphorylation proteins cytochrome c, cytochrome oxidase complex III, and cytochrome oxidase complex IV in the EDL of AICAR treated mice, indicating increased oxidative capacity in the fast, glycolytic muscles of AICAR treated mice (Table 4.2). This increase in oxidative phosphorylation has been documented before, with a significant increase in cytochrome oxidase IV activity shown by Ljubicic et al. (24).

There was also a shift towards a slower phenotype, as the EDL muscles of AICAR treated mice showed an increase in expression of slow troponin c type 1. In addition, they had a higher number

of fibers expressing MHC II A. Troponin c type 1 is an isoform of troponin c that is coded by the *TNNC1* gene and expressed in cardiac and slow skeletal muscle, so its increase indicates development of a slower phenotype (76). MHC II A is the MHC-a isoform with the slowest contraction velocity (Vmax), so a greater number of fibers expressing it could also indicate a shift towards a slower phenotype (77). Overall, these results show, as expected, that chronic AICAR treatment induced an oxidative, possibly slower phenotype in the skeletal muscles of mdx mice, which is in agreement with the literature. Importantly, and as expected from our results showing increased in expression of signaling molecules that promote the slow, oxidative myogenic program, we showed that dKO mice are also capable of expressing a slower, more oxidative skeletal muscle phenotype when treated with the appropriate pharmacological agents (Table 4.2).

Table 4.2: The effects of AICAR treatment on the expression of important phenotype indicators in the fast, glycolytic muscles of dKO and mdx mice.

Phenotype indicator	dKO-AICAR	mdx-AICAR
Oxidative proteins		
Cytochrome c	Up 70%	Up 70%
Cytochrome oxidase III	Up 50%	Up 60%
Cytochrome oxidase IV	Up 50%	Up 100%
Contractile proteins		
Slow troponin c	Up 60%	Up 70%
MHC II A	Up 40%	Up 40%
DAPC		
Utrophin A	NA	Up 100%

4.5 Chronic AICAR treatment increases utrophin A expression and promotes reassembly of the DAPC in the fast, glycolytic muscles of mdx mice, but not dKO mice

A central aspect of the slow, oxidative phenotype to this project is the increase in utrophin A protein expression that has been reported in the past (24,46,47,219). We saw this same upregulation of utrophin A in mdx mice (Table 4.2). dKO mice, on the other hand, did not express any utrophin A due to their utrophin A-null genotype. In non-dystrophic muscles, dystrophin is found along the entire sarcolemma, while utrophin A is localized to the neuromuscular junction (78). As important as the increased expression, our immunofluorescence results show that the AICAR treatment upregulated utrophin A throughout the sarcolemma, not only in the neuromuscular junction. This likely allows utrophin A to better serve as a replacement to dystrophin in functions such as recruiting the DAPC proteins to the sarcolemma and stabilizing it. The C-terminus of utrophin A can bind DAPC proteins such as α-dystrobrevin-1 and β-DG (79,80). Also, like dystrophin, utrophin A binds β-DG through its ZZ domain, though their modes of binding differ slightly (79).

To verify the ability of utrophin A to recruit the DAPC, we looked at the expression and localization of β-DG to the sarcolemma. β-DG expression in the EDL muscle of mdx mice was significantly increased. This is consistent with earlier studies, which show that AMPK activation has significant effects on the protein profile of cell membranes in skeletal muscle and other tissues (24,81-83). On the other hand, β-DG expression was not increased in AICAR-treated dKO mice. This suggests that the reassembly of the DAPC in the mdx mice was facilitated by the AICAR-mediated increase in utrophin A expression.

4.6 Chronic AICAR treatment improves skeletal muscle morphology and function in the utrophin A expressing mdx mice, but not the utrophin A negative dKO mice

Our central objective was determine whether or not the slower, more oxidative phenotype that we induced in the mice increased the resilience of their muscles to dystrophy and improved their function independently of utrophin A. We looked at various parameters for an indication of this. Muscle fiber central nucleation is a good indicator of muscle regeneration as a result of prior necrosis. The more centrally nucleated fibers in the muscle, the greater the amount of damage this muscle has seen and is regenerating from (84,85). Our results indicated that AICAR-treated mdx mice were experiencing reduced necrosis, as has been reported in previous studies (24,57,231) (Table 4.3). Another indicator of muscle damage is IgM staining. IgM is an immunoglobin that is normally found in the serum. When the sarcolemma is compromised, IgM can penetrate the muscle fibers and accumulate in them (50). The results of this experiment supported the results of the previous experiment, as well as the results of previous studies, indicating reduced muscle damage as a result of the AICAR treatment in mdx mice (24,57,231) (Table 4.3).

We also looked at muscle resistance to damage from eccentric contractions, which can cause sarcomere as well as sarcolemmal damage (86). As a result of this damage, the peak tetanic force generated by the muscles is reduced in successive eccentric contractions (87). After 12 eccentric contractions, our results indicated that the AICAR treatment did not improve the force maintenance in the mdx mice, which agrees with what has been shown previously by Ljubicic et al. (24).

However, the eccentric contraction experiment was accompanied by trypan blue staining. Trypan blue, a diazo dye, is used to selectively stain dead tissues or cells. Trypan blue is negatively charged, so it is unable to pass through cell membranes unless they are damaged. Cells that exclude the dye have undamaged membranes, while cells that display trypan blue fluorescence have damaged membranes and are likely non-viable (90). The trypan blue staining results showed that the AICAR treatment protected the mdx mice from muscle damage but could not do the same for the dKO mice (Table 4.3). Such a result has been shown before, though with a different dye, in mdx mice with AICAR treatment, but it is novel in dKO mice (24).

We performed one more test of muscle function, the forelimb grip strength test. This method can measure disease progression and test the benefits of therapeutic interventions. It has been shown previously that dystrophic mice had significantly reduced grip strength compared to wt mice, and reduced grip strength has been attributed to several factors including declining muscle mass and increased fibrosis, which are symptoms of DMD progression (91,92). Our results showed that the AICAR treatment significantly improved the grip strength of mdx mice, indicating slowed DMD progression and improved muscle function, as has been shown previously (93,94).

These results in the mdx mice indicate that the AICAR treatment, and the resulting induction of the slow, oxidative myogenic program caused an improvement in the resistance of skeletal muscles to DMD. As stated earlier, these results are in agreement with what has been shown in previous studies (24,57,238). On the other hand, we documented an important and stark difference in the ability of dKO mice to benefit from the slower, more oxidative phenotype. Unlike the mdx mice, we found that chronic treatment with AICAR elicits no structural or functional improvements in dKO mice (Table 4.3). Central nucleation was constant between AICAR treated and control dKO mice, indicating that necrosis and resulting regeneration was not reduced by the AICAR treatment.

Muscle fiber damage, as indicated by IgM penetration, was also unchanged by the AICAR treatment. Muscles from ACIAR treated dKO mice did not have greater resistance to damage from eccentric contractions, as indicated by trypan blue staining. Finally, the AICAR treatment did not increase the forelimb strength of the dKO mice. This inability of the dKO mouse muscles to benefit structurally or functionally from the slow, oxidative myogenic program points to a finding that is central to our study: utrophin A is important to the benefits conferred on dystrophic mice by the slow, oxidative myogenic program.

Table 4.3: The effects of AICAR treatment on indicators of the DMD pathology in the fast, glycolytic muscles of dKO and mdx mice.

Indicator of pathology	dKO-AICAR	mdx-AICAR
Morphological indicators		
Central nucleation	uchanged	Down 40%
IgM staining	unchanged	Down 30%
Functional indicators		
ECC induced damage	Unchanged	Down 30%
Grip strength	Unchanged	Up 16%
DAPC		
β-Dystroglycan	Unchanged	Up 50%

4.7 Utrophin A is directly linked to the benefits of the slow, oxidative phenotype in models of DMD

Several aspects of the slow, oxidative phenotype have been hypothesized to provide benefits to dystrophic muscles. These include improved mitochondrial function, reduced mitochondrially mediated apoptosis, reduced proapoptotic caspase activity and oxidative stress, and improved autophagy. Abnormalities in mitochondrial function have been found in DMD patients and carriers, and have been especially linked to DMD's early progression (226). A key aspect of the slow oxidative myogenic program, mitochondrial biogenesis, has been shown to improve some deficiencies found in dystrophic skeletal muscle that are linked to mitochondrial abnormalities, including exercise intolerance, fatigue, and exaggerated lactic acid production (101).

Another deficiency found in dystrophic skeletal muscle is its vulnerability to atrophy, which can be caused by mitochondrially mediated apoptosis (102). It occurs when mitochondrial proteins, such as cytochrome c and apoptosis inducing factor (AIF), are released into the cytosol, causing DNA fragmentation and cell death. The release of these proteins is facilitated by specialized pores, such as the mitochondrial permeability transition pore (mtPTP) (102). The slow, oxidative myogenic program has been shown to reduce mitochondrially mediated apoptosis by reducing mtPTP opening succeptibility, and reducing calcium overload induced swelling of the mitochondria, which is specifically linked to apoptosis and atrophy in dystrophic fibers (103). In addition, the slow, oxidative myogenic program has been shown to reduce the pro-apoptotic activity of the calcium dependent protease calpain, and the caspases, which are a group of cysteine proteases involved in apoptosis and necrosis (54). Furthermore, the improved mitochondrial

function elicited by the program is also associated with reduced damage to dystrophic fibers from reactive oxygen species (104).

Increased AMPK activation, which elicits the slow, oxidative myogenic program, has been associated with improved autophagy, which is thought to provide structural and functional benefits to dystrophic muscles (13). Despite these multiple beneficial adaptations provided by the slow, oxidative myogenic program to dystrophic fibers, our results show that the increased utrophin A expression is the vital ingredient to the palpable structural and functional improvements that are seen in mdx mice upon induction of the program.

While AICAR treatment successfully activated a slower, more oxidative phenotype in both strains of mice, only the mdx mice were able to benefit from this transformation. Since we showed that dKO mice have the same signaling capacity as mdx mice, which allows them to respond to AICAR treatment and express the slow, oxidative phenotype properly, the main skeletal muscle difference that remains between the two strains is the absence of utrophin A from the dKO mice.

Over the past years, there has been a hypothesis in our lab that utrophin A is vital to the benefits that the slow, oxidative myogenic program confers on mdx mice (24,43-50). This seemed logical, since utrophin A is an analog of dystrophin, binding the same proteins that comprise the DAPC, and has been shown to be highly expressed in slow, oxidative muscles, which are less damaged by DMD (41,42). In addition, transgenic overexpression of utrophin A has been shown to alleviate the symptoms of DMD, and it has been determined that upregulation of utrophin A by ~2 fold in dystrophic mice can significantly improve their resistance to the disease (87,88,95,96). Interestingly, this ~2 fold increase in utrophin A expression is what we saw in the TA muscles of our AICAR treated mdx mice, similar to what Ljubicic et al. showed (24). There is a body of evidence that shows that utrophin A upregulation allows mdx mice to be phenotypically

indistinguishable from wt mice in sedentary conditions, including in terms of myofiber size variability and rates of degeneration and regeneration (87,97,98). Utrophin A stabilizes the sarcolemma, and even improves higher models of DMD such as the GRMD dog (87,97,98). Considering this evidence, and the fact that the slow, oxidative myogenic program upregulates utrophin A expression to a physiologically relevant degree, it is clear that utrophin A is vital to the benefits conferred on dystrophic mice by the slow, oxidative myogenic program.

In a recent publication by Chan et al. (2014), it was shown that upregulation of the slow, oxidative myogenic program can improve muscle strength and function in both dKO and mdx mice, and it was therefore claimed that utrophin A is not necessary for these improvements. In that study, they rely on two main experiments to come to this conclusion. First, they show that PGC-1b does not upregulate utrophin A or other proteins of the neuromuscular junction, while it still induces a more oxidative phenotype in skeletal muscles. Through use of the muscle creatine kinase (MCK) promoter, PGC-1b is transgenically upregulated in the skeletal muscles mdx mice. These MCK-PGC-1β mice are shown to have improved muscle morphology and function, independently of utrophin A. Moreover, MCK-PGC-1a dKO mice, which cannot express utrophin A, also showed improved muscle morphology and function. Based on this, Chan et al. stipulate that utrophin A is not necessary for the benefits of the slow, oxidative myogenic program to dystrophic mice. However, in both of the above cases, the mice had overexpression of PGC-1a or PGC-1b as soon as their muscles started to develop, and so expressed a slow, oxidative muscle phenotype prior to birth. *In utero* overexpression of PGC likely reduces some of the prenatal abnormalities associated with DMD, which results in improved resistance to the postnatal dystrophic phenotype, but is unlikely to be replicated in a clinical setting (178,227).

For example, PGC-1a is known to protect muscles from Forkhead box protein O (FoxO) mediated atrophy, so having this advantage prior to the onset of dystrophy might reduce the loss of skeletal muscle mass after its onset (225). In addition, there are other benefits besides, utrophin A upregulation, that the slow, oxidative phenotype bestows on dystrophic mice, such as improved autophagy, reduced apoptotic susceptibility, and decreased metabolic abnormalities (13,100-102). When given a long time and allowed to function in the muscles as they develop, these adaptations may pose a viable defense against dystrophy, but this is unrealistic in a clinical setting, where patients are usually already dystrophic by the time they are diagnosed at approximately 5 years of age (241). If these adaptations are only beneficial in the longer term, then inducing them postnatally might not give them enough time to produce palpable benefits before the dystrophy produces irreversible damage.

In fact, this is supported by the last part of the study by Chan et al., in which PGC was upregulated in the mice postnatally using the inducible tet-response element promoter. Thus PGC-1a overexpression was only induced in the mice after removal of doxycycline from their chow at 3 weeks of age. In that part, only PGC-1a overexpression, which is associated with utrophin A upregulation, was shown to ameliorate the dystrophic phenotype and it was only shown doing so in mice that were capable of expressing utrophin A, the mdx mice. This part of the study follows the same timeline as our study, which is more realistic for clinical interventions in humans. Therefore, the multiple beneficial aspects of the slow, oxidative phenotype, other than utrohpin expression, can not be ruled out in providing benefits to dystrophic muscles, but utrophin A upregulation is vital to the realization of these benefits in a scenario that is more clinically relevant, when the mice are already dystrophic and require treatment.

5: CONCLUSION AND FUTURE DIRECTIONS

Our findings showed that dKO and mdx mouse skeletal muscles have similar signaling capacity and display a similar phenotype, in terms of oxidative capacity and contractile proteins, based on our measurements. When treated with AICAR, both mice displayed a significant increase in oxidative capacity with expression of proteins indicating a possible shift towards a slower phenotype. This shift in phenotype was associated with a significant increase in utrophin A expression in the mdx mice, while the dKO mice could not express utrophin A. When tested for functional and morphological signs of overcoming DMD, only the mdx mice, which had increased utrophin A expression, showed improvements. These results indicate that utrophin A is directly linked to the improvements incurred by the slow, oxidative myogenic program on dystrophic mice.

Our result confirm the hypothesis that was posed at the beginning of this study. This conclusion verifies that utrophin A is an important therapeutic target for DMD, and that the slow, oxidative myogenic program is a valid mechanism to upregulate utrophin A expression in models of DMD. However, the extent to which the slow, oxidative myogenic program and the resulting utrophin A upregulation benefits these models across their lifetime is still an area that needs investigation. A study where the slow, oxidative myogenic program is induced in mdx mice throughout their lives would provide interesting insights into how the benefits of the program change as the mice get older, and whether or not the program can prolong the lives of mdx mice to match the lifespan of wt mice. In addition, in a clinical setting, DMD patients might be identified very early or very late, depending on the use of technologies like genetic testing or the absence of proper healthcare infrastructure. Therefore, a study on the benefits of the slow, oxidative myogenic program to models of DMD if treatment is started at a very early age or at a late age would provide further insight into the improvements the program can offer in a clinical setting. In addition, it would be

worthwhile to assess markers of non-utrophin A-related, beneficial slow, oxidative phenotype adaptations, such as autophagy, in the AICAR-treated dKO and mdx mice. If these non-utrophin A-mediated changes occur equally in both dKO and mdx mice, then the case for utrophin As the vital component behind slow, oxidative phenotype's resistance to dystrophy would be made even stronger.

As mentioned earlier, there are many therapeutic options for DMD. A plethora of therapeutic targets have been identified and there many ways to influence them, pharmacologically or otherwise. Combining the utrophin A-mediated benefits of the slow, oxidative myogenic program with other beneficial adaptations can help further improve the resistance of DMD models to the disease. Several pathological conditions have been linked to increased necrosis and progression of muscular dystrophies including DMD. Inflammation is part of the immune response to DMD and has been shown to contribute to the progression of its pathology (105). Reduction of inflammation has been shown to improve the DMD pathology in human patients and animal models (106,107). Therefore, combining the slow, oxidative myogenic program with an anti-inflammatory drug like VBP15, may lead to further improvements of the DMD pathology (106). Related to inflammation is fibrosis, the penetration of skeletal muscles by fibrotic tissue, which directly contributes to progressive muscle dysfunction and the lethal phenotype of DMD (109). There are therapeutic options to reduce fibrosis in human patients and models of DMD, such as andrographolide, and combining treatments like this with the slow, oxidative myogenic program might lead to greater improvements in pathology (108). A combination of the known utrophin A-mediated beneficial effects of the slow, oxidative myogenic program and other therapeutic avenues may open the door to a potent combintatorial treatment that will not only improve models of DMD, but provide relief to human patients of the disease.

6: REFERENCES

1. Vrbova G.(1963) The effect of motoneurone activity on the speed of contraction of striated muscle. J. Physiol. (London) 169:513–526.
2. Williams R.S., Salmons S., Newsholme E.A., Kaufman R.E., Mellor J.(1986) Regulation of nuclear and mitochondrial gene expression by contractile activity in skeletal muscle. J. Biol. Chem. 261:376–380.
3. Pette D., Vrbova G.(1992) Adaptation of mammalian skeletal muscle fibers to chronic electrical stimulation. Rev. Physiol. Biochem. Pharmacol. 120:115–202.
4. Chin E.R., Olson, E.N., Richardson, J.A., Yang, Q., Humphries, C., Shelton, J.M., Wu, H., Zhu, W., Bassel-Duby, R., and Williams, R.S. 1998. A calcineurin-dependent transcriptional pathway controls skeletal muscle fiber type. Genes & Dev. 12: 2499-2509.
5. Ljubicic, V. Burt, M. Jasmin, B. 2014. The therapeutic potential of skeletal muscle plasticity in Duchenne muscular dystrophy: phenotypic modifiers as pharmacologic targets. FASEB Journal. 28 (2): 548-568.
6. Deconinck AE, Rafael JA, Skinner JA, et al. 1997. Utrophin A–dystrophin-deficient mice as a model for Duchenne muscular dystrophy. Cell 90: 717–727.
7. Li Wang, Yi Jia, Heather Rogers, Norio Suzuki, Max Gassmann, Qian Wang, Alexandra C. McPherron, Jeffery B. Kopp, Masayuki Yamamoto, Constance Tom Noguchi. 2013. Erythropoietin contributes to slow oxidative muscle fiber specification via PGC-1α and AMPK activation. The International Journal of Biochemistry & Cell Biology. 45(7): 1155-1164.
8. Vitzel KF, Bikopoulos G, Hung S, Pistor KE, Patterson JD, et al. (2013) Chronic Treatment with the AMP-Kinase Activator AICAR Increases Glycogen Storage and Fatty Acid Oxidation in Skeletal Muscles but Does Not Reduce Hyperglucagonemia and Hyperglycemia in Insulin Deficient Rats. PLoS ONE 8(4): e62190.doi: 10.1371/journal.pone.0062190
9. Thomson DM, Porter BB, Tall JH, Kim HJ, Barrow JR, Winder WW (January 2007). "Skeletal muscle and heart LKB1 deficiency causes decreased voluntary running and reduced muscle mitochondrial marker enzyme expression in mice". Am. J. Physiol. Endocrinol. Metab.292 (1): E196–202.

10. Winder W.W. Energy-sensing and signaling by AMP-activated protein kinase in skeletal muscle. J. Appl. Physiol. 2001;91:1017-1028.
11. Durante PE, Mustard KJ, Park SH, Winder WW, Hardie DG (July 2002). "Effects of endurance training on activity and expression of AMP-activated protein kinase isoforms in rat muscles". Am. J. Physiol. Endocrinol. Metab. 283 (1): E178–86.
12. Minokoshi, Y., et al. "Leptin Stimulates Fatty-Acid Oxidation by Activating AMP-Activated Protein Kinase." Nature 415.6869 (2002): 339-43. SCOPUS. Web. 7 May 2014.
13. Ljubicic V, Jasmin BJ. 2013. AMP-activated protein kinase at the nexus of therapeutic skeletal muscle plasticity in Duchenne muscular dystrophy. Trends in Molecular Medicine. 19(10): 614-624.
14. Lin J., Wu H., Tarr P.T., Zhang C.Y., Wu Z., Boss O., Michael L.F., Puigserver P., Isotani E., Olson E.N., et al. Transcriptional co-activator PGC-1 alpha drives the formation of slow-twitch muscle fibres. Nature 2002;418:797-801.
15. Lira V.A., Benton C.R., Yan Z., Bonen A. PGC-1alpha regulation by exercise training and its influences on muscle function and insulin sensitivity. Am. J. Physiol. Endocrinol. Metab. 2010;299:E145-E161.
16. Blair E. Warren , Phing-How Lou , Eliana Lucchinetti , Liyan Zhang , Alexander S. Clanachan , Andreas Affolter , Martin Hersberger , Michael Zaugg , Hélène Lemieux. 2014. Early mitochondrial dysfunction in glycolytic muscle, but not oxidative muscle, of the fructose-fed insulin-resistant rat. American Journal of Physiology - Endocrinology and Metabolism. 306: E658-E667.
17. Shin Terada , Izumi Tabata. 2004. Effects of acute bouts of running and swimming exercise on PGC-1α protein expression in rat epitrochlearis and soleus muscle. American Journal of Physiology - Endocrinology and Metabolism. 286: E208-E216.
18. Sibylle Jäger, Christoph Handschin, Julie St.-Pierre, and Bruce M. Spiegelman. 2007. AMP-activated protein kinase (AMPK) action in skeletal muscle via direct phosphorylation of PGC-1α. PNAS. 104 (29) 12017-12022.
19. Orsolya M. Palacios, Juan J. Carmona, Shaday Michan, Ke Yun Chen, Yasuko Manabe, Jack Lee Ward III, Laurie J. Goodyear, and Qiang Tong. 2009. Diet and exercise signals

regulate SIRT3 and activate AMPK and PGC-1α in skeletal muscle. Aging. 1(9): 771-783.

20. Patricia S. Pardo and Aladin M. Boriek. 2011. The physiological roles of Sirt1 in skeletal muscle. Aging. 3(4): 430-437.
21. Cantó C., Gerhart-Hines Z., Feige J.N., Lagouge M., Noriega L., Milne J.C., Elliott P.J., Puigserver P., Auwerx J. AMPK regulates energy expenditure by modulating NAD+ metabolism and SIRT1 activity. Nature 2009;458:1056-1060.
22. Cantó C., Jiang L.Q., Deshmukh A.S., Mataki C., Coste A., Lagouge M., Zierath J.R., Auwerx J. Interdependence of AMPK and SIRT1 for metabolic adaptation to fasting and exercise in skeletal muscle. Cell Metab. 2010;11:213-219.
23. Seth A., Steel J.H., Nichol D., Pocock V., Kumaran M.K., Fritah A., Mobberley M., Ryder T.A., Rowlerson A., Scott J., et al. The transcriptional corepressor RIP140 regulates oxidative metabolism in skeletal muscle. Cell Metab. 2007;6:236-245.
24. V. Ljubicic, P. Miura, M. Burt, L. Boudreault, S. Khogali, J.A. Lunde, J.M. Renaud, B.J. Jasmin. 2011. Chronic AMPK activation evokes the slow, oxidative myogenic program and triggers beneficial adaptations in mdx mouse skeletal muscle. Hum Mol Genet. 20: 3478–3493.
25. Fritah A, Steel JH, Parker N, Nikolopoulou E, Christian M, et al. (2012) Absence of RIP140 Reveals a Pathway Regulating glut4-Dependent Glucose Uptake in Oxidative Skeletal Muscle through UCP1-Mediated Activation of AMPK. PLoS ONE 7(2): e32520.
26. Daisuke Hoshino , Yuko Yoshida , Graham P. Holloway , James Lally , Hideo Hatta , Arend Bonen. 2012. Clenbuterol, a β2-adrenergic agonist, reciprocally alters PGC-1 alpha and RIP140 and reduces fatty acid and pyruvate oxidation in rat skeletal muscle. American Journal of Physiology - Regulatory, Integrative and Comparative Physiology. 302: R373-R384.
27. Saltin B., Gollnick P.D. (1983) Skeletal muscle adaptability: Significance for metabolism and performance. in Handbook of physiology: Skeletal muscle, ed Peachey L.D.D.(American Physiological Society, Bethesda, MD), pp 555–632.
28. Booth F.W., Baldwin K.M. (1996) Muscle plasticity: Energy demand and supply processes. in The handbook of physiology: Integration of motor, circulatory, respiratory

and metabolic control during exercise, eds Rowell L.B., Shepard J.T.(American Physiology Society, Bethesda, MD), pp 1075–1123.

29. Schiaffino S., Reggiani C.(1996) Molecular diversity of myofibrillar proteins: Gene regulation and functional significance. Physiol. Rev. 76:371–423.
30. Hoppeler, H. (1986). Exercise-induced ultrastructural changes in skeletal muscle. Int. J. Sports Med. 7,187 -204.
31. Brooke MH, Kaiser KK. Muscle fiber types: how many and what kind? Arch Neurol 23: 369–379, 1970.
32. Edstrom L, Kugelberg E. Histochemical composition, distribution of fibres and fatiguability of single motor units. Anterior tibial muscle of the rat. J Neurol Neurosurg Psychiatry 31: 424–433, 1968.
33. Guth L, Samaha FJ. Qualitative differences between actomyosin ATPase of slow and fast mammalian muscle. Exp Neurol 25: 138–152, 1969.
34. Schiaffino S, Hanzlikova V, Pierobon S. Relations between structure and function in rat skeletal muscle fibers. J Cell Biol 47: 107–119, 1970.
35. Reed, JC. 1997. Cytochrome c: can't live with it--can't live without it. Cell. 91(5): 559-62.
36. Tafani M, Karpinich NO, Hurster KA, Pastorino JG, Schneider T, Russo MA, Farber JL (March 2002). "Cytochrome c release upon Fas receptor activation depends on translocation of full-length bid and the induction of the mitochondrial permeability transition". J. Biol. Chem. 277 (12): 10073–82.
37. P. Kischel , B. Bastide , L. Stevens , Y. Mounier. 2001. Expression and functional behavior of troponin C in soleus muscle fibers of rat after hindlimb unloading. Journal of Applied Physiology. 90: 1095-1101.
38. M. Campione , S. Ausoni , C. Y. Guezennec , S. Schiaffino. 1993. Myosin and troponin changes in rat soleus muscle after hindlimb suspension. Journal of Applied Physiology. 74: 1156-1160.
39. Baker PE, Kearney JA, Gong B, Merriam AP, Kuhn DE, Porter JD, Rafael-Fortney JA. 2006. Analysis of gene expression differences between utrophin/dystrophin-deficient vs mdx skeletal muscles reveals a specific upregulation of slow muscle genes in limb muscles. Neurogenetics. 7(2): 81-91.

40. Deconinck N, Rafael JA, Beckers-Bleukx G, Kahn D, Deconinck AE, Davies KE, Gillis JM. 1998. Consequences of the combined deficiency in dystrophin and utrophin A on the mechanical properties and myosin composition of some limb and respiratory muscles of the mouse. Neuromuscul Disord. 8(6): 362-70.
41. Webster C., Silberstein L., Hays P., Blau M. (1988) Fast muscle fibers are preferentially affected in Duchenne muscular dystrophy. Cell 52, 503–513.
42. Moens P., Baatsen P. H., Maréchal G. (1993) Increased susceptibility of EDL muscles from mdx mice to damage induced by contractions with stretch. J. Muscle Res. Cell Motil. 14, 446–451.
43. Angus L. M., Chakkalakal J. V., Méjat A., Eibl J. K., Bélanger G., Megeney L. A., Chin E. R., Schaeffer L., Michel R. N., Jasmin B. J. (2005) Calcineurin-NFAT signaling, together with GABP and peroxisome PGC-1a, drives utrophin A gene expression at the neuromuscular junction. Am. J. Physiol. Cell Physiol. 289, C908–C917.
44. Chakkalakal J. V., Harrison M.-A., Carbonetto S., Chin E., Michel R. N., Jasmin B. J. (2004) Stimulation of calcineurin signaling attenuates the dystrophic pathology in mdx mice. Hum. Mol. Genet. 13, 379–388.
45. Chakkalakal J. V., Michel S. a, Chin E. R., Michel R. N., Jasmin B. J. (2006) Targeted inhibition of Ca2+/calmodulin signaling exacerbates the dystrophic phenotype in mdx mouse muscle. Hum. Mol. Genet. 15, 1423–1435.
46. Chakkalakal J. V., Stocksley M. A., Harrison M.-A., Angus L. M., Deschenes-Furry J., St-Pierre S., Megeney L. A., Chin E. R., Michel R. N., Jasmin B. J. (2003) Expression of utrophin A mRNA correlates with the oxidative capacity of skeletal muscle fiber types and is regulated by calcineurin/NFAT signaling. Proc. Natl. Acad. Sci. U. S. A. 100, 7791–7796.
47. Gramolini A. O., Bélanger G., Thompson J. M., Chakkalakal J. V., Jasmin B. J. (2001) Increased expression of utrophin A in a slow vs. a fast muscle involves posttranscriptional events. Am. J. Physiol. Cell Physiol. 281, C1300–C1309.
48. Ljubicic V., Jasmin B. J. (2013) AMP-activated protein kinase at the nexus of therapeutic skeletal muscle plasticity in Duchenne muscular dystrophy. Trends Mol. Med. 19, 614–624.

49. Ljubicic V., Khogali S., Renaud J.-M., Jasmin B. J. (2012) Chronic AMPK stimulation attenuates adaptive signaling in dystrophic skeletal muscle. Am. J. Physiol. Cell Physiol. 302, C110–C121.
50. Miura P., Chakkalakal J. V., Boudreault L., Bélanger G., Hébert R. L., Renaud J.-M., Jasmin B. J. (2009) Pharmacological activation of PPARbeta/delta stimulates utrophin A expression in skeletal muscle fibers and restores sarcolemmal integrity in mature mdx mice. Hum. Mol. Genet. 18, 4640–4649.
51. Baltgalvis K. A., Call J. A., Cochrane G. D., Laker R. C., Yan Z., Lowe D. A. (2012) Exercise training improves plantarflexor muscle function in mdx mice. Med. Sci. Sports Exerc. 44, 1671–1679.
52. Blanchet E., Annicotte J.-S., Pradelli L. A., Hugon G., Matecki S., Mornet D., Rivier F., Fajas L. (2012) E2F transcription factor-1 deficiency reduces pathophysiology in the mouse model of Duchenne muscular dystrophy through increased muscle oxidative metabolism. Hum. Mol. Genet. 21, 3910–3917.
53. Bueno Júnior C. R., Pantaleão L. C., Voltarelli V. A., Bozi L. H. M., Brum P. C., Zatz M. (2012) Combined effect of AMPK/PPAR agonists and exercise training in mdx mice functional performance. PloS ONE 7, e45699.
54. Godin R., Daussin F., Matecki S., Li T., Petrof B. J., Burelle Y. (2012) Peroxisome proliferator-activated receptor γ coactivator1-α gene transfer restores mitochondrial biomass and improves mitochondrial calcium handling in post-necrotic mdx mouse skeletal muscle. J. Phsyiol. 590, 5487–5502.
55. Gordon B. S., Delgado D. C., Kostek M. C. (2013) Resveratrol decreases in flammation and increases utrophin A gene expression in the mdx mouse model of Duchenne muscular dystrophy. Clin. Nutr. 32, 104–111.
56. Handschin C., Kobayashi Y. M., Chin S., Seale P., Campbell K. P., Spiegelman B. M. (2007) PGC-1alpha regulates the neuromuscular junction program and ameliorates Duchenne muscular dystrophy. Genes Dev. 21, 770–783.
57. Jahnke V. E., Meulen Van J. H. Der, Johnston H. K., Ghimbovschi S., Partridge T., Hoffman E. P., Nagaraju K. (2012) Metabolic remodeling agents show beneficial effects in the dystrophin-deficient mdx mouse model. Skelet. Muscle 2, 16.

58. Matsakas A., Yadav V., Lorca S., Narkar V. (2013) Muscle ERRγ mitigates Duchenne muscular dystrophy via metabolic and angiogenic reprogramming. FASEB J. 27, 4004–4016.
59. Selsby J. T., Morine K. J., Pendrak K., Barton E. R., Sweeney H. L. (2012) Rescue of dystrophic skeletal muscle by PGC-1α involves a fast to slow fiber type shift in the mdx mouse. PloS ONE 7, e30063.
60. Stupka N., Plant D. R., Schertzer J. D., Emerson T. M., Bassel-Duby R., Olson E. N., Lynch G. S. (2006) Activated calcineurin ameliorates contraction-induced injury to skeletal muscles of mdx dystrophic mice. J. Physiol. 575.2, 645–656.
61. Von Maltzahn J., Renaud J.-M., Parise G., Rudnicki M. A. (2012) Wnt7a treatment ameliorates muscular dystrophy. Proc. Natl. Acad. Sci. U. S. A. 109, 20614–20619.
62. V.A. Narkar et al. 2008. AMPK and PPARδ agonists are exercise mimetics. Cell. 134: 405–415.
63. Winder, W.W. , Holmes, B.F., Rubink, D.S., Jensen, E.B., Chen, M., Holloszy, J.O. 2000. Activation of AMP-activated protein kinase increases mitochondrial enzymes in skeletal muscle. Journal of Applied Physiology. 88(6): 2219-2226.
64. Suwa, M., Nakano, H., Kumagai, S. 2003. Effects of chronic AICAR treatment on fiber composition, enzyme activity, UCP3, and PGC-1 in rat muscles. Journal of Applied Physiology. 95(3): 960-968.
65. Fillmore, N., Jacobs, D.L., Mills, D.B., Winder, W.W., Hancock, C.R. 2010. Chronic AMP-activated protein kinase activation and a high-fat diet have an additive effect on mitochondria in rat skeletal muscle. Journal of Applied Physiology. 109(2): 511-520.
66. Yaarit Adamovich, Amir Shlomai, Peter Tsvetkova, Kfir B. Umansky, Nina Reuven, Jennifer L. Estall, Bruce M. Spiegelman and Yosef Shaul. 2013. The Protein Level of PGC-1α, a Key Metabolic Regulator, Is Controlled by NADH-NQO1. Mol. Cell. Biol. 33(13): 2603-2613.
67. Lin J , Handschin C , Spiegelman BM. 2005. Metabolic control through the PGC-1 family of transcription coactivators. Cell Metab. 1: 361–370.
68. David A. Hood, Isabella Irrcher, Vladimir Ljubicic and Anna-Maria Joseph. 2006. Coordination of metabolic plasticity in skeletal muscle. J Exp Biol. 209: 2265-2275.

69. Ljubicic V, Burt M, Lunde JA, Jasmin BJ. 2014. Resveratrol induces expression of the slow, oxidative phenotype in mdx mouse muscle together with enhanced activity of the SIRT1-PGC-1α axis. Am J Physiol Cell Physiol. 2014 Apr 23. [Epub ahead of print].
70. White R, Morganstein D, Christian M, Seth A, Herzog B, Parker MG. 2008. Role of RIP140 in metabolic tissues: connections to disease. FEBS Lett 582: 39–45.
71. Hallberg M, Morganstein DL, Kiskinis E, Shah K, Kralli A, Dilworth SM, White R, Parker MG, Christian M. 2008. A functional interaction between RIP140 and PGC-1alpha regulates the expression of the lipid droplet protein CIDEA. Mol Cell Biol 28: 6785–6795.
72. Williams D.B., Sutherland L.N., Bomhof M.R., Basaraba S.A., Thrush A.B., Dyck D.J., Field C.J., Wright D.C. Muscle-specific differences in the response of mitochondrial proteins to beta-GPA feeding: an evaluation of potential mechanisms. Am. J. Physiol. Endocrinol. Metab. 2009;296:E1400-E1408.
73. Holloszy, J. O. (1967). Biochemical adaptations in muscle. Effects of exercise on mitochondrial oxygen uptake and respiratory enzyme activity in skeletal muscle. J. Biol. Chem. 242,2278 -2282.
74. Biswas, G., Adebanjo, O. A., Freedman, B. D., Anandatheerthavarada, H. K., Vijayasarathy, C., Zaidi, M., Kotlikoff, M. and Avadhani, N. G. (1999). Retrograde Ca2+ signaling in C2C12 skeletal myocytes in response to mitochondrial genetic and metabolic stress: a novel mode of inter-organelle crosstalk. EMBO J. 18,522 -533.
75. Marusich, M. F., Robinson, B. H., Taanman, J. W., Kim, S. J., Schillace, R., Smith, J. L. and Capaldi, R. A. (1997). Expression of mtDNA and nDNA encoded respiratory chain proteins in chemically and genetically-derived Rho0 human fibroblasts: a comparison of subunit proteins in normal fibroblasts treated with ethidium bromide and fibroblasts from a patient with mtDNA depletion syndrome. Biochim. Biophys. Acta 1362,145 -159.
76. Song, W.-J., Van Keuren, M. L., Drabkin, H. A., Cypser, J. R., Gemmill, R. M., Kurnit, D. M. 1996. Assignment of the human slow twitch skeletal muscle/cardiac troponin C gene (TNNC1) to human chromosome 3p21.3-3p14.3 using somatic cell hybrids. Cytogenet. Cell Genet. 75: 36-37.

77. Carol A. Sartorius, Brian D. Lu, Leslie Acakpo-Satchivi, Renee P. Jacobsen, William C. Byrnes, and Leslie A. Leinwand. 1998. Myosin Heavy Chains IIa and IId Are Functionally Distinct in the Mouse. J Cell Biol. 141(4): 943–953.
78. Rebecca J. Fairclough, Akshay Bareja and Kay E. Davies. 2011. Progress in therapy for Duchenne muscular dystrophy. Exp Physiol. 96(11): 1101–1113.
79. Ishikawa-Sakurai M, Yoshida M, Imamura M, Davies KE & Ozawa E. 2004. ZZ domain is essentially required for the physiological binding of dystrophin and utrophin A to β-dystroglycan. Hum Mol Genet. 13: 693–702.
80. Peters MF, Sadoulet-Puccio HM, Grady RM, Kramarcy NR, Kunkel LM, Sanes JR, Sealock R & Froehner SC. 1998. Differential membrane localization and intermolecular associations of α-dystrobrevin isoforms in skeletal muscle. J Cell Biol. 142: 1269–1278.
81. Niu W., Bilan P.J., Ishikura S., Schertzer J.D., Contreras-Ferrat A., Fu Z., Liu J., Boguslavsky S., Foley K.P., Liu Z., et al. 2010. Contraction-related stimuli regulate GLUT4 traffic in C2C12-GLUT4myc skeletal muscle cells. Am. J. Physiol. Endocrinol. Metab. 298: E1058-E1071.
82. Pandke K.E., Mullen K.L., Snook L.A., Bonen A., Dyck D.J. 2008. Decreasing intramuscular phosphagen content simultaneously increases plasma membrane FAT/CD36 and GLUT4 transporter abundance. Am. J. Physiol. Regul. Integr. Comp. Physiol. 295: R806-R813.
83. Terunuma M., Vargas K.J., Wilkins M.E., Ramírez O.A., Jaureguiberry-Bravo M., Pangalos M.N., Smart T.G., Moss S.J., Couve A. 2010. Prolonged activation of NMDA receptors promotes dephosphorylation and alters postendocytic sorting of GABAB receptors. Proc. Natl Acad. Sci. USA. 107: 13918-13923.
84. George Karpati, Yannick Pouliot, Elizabeth, Zubrzycka-Gaarn,t Stirling Carpenter, Peter N. Ray, Ronald G. Worton,t and Paul Holland. 1989. Dystrophin is Expressed in mdx Skeletal Muscle Fibers After Normal Myoblast Implantation. American Journal of Pathology. 135(1): 27-32.
85. Ebihara S, Guibinga GH, Gilbert R, Nalbantoglu J, Massie B, Karpati G, Petrof BJ. 2000. Differential effects of dystrophin and utrophin A gene transfer in immunocompetent muscular dystrophy (mdx) mice. Physiol Genomics. 3(3): 133-44.

86. Proske, U. and Morgan, D. L. 2001. Muscle damage from eccentric exercise: mechanism, mechanical signs, adaptation and clinical applications. Journal of Physiology. 537(2): 333–345.
87. Tinsley J, Deconinck N, Fisher R, Kahn D, Phelps S, Gillis JM, Davies K. 1998. Expression of full-length utrophin A prevents muscular dystrophy in mdx mice. Nat Med. 4(12): 1441-4.
88. Squire S, Raymackers JM, Vandebrouck C, Potter A, Tinsley J, Fisher R, Gillis JM & Davies KE (2002). Prevention of pathology in mdx mice by expression of utrophin A: analysis using an inducible transgenic expression system. Hum Mol Genet 11, 3333–3344.
89. Liu M, Yue Y, Harper SQ, Grange RW, Chamberlain JS & Duan D (2005). Adeno-associated virus-mediated microdystrophin expression protects young mdx muscle from contraction-induced injury. Molecular Therapy: the Journal of the American Society of Gene Therapy 11, 245–256.
90. Tran S-L, Puhar A, Ngo-Camus M, Ramarao N. 2011. Trypan Blue Dye Enters Viable Cells Incubated with the Pore-Forming Toxin HlyII of Bacillus cereus. PLoS ONE. 6(9): e22876.
91. Connolly AM, Keeling RM, Mehta S, Pestronk A, Sanes JR. 2001. Three mouse models of muscular dystrophy: the natural history of strength and fatigue in dystrophin-, dystrophin/utrophin A-, and laminin alpha2-deficient mice. Neuromusc. Disorders 11: 703-712.
92. Douglas A. Kallman, Chris C. Plato, and Jordan D. Tobin. 1990. The Role of Muscle Loss in the Age-Related Decline of Grip Strength: Cross-sectional and Longitudinal Perspectives. Journal of Gerontology: MEDICAL SCIENCES. 45(3): M82-88.
93. Vanessa E Jahnke, Jack H Van Der Meulen, Helen K Johnston, Svetlana Ghimbovschi, Terrence Partridge, Eric P Hoffman and Kanneboyina Nagaraju. 2012. Metabolic remodeling agents show beneficial effects in the dystrophin-deficient mdx mouse model. Skeletal Muscle. 2: 16.
94. Bueno Júnior CR, Pantaleão LC, Voltarelli VA, Bozi LHM, Brum PC, et al. (2012) Combined Effect of AMPK/PPAR Agonists and Exercise Training in mdx Mice Functional Performance. PLoS ONE 7(9): e45699.

95. Krag T.O., Bogdanovich S., Jensen C.J., Fischer M.D., Hansen-Schwartz J., Javazon E.H., Flake A.W., Edvinsson L., Khurana T.S. 2004. Heregulin ameliorates the dystrophic phenotype in mdx mice. Proc. Natl Acad. Sci. 101: 13856-13860.
96. Rafael J.A., Tinsley J.M., Potter A.C., Deconinck A.E., Davies K.E. 1998. Skeletal muscle-specific expression of a utrophin A transgene rescues utrophin A-dystrophin deficient mice. Nat. Genet. 19: 79-82.
97. M. Cerletti et al. 2003. Dystrophic phenotype of canine X-linked muscular dystrophy is mitigated by adenovirus-mediated utrophin A gene transfer. Gene Ther. 10 : 750–757.
98. Miura and Jasmin. 2006. Utrophin A upregulation for treating Duchenne or Becker muscular dystrophy: how close are we? Trends in Molecular Medicine. 12(3): 122-129.
99. Chan MC, Rowe GC, Raghuram S, Patten IS, Farrell C, Arany Z. 2014. Post-natal induction of PGC-1α protects against severe muscle dystrophy independently of utrophin A. Skelet Muscle. 4(1): 2.
100. Hood D.A. Invited Review: contractile activity-induced mitochondrial biogenesis in skeletal muscle. J. Appl. Physiol. 2001;90:1137-1157.
101. Adhihetty P.J., O'Leary M.F., Hood D.A. 2008. Mitochondria in skeletal muscle: adaptable rheostats of apoptotic susceptibility. Exerc. Sport Sci. Rev. 36: 116-121.
102. Pagel-Langenickel I., Bao J., Pang L., Sack M.N. 2010. The role of mitochondria in the pathophysiology of skeletal muscle insulin resistance. Endocr. Rev. 31: 25-51.
103. Millay D.P., Sargent M.A., Osinska H., Baines C.P., Barton E.R., Vuagniaux G., Sweeney H.L., Robbins J., Molkentin J.D. 2008. Genetic and pharmacologic inhibition of mitochondrial-dependent necrosis attenuates muscular dystrophy. Nat. Med. 14: 442-447.
104. Menazza S., Blaauw B., Tiepolo T., Toniolo L., Braghetta P., Spolaore B., Reggiani C., Di Lisa F., Bonaldo P., Canton M. 2010. Oxidative stress by monoamine oxidases is causally involved in myofiber damage in muscular dystrophy. Hum. Mol. Genet. 19: 4207-4215.
105. Tidball JG1, Wehling-Henricks M. 2005. Damage and inflammation in muscular dystrophy: potential implications and relationships with autoimmune myositis. Curr Opin Rheumatol. 17(6): 707-13.
106. Christopher R. Heier, Jesse M. Damsker, Qing Yu, Blythe C. Dillingham, Tony Huynh, Jack H. Van der Meulen, Arpana Sali, Brittany K. Miller, Aditi Phadke, Luana Scheffer,

James Quinn, Kathleen Tatem, Sarah Jordan, Sherry Dadgar, Olga C. Rodriguez, Chris Albanese, Michael Calhoun, Heather Gordish-Dressman, Jyoti K. Jaiswal, Edward M. Connor, John M. McCall, Eric P. Hoffman, Erica K. M. Reeves andKanneboyina Nagaraju. 2013. VBP15, a novel anti-inflammatory and membrane-stabilizer, improves muscular dystrophy without side effects. EMBO Molecular Medicine. 5(10): 1569-1585.

107. Mariam Chahbouni, Germaine Escames, Carmen Venegas, Bele´n Sevilla, Jose´ Antonio Garcı´a, Luis C. Lo´pez, Antonio Mun˜oz-Hoyos, Antonio Molina-Carballo and Darı´o Acun˜a-Castroviejo. 2010. Melatonin treatment normalizes plasma pro-inflammatory cytokines and nitrosative/oxidative stress in patients suffering from Duchenne muscular dystrophy. J. Pineal Res. 48: 282–289

108. Daniel Cabrera, Jaime Gutiérrez, Claudio Cabello-Verrugio, Maria Gabriela Morales, Sergio Mezzano, Ricardo Fadic, Juan Carlos Casar, Juan L Hancke and Enrique Brandan. 2014. Andrographolide attenuates skeletal muscle dystrophy in mdx mice and increases efficiency of cell therapy by reducing fibrosis. Skeletal Muscle. 4: 6.

109. Morales MG, Gutierrez J, Cabello-Verrugio C, Cabrera D, Lipson KE, Goldschmeding R, Brandan E. 2013. Reducing CTGF/CCN2 slows mdx muscle dystrophy and improves cell-therapy. Hum Mol Genet. 22:4938-4951.

110. Feldman ME, Apsel B, Uotila A, Loewith R, Knight ZA, Ruggero D, Shokat KM. 2009. Active-site inhibitors of mTOR target rapamycin-resistant outputs of mTORC1 and mTORC2. PLoS Biol. 7:e38

111. Thoreen CC, Kang SA, Chang JW, Liu Q, Zhang J, Gao Y, Reichling LJ, Sim T, Sabatini DM, Gray NS. 2009. An ATP-competitive mammalian target of rapamycin inhibitor reveals rapamycin-resistant functions of mTORC1. J. Biol. Chem. 284:8023–8032.

112. Hackman P., J. Sarparanta, S. Lehtinen et al. 2013. Welander distal myopathy is caused by a mutation in the RNA-binding protein TIA1. Ann Neurol, 73: 500–509.

113. Huichalaf C1, Sakai K, Jin B, Jones K, Wang GL, Schoser B, Schneider-Gold C, Sarkar P, Pereira-Smith OM, Timchenko N, Timchenko L. 2010. Expansion of CUG RNA repeats causes stress and inhibition of translation in myotonic dystrophy 1 (DM1) cells. FASEB J. 24(10): 3706-19.

114. E Meryon. 1851. On fatty degeneration of the voluntary muscles: report of the Royal Medical and Chirurgical Society. Lancet. 2: 588–589.

115. E Meryon. 1852. On granular and fatty degeneration of the voluntary muscles. Medico-Chirurgical Trans. 35: 73–84.
116. Dubowitz, D. 1989. The Duchenne Dystrophy Story: From Phenotype to Gene and Potential Treatment. Journal of Child Neurology. 4: 240-250.
117. K Kobayashi, Y Nakahori, M Miyake, Matsumura, K., Kondo-Iid, E., Nomura, Y., Segawa, M., Yoshioka, M., Saito, K., Osawa, M., Hamano, K., Sakakihara, Y., Nonaka, I., Nakagome, Y., Kanazawa, I., Nakamura, Y., Tokunaga, K., Toda. 1998. An ancient retrotransposal insertion causes Fukuyama-type congenital muscular dystrophy. Nature. 394: 388-392.
118. D.J. Blake, A. Wier, S.E. Newey, K.E. Davies. 2002. Function and genetics of dystrophin and dystrophin-related proteins in muscle. Physiol Rev. 82: 291–329.
119. T.A. Rando. 2001. The dystrophin–glycoprotein complex, cellular signaling, and the regulation of cell survival in the muscular dystrophies. Muscle and Nerve. 24: 1575–1594.
120. Koenig M, Monaco AP & Kunkel LM. 1988. The complete sequence of dystrophin predicts a rod-shaped cytoskeletal protein. Cell. 53: 219–228.
121. Amann KJ, Guo AW & Ervasti JM. 1999. Utrophin A lacks the rod domain actin binding activity of dystrophin. J Biol Chem. 274: 35375–35380.
122. Williamson, R. A., Henry, M. D., Daniels, K. J., Hrstka, R. F., Lee, J. C., Sunada, Y., Ibraghimov-Beskrovnaya, O. and Campbell, K. P. 1997. Dystroglycan is essential for early embryonic development: disruption of Reichert's membrane in Dag1-null mice. Hum. Mol. Genet. 6: 831 -841.
123. Ehmsen J, Poon E, Davies K. 2002. The dystrophin-associated protein complex. J. Cell. Sci. 115(14): 2801–3.
124. Chan, Y. M., Bonnemann, C. G., Lidov, H. G. and Kunkel, L. M. 1998. Molecular organization of sarcoglycan complex in mouse myotubes in culture. J. Cell Biol. 143: 2033 -2044.
125. Bushby, K. M. 1999. Making sense of the limbgirdle muscular dystrophies. Brain 122: 1403 -1420.

126. Crosbie, R. H., Heighway, J., Venzke, D. P., Lee, J. C. and Campbell, K. P. 1997. Sarcospan, the 25-kDa transmembrane component of the dystrophin-glycoprotein complex. J. Biol. Chem. 272: 31221 -31224.
127. Lebakken, C. S., Venzke, D. P., Hrstka, R. F., Consolino, C. M., Faulkner, J. A., Williamson, R. A. and Campbell, K. P. 2000. Sarcospan-deficient mice maintain normal muscle function. Mol. Cell. Biol. 20: 1669 -1677.
128. Kameya, S., Miyagoe, Y., Nonaka, I., Ikemoto, T., Endo, M., Hanaoka, K., Nabeshima, Y. and Takeda, S. 1999. Alpha1-syntrophin gene disruption results in the absence of neuronal-type nitric-oxide synthase at the sarcolemma but does not induce muscle degeneration. J. Biol. Chem. 274: 2193 -2200.
129. Adams, M. E., Kramarcy, N., Krall, S. P., Rossi, S. G., Rotundo, R. L., Sealock, R. and Froehner, S. C. 2000. Absence of alpha-syntrophin leads to structurally aberrant neuromuscular synapses deficient in utrophin A. J. Cell Biol. 150: 1385 -1398.
130. Crawford, G. E., Faulkner, J. A., Crosbie, R. H., Campbell, K. P., Froehner, S. C. and Chamberlain, J. S. 2000. Assembly of the dystrophin-associated protein complex does not require the dystrophin COOH-terminal domain. J. Cell Biol. 150: 1399 -1410.
131. Thomas GD, Sander M, Lau KS, Huang PL, Stull JT & Victor RG. 1998. Impaired metabolic modulation of α-adrenergic vasoconstriction in dystrophin-deficient skeletal muscle. Proc Natl Acad Sci. 95: 15090–15095.
132. Lai Y, Thomas GD, Yue Y, Yang HT, Li D, Long C, Judge L, Bostick B, Chamberlain JS, Terjung RL & Duan D. 2009. Dystrophins carrying spectrin-like repeats 16 and 17 anchor nNOS to the sarcolemma and enhance exercise performance in a mouse model of muscular dystrophy. J Clin Invest. 119: 624–635.
133. Gail D. Thomas. 2013. Functional muscle ischemia in Duchenne and Becker muscular dystrophy. Front Physiol. 4: 381.
134. Rybakova IN, Patel JR & Ervasti JM (2000). The dystrophin complex forms a mechanically strong link between the sarcolemma and costameric actin. J Cell Biol 150, 1209–1214.
135. A.H. Ahn, L.M. Kunkel. 1993. The structural and functional diversity of dystrophin. Nat. Genet. 3: 283–291.

136. S.J. Winder. 1997. The membrane-cytoskeleton interface: the role of dystrophin and utrophin A. J. Muscle Res. Cell Motil. 18: 617–629.
137. M. Koenig, L.M. Kunkel. 1990. Detailed analysis of the repeat domain of dystrophin reveals four potential hinge segments that may confer flexibility. J. Biol. Chem. 265: 4560–4566.
138. Newey S., Howman, E.V., Ponting, C.P., Benson, M.A., Nawrotzki, R., Loh, N.Y., Davies, K.E., Blake, D.J. 2001. Syncoilin, a novel member of the intermediate filament superfamily That Interacts with α-dystrobrevin in skeletal muscle. J. Biol. Chem. 276: 6645–6655.
139. J. Chamberlain. 2006. The structure and function of dystrophin. Molecular Mechanisms of Muscular Dystrophies. Landes Bioscience. 14–34.
140. Gieseler K, Bessou C, Segalat L. 1999. Dystrobrevin- and dystrophin-like mutants display similar phenotypes in the nematode Caenorhabditis elegans. Neurogenetics. 2: 87–90.
141. Yang B, Jung D, Motto D, Meyer J, Koretzky G, Campbell KP. 1995. SH3 domain-mediated interaction of dystroglycan and Grb2. J Biol Chem. 270: 11711–11714.
142. Taverna D, Disatnik MH, Rayburn H, Bronson RT, Yang J, Rando TA, Hynes RO. 1998. Dystrophic muscle in mice chimeric for expression of α5 integrin. J Cell Biol. 143: 849–859.
143. Minetti C, Sotgia F, Bruno C, Scartezzini P, Broda P, Bado M, Masetti E, Mazzocco M, Egeo A, Donati MA, Volonte D, Galbiati F, Cordone G, Bricarelli FD, Lisanti MP, Zara F. 1998. Mutations in the caveolin-3 gene cause autosomal dominant limb-girdle muscular dystrophy. Nat Genet. 18: 365–368.
144. Petrof BJ, Shrager JB, Stedman HH, Kelly AM & Sweeney HL 1993. Dystrophin protects the sarcolemma from stresses developed during muscle contraction. Proc Natl Acad Sci. 90: 3710–3714.
145. J.M. Alderton, R.A. Steinhardt. 2000. calcium influx through calcium leak channels Is responsible for the elevated levels of calcium-dependent proteolysis in dystrophic myotubes. J. Biol. Chem. 275: 9452–9460.

146. Chen YW, Zhao P, Borup R & Hoffman EP. 2000. Expression profiling in the muscular dystrophies: identification of novel aspects of molecular pathophysiology. J Cell Biol. 151: 1321–133.
147. Morrison J, Lu QL, Pastoret C, Partridge T & Bou-Gharios G. 2000. T-cell-dependent fibrosis in the mdx dystrophic mouse. Lab Invest. 80: 881–891.
148. Bertorini TE, Bhattacharya SK, Palmieri GM, Chesney CM, Pifer D, Baker B. 1982. Muscle calcium and magnesium content in Duchenne muscular dystrophy. Neurology. 32: 1088-1092.
149. Chang WJ, Iannaccone ST, Lau KS, Masters BS, McCabe TJ, McMillan K, Padre RC, Spencer MJ, Tidball JG & Stull JT. 1996. Neuronal nitric oxide synthase and dystrophin-deficient muscular dystrophy. Proc Natl Acad Sci. 93: 9142–9147.
150. Sander M, Chavoshan B, Harris SA, Iannaccone ST, Stull JT, Thomas GD & Victor RG. 2000. Functional muscle ischemia in neuronal nitric oxide synthase-deficient skeletal muscle of children with Duchenne muscular dystrophy. Proc Natl Acad Sci. 97: 13818–13823.
151. Acharyya S, Butchbach MER, Sahenk Z, Wang HT, Saji M, Carathers M, Ringel MD, Skipworth RJE, Fearon KCH, Hollingsworth MA, Muscarella P, Burghes AHM, Rafael-Fortney JA & Guttridge DC. 2005. Dystrophin glycoprotein complex dysfunction: a regulatory link between muscular dystrophy and cancer cachexia. Cancer Cell. 8: 421–432.
152. Bulfield G; Siller WG; Wight PA; Moore KJ. 1984. X chromosome-linked muscular dystrophy (mdx) in the mouse. Proc Natl Acad Sci. 81(4): 1189-92.
153. Ryder-Cook AS; Sicinski P; Thomas K; Davies KE; Worton RG; Barnard EA; Darlison MG; Barnard PJ. 1988. Localization of the mdx mutation within the mouse dystrophin gene. EMBO J. 7(10): 3017-21.
154. Sicinski P; Geng Y; Ryder-Cook AS; Barnard EA; Darlison MG; Barnard PJ. 1989. The molecular basis of muscular dystrophy in the mdx mouse: a point mutation. Science. 244(4912): 1578-80.
155. Bushby, K. et al. 2010. Diagnosis and management of Duchenne muscular dystrophy, part 1: diagnosis, and pharmacological and psychosocial management. Lancet Neurol. 9: 77–93.

156. Bushby, K. et al. 2010. Diagnosis and management of Duchenne muscular dystrophy, part 2: implementation of multidisciplinary care. Lancet Neurol. 9: 177–189.
157. Pichavant, C. et al. 2011. Current status of pharmaceutical and genetic therapeutic approaches to treat DMD. Mol. Ther. 19: 830–840.
158. Webster, C. et al. 1988. Fast muscle fibers are preferentially affected in Duchenne muscular dystrophy. Cell. 52: 503–513.
159. Moens, P. et al. 1993. Increased susceptibility of EDL muscles from mdx mice to damage induced by contractions with stretch. J. Muscle Res. Cell Motil. 14: 446–451.
160. Aartsma-Rus A, Fokkema I, Verschuuren J, Ginjaar I, van Deutekom J, van Ommen GJ & den Dunnen JT. 2009. Theoretic applicability of antisense-mediated exon skipping for Duchenne muscular dystrophy mutations. Hum Mutat. 30: 293–299.
161. Alter J, Lou F, Rabinowitz A, Yin HF, Rosenfeld J, Wilton SD, Partridge TA & Lu QL. 2006. Systemic delivery of morpholino oligonucleotide restores dystrophin expression bodywide and improves dystrophic pathology. Nat Med. 12: 175–177.
162. Goyenvalle A, Babbs A, Powell D, Kole R, Fletcher S, Wilton SD & Davies KE. 2010. Prevention of dystrophic pathology in severely affected dystrophin/utrophin A-deficient mice by morpholino-oligomer-mediated exon-skipping. Mol Ther. 18: 198–205.
163. Manuvakhova M, Keeling K & Bedwell DM. 2000. Aminoglycoside antibiotics mediate context-dependent suppression of termination codons in a mammalian translation system. RNA: 6: 1044–1055.
164. Welch EM, Barton ER, Zhuo J, Tomizawa Y, Friesen WJ, Trifillis P, Paushkin S, Patel M, Trotta CR, Hwang SW, Wilde RG, Karp G, Takasugi J, Chen GM, Jones S, Ren H, Moon YC, Corson D, Turpoff AA, Campbell JA, Conn MM, Khan A, Almstead NG, Hedrick J, Mollin A, Risher N, Weetall M, Yeh S, Branstrom AA, Colacino JM, Babiak J, Ju WD, Hirawat S, Northcutt VJ, Miller LL, Spatrick P, He F, Kawana M, Feng H, Jacobson A, Peltz SW & Sweeney HL. 2007. PTC124 targets genetic disorders caused by nonsense mutations. Nature. 447: 87–91.
165. Partridge TA. 1991. Invited review: myoblast transfer: a possible therapy for inherited myopathies? Muscle Nerve. 14: 197–212.

166. El Fahime E, Mills P, Lafreniere JF, Torrente Y & Tremblay JP. 2002. The urokinase plasminogen activator: an interesting way to improve myoblast migration following their transplantation. Exp Cell Res. 280: 169–178.
167. Torrente Y, El Fahime E, Caron NJ, Bresolin N & Tremblay JP. 2000. Intramuscular migration of myoblasts transplanted after muscle pretreatment with metalloproteinases. Cell Transplant. 9: 539–549.
168. Goyenvalle A & Davies KE. 2011. Challenges to oligonucleotides-based therapeutics for Duchenne muscular dystrophy. Skelet Muscle. 1: 8.
169. Pichavant C, Chapdelaine P, Cerri DG, Dominique JC, Quenneville SP, Skuk D, Kornegay JN, Bizario JC, Xiao X & Tremblay JP. 2010. Expression of dog microdystrophin in mouse and dog muscles by gene therapy. Mol Ther. 18: 1002–1009.
170. Mendell JR, Campbell K, Rodino-Klapac L, Sahenk Z, Shilling C, Lewis S, Bowles D, Gray S, Li C, Galloway G, Malik V, Coley B, Clark KR, Li J, Xiao X, Samulski J, McPhee SW, Samulski RJ & Walker CM. 2010. Dystrophin immunity in Duchenne's muscular dystrophy. N Engl J Med. 363: 1429–1437.
171. Tinsley JM, Blake DJ, Roche A, Fairbrother U, Riss J, Byth BC, Knight AE, Kendrick Jones J, Suthers GK, Love DR, Edwards YH & Davies KE. 1992. Primary structure of dystrophin-related protein. Nature. 360: 591–593.
172. Perkins K.J., Davies K.E. 2002. The role of utrophin A in the potential therapy of Duchenne muscular dystrophy. Neuromuscul. Disord. 12: S78-S89.
173. Khurana T.S., Watkins S.C., Chafey P., Chelly J., Tomé F.M., Fardeau M., Kaplan J.C., Kunkel L.M. 1991. Immunolocalization and developmental expression of dystrophin related protein in skeletal muscle. Neuromuscul. Disord. 1: 185-194.
174. Ohlendieck K., Ervasti J.M., Matsumura K., Kahl S.D., Leveille C.J., Campbell K.P. 1991. Dystrophin-related protein is localized to neuromuscular junctions of adult skeletal muscle. Neuron. 7: 499-508.
175. J.R. Mendell et al. 2012. Gene therapy for muscular dystrophy: lessons learned and path forward. Neurosci. Lett. 527: 90–99.
176. Deconinck AE, Rafael JA, Skinner JA, Brown SC, Potter AC, Metzinger L, Watt DJ, Dickson JG, Tinsley JM, Davies KE. 1997. Utrophin A-dystrophin-deficient mice as a model for Duchenne muscular dystrophy. Cell. 90(4):717-27.

177. Grady RM, Teng H, Nichol MC, Cunningham JC, Wilkinson RS, Sanes JR. 1997. Skeletal and cardiac myopathies in mice lacking utrophin And dystrophin: a model for Duchenne muscular dystrophy. Cell. 90(4):729-38.
178. Schiaffino S., Sandri M., Murgia M.2007. Activity-dependent signaling pathways controlling muscle diversity and plasticity. Physiology (Bethesda). 22: 269-278.
179. Luquet S., Lopez-Soriano J., Holst D., Fredenrich A., Melki J., Rassoulzadegan M., Grimaldi P.A. 2003. Peroxisome proliferator-activated receptor delta controls muscle development and oxidative capability. FASEB J. 17: 2299-2301.
180. Wang Y.X., Zhang C.L., Yu R.T., Cho H.K., Nelson M.C., Bayuga-Ocampo C.R., Ham J., Kang H., Evans R.M. 2004. Regulation of muscle fiber type and running endurance by PPARdelta. PLoS Biol. 2: 1532-1539.
181. Puigserver P, Spiegelman BM. 2003. Peroxisome proliferator-activated receptor-gamma coactivator 1 alpha (PGC-1 alpha): transcriptional coactivator and metabolic regulator. Endocr Rev. 24: 78–90.
182. Zhang, L., Frederich, M., He, H., & Balschi, J. a. 2006. Relationship between 5-aminoimidazole-4-carboxamide-ribotide and AMP-activated protein kinase activity in the perfused mouse heart. American journal of physiology. Heart and circulatory physiology. 290(3): H1235-43.
183. Foster H, Popplewell L, Dickson G. 2012. Genetic therapeutic approaches for duchenne muscular dystrophy. *Hum Gene Ther*. 23(7): 676-687.
184. Goemans NM, Tulinius M, Buyse G, Wilson R, de Kimpe R, van Deutekom JCT & Campion G. 2010. 24 week follow-up data from a phase I/IIa extension study of PRO051/GSK2402968 in subjects with Duchenne muscular dystrophy. Neuromusc Disord. 20: 639.
185. Shrewsbury SB, Cirak S, Guglieri M, Bushby K & Muntoni F. 2010. Current progress and preliminary results with the systemic administration trial of AVI-4658, a novel phosphorodiamidate morpholino oligomer (PMO) skipping dystrophin exon 51 in Duchenne muscular dystrophy (DMD). In Neuromuscular Disorders. 20: 639–640.
186. Jearawiriyapaisarn N, Moulton HM, Buckley B, Roberts J, Sazani P, Fucharoen S, Iversen PL & Kole R. 2008. Sustained dystrophin expression induced by peptide-conjugated morpholino oligomers in the muscles of mdx mice. Mol Ther. 16: 1624–1629.

187. Yin H, Lu Q & Wood M. 2008. Effective exon skipping and restoration of dystrophin expression by peptide nucleic acid antisense oligonucleotides in mdx mice. Mol Ther. 16: 38–45.
188. Watt DJ, Lambert K, Morgan JE, Partridge TA & Sloper JC. 1982. Incorporation of donor muscle precursor cells into an area of muscle regeneration in the host mouse. J Neurol Sci 57: 319–331.
189. Partridge TA, Morgan JE, Coulton GR, Hoffman EP & Kunkel LM. 1989. Conversion of mdx myofibres from dystrophin-negative to -positive by injection of normal myoblasts. Nature. 337: 176–179.
190. Morgan JE & Partridge TA. 1992. Cell transplantation and gene therapy in muscular dystrophy. Bioessays. 14: 641–645.
191. Vilquin JT, Asselin I, Guerette B, Kinoshita I, Lille S, Roy R & Tremblay JP. 1994. Myoblast allotransplantation in mice: degree of success varies depending on the efficacy of various immunosuppressive treatments. Transplant Proc. 26: 3372–3373.
192. Gussoni E, Pavlath GK, Lanctot AM, Sharma KR, Miller RG, Steinman L & Blau HM. 1992. Normal dystrophin transcripts detected in Duchenne muscular dystrophy patients after myoblast transplantation. Nature. 356: 435–438.
193. Karpati G, Ajdukovic D, Arnold D, Gledhill RB, Guttmann R, Holland P, Koch PA, Shoubridge E, Spence D, Vanasse M, Watters GV, Abrahamowicz M, Duff C & Worton RG. 1993. Myoblast transfer in Duchenne muscular dystrophy. Ann Neurol. 34: 8–17.
194. Mendell JR, Kissel JT, Amato AA, King W, Signore L, Prior TW, Sahenk Z, Benson S, McAndrew PE, Rice R, Nagaraja H, Stephens R, Lantry L, Morris GE & Burghes AHM. 1995. Myoblast transfer in the treatment of Duchenne's muscular dystrophy. N Engl J Med. 333: 832–838.
195. Fan Y, Beilharz MW & Grounds MD. 1996. A potential alternative strategy for myoblast transfer therapy: the use of sliced muscle grafts. Cell Transplant. 5: 421–429.
196. Li S, Kimura E, Fall BM, Reyes M, Angello JC, Welikson R, Hauschka SD & Chamberlain JS. 2005. Stable transduction of myogenic cells with lentiviral vectors expressing a minidystrophin. Gene Ther. 12: 1099–1108.
197. Kazuki Y, Hiratsuka M, Takiguchi M, Osaki M, Kajitani N, Hoshiya H, Hiramatsu K, Yoshino T, Kazuki K, Ishihara C, Takehara S, Higaki K, Nakagawa M, Takahashi K,

Yamanaka S & Oshimura M. 2010. Complete genetic correction of iPS cells from Duchenne muscular dystrophy. Mol Ther. 18: 386–393.

198. Love DR, Hill DF, Dickson G, et al. 1989. An autosomal transcript in skeletal muscle with homology to dystrophin. Nature. 339(6219): 55-58.

199. Khurana TS, Hoffman EP, Kunkel LM. 1990. Identification of a chromosome 6-encoded dystrophin-related protein. J Biol Chem. 265(28): 16717-16720.

200. Jasmin BJ, Cartaud A, Ludosky MA, Changeux JP, Cartaud J. 1990. Asymmetric distribution of dystrophin in developing and adult torpedo marmorata electrocyte: Evidence for its association with the acetylcholine receptor-rich membrane. Proc Natl Acad Sci U S A. 87(10): 3938-3941.

201. Amann KJ, Renley BA & Ervasti JM. 1998. A cluster of basic repeats in the dystrophin rod domain binds F-actin through an electrostatic interaction. J Biol Chem. 273: 28419–28423.

202. Rybakova IN & Ervasti JM. 2005. Identification of spectrin-like repeats required for high affinity utrophin A-actin interaction. J Biol Chem. 280: 23018–23023.

203. Muthu M, Richardson KA, Sutherland-Smith AJ. 2012. The crystal structures of dystrophin and utrophin A spectrin repeats: Implications for domain boundaries. PLoS One. 7(7): e40066.

204. Burton EA, Tinsley JM, Holzfeind PJ, Rodrigues NR, Davies KE. 1999. A second promoter provides an alternative target for therapeutic up-regulation of utrophin A in duchenne muscular dystrophy. Proc Natl Acad Sci. 96(24):14025-14030.

205. Kleopa KA, Drousiotou A, Mavrikiou E, Ormiston A & Kyriakides T. 2006. Naturally occurring utrophin A correlates with disease severity in Duchenne muscular dystrophy. Hum Mol Genet. 15: 1623–1628.

206. Mizuno Y, Nonaka I, Hirai S, Ozawa E. 1993. Reciprocal expression of dystrophin and utrophin A in muscles of duchenne muscular dystrophy patients, female DMD-carriers and control subjects. J Neurol Sci. 119(1): 43-52.

207. De la Porte S, Morin S, Koenig J. 1999. Characteristics of skeletal muscle in mdx mutant mice. Int Rev Cytol. 191: 99-148.

208. Deol JR, Danialou G, Larochelle N, et al. 2007. Successful compensation for dystrophin deficiency by a helper-dependent adenovirus expressing full-length utrophin A. Mol Ther. 15(10): 1767-1774.
209. Odom GL, Gregorevic P, Allen JM, Finn E, Chamberlain JS. 2008. Microutrophin A delivery through rAAV6 increases lifespan and improves muscle function in dystrophic dystrophin/utrophin A-deficient mice. Mol Ther. 16(9): 1539-1545.
210. Lin AY, Prochniewicz E, Henderson DM, Li B, Ervasti JM, Thomas DD. 2012. Impacts of dystrophin and utrophin A domains on actin structural dynamics: Implications for therapeutic design. J Mol Biol. 420(1-2): 87-98.
211. Sonnemann KJ, Heun-Johnson H, Turner AJ, Baltgalvis KA, Lowe DA, Ervasti JM. 2009. Functional substitution by TAT-utrophin A in dystrophin-deficient mice. PLoS Med. 6(5): e1000083.
212. Call JA, Ervasti JM, Lowe DA. 2011. TAT-muUtrophin A mitigates the pathophysiology of dystrophin and utrophin A double-knockout mice. J Appl Physiol. 111(1): 200-205.
213. Amenta AR, Yilmaz A, Bogdanovich S, et al. 2011. Biglycan recruits utrophin A to the sarcolemma and counters dystrophic pathology in mdx mice. Proc Natl Acad Sci U S A. 108(2): 762-767.
214. Chaubourt E, Fossier P, Baux G, Leprince C, Israel M, De La Porte S. 1999. Nitric oxide and l-arginine cause an accumulation of utrophin At the sarcolemma: A possible compensation for dystrophin loss in duchenne muscular dystrophy. Neurobiol Dis. 6(6): 499-507.
215. Tinsley JM, Fairclough RJ, Storer R, et al. 2011. Daily treatment with SMTC1100, a novel small molecule utrophin A upregulator, dramatically reduces the dystrophic symptoms in the mdx mouse. PLoS One. 6(5): e19189.
216. Karpati G, Carpenter S, Morris GE, Davies KE, Guerin C, Holland P. 1993. Localization and quantitation of the chromosome 6-encoded dystrophin-related protein in normal and pathological human muscle. J Neuropathol Exp Neurol. 52(2): 119-128.
217. Voisin V, Sebrie C, Matecki S, et al. 2005. L-arginine improves dystrophic phenotype in mdx mice. Neurobiol Dis. 20(1): 123-130.

218. Archer JD, Vargas CC, Anderson JE. 2006. Persistent and improved functional gain in mdx dystrophic mice after treatment with L-arginine and deflazacort. FASEB J. 20(6): 738-740.
219. Chakkalakal JV, Miura P, Bélanger G, Michel RN, Jasmin BJ. 2008. Modulation of utrophin A mRNA stability in fast versus slow muscles via an AU-rich element and calcineurin signaling. Nucleic Acids Res. 36(3): 826-38.
220. Long YC, Zierath JR. 2008. Influence of AMP-activated protein kinase and calcineurin on metabolic networks in skeletal muscle. Am J Physiol Endocrinol Metab. 295: E545–52.
221. Stupka N, Gregorevic P, Plant DR, Lynch GS. 2004. The calcineurin signal transduction pathway is essential for successful muscle regeneration in mdx dystrophic mice. Acta Neuropathol. 107(4): 299-310.
222. Stupka N, Gregorevic P, Plant DR, Lynch GS. 2007. The calcineurin signal transduction pathway is essential for successful muscle regeneration in mdx dystrophic mice. Acta Neuropathol. 107(4): 299-310.
223. Muoio DM, MacLean PS, Lang DB, et al. 2002. Fatty acid homeostasis and induction of lipid regulatory genes in skeletal muscles of peroxisome proliferator-activated receptor (PPAR) 128 alpha knock-out mice. evidence for compensatory regulation by PPAR delta. J Biol Chem. 277(29): 26089-26097.
224. Ehrenborg E, Krook A. 2009. Regulation of skeletal muscle physiology and metabolism by peroxisome proliferator-activated receptor delta. Pharmacol Rev. 61(3): 373-393.
225. Schiaffino S., Mammucari C. 2011. Regulation of skeletal muscle growth by the IGF1-Akt/PKB pathway: insights from genetic models. Skeletal muscle. 1: 4.
226. Katsetos S., Koutzaki S., Melvin J. 2013. Mitochondrial dysfunction in neuromuscular disorders. Seminars in Pediatric Neurology. 20(3): 202-215.
227. Merrick D, Stadler LK, Larner D, Smith J. 2009. Muscular dystrophy begins early in embryonic development deriving from stem cell loss and disrupted skeletal muscle formation. Disease Models & Mechanisms. 4: 374–388.
228. Blanchet, E. et al. 2012. E2F transcription factor-1 deficiency reduces pathophysiology in the mouse model of Duchenne muscular dystrophy through increased muscle oxidative metabolism. Hum. Mol. Genet. 21: 3910–3917.

229. Aguilar V., Fajas L. 2010. Cycling through metabolism. EMBO Mol. Med. 2: 338-348.
230. Blanchet E., Annicotte J.S., Fajas L. 2009. Cell cycle regulators in the control of metabolism. Cell Cycle. 8: 4029-4031.
231. Bueno Júnior CR, Pantaleão LC, Voltarelli VA, Bozi LH, Brum PC, Zatz M. 2012. Combined effect of AMPK/PPAR agonists and exercise training in mdx mice functional performance. PLoS One. 7(9): e45699.
232. Lagouge M., Argmann C., Gerhart-Hines Z., Meziane H., Lerin C., Daussin F., Messadeq N., Milne J., Lambert P., Elliott P., et al. 2006. Resveratrol improves mitochondrial function and protects against metabolic disease by activating SIRT1 and PGC-1alpha. Cell. 127: 1109-1122.
233. Bergeron R., Ren J.M., Cadman K.S., Moore I.K., Perret P., Pypaert M., Young L.H., Semenkovich C.F., Shulman G.I. 2001. Chronic activation of AMP kinase results in NRF-1 activation and mitochondrial biogenesis. Am. J. Physiol. Endocrinol. Metab. 281: E1340-E1346.
234. Steinberg G.R., O'Neill H.M., Dzamko N.L., Galic S., Naim T., Koopman R., Jørgensen S.B., Honeyman J., Hewitt K., Chen Z.P., et al. 2010. Whole body deletion of AMP-activated protein kinase β2 reduces muscle AMPK activity and exercise capacity. J. Biol. Chem. 285: 37198-37209.
235. Zong H., Ren J.M., Young L.H., Pypaert M., Mu J., Birnbaum M.J., Shulman G.I. 2002. AMP kinase is required for mitochondrial biogenesis in skeletal muscle in response to chronic energy deprivation. Proc. Natl Acad. Sci. 99: 15983-15987.
236. Straub V., Rafael J.A., Chamberlain J.S., Campbell K.P. 1997. Animal models for muscular dystrophy show different patterns of sarcolemmal disruption. J. Cell Biol. 139: 375-385.
237. Quinn JL, Huynh T, Uaesoontrachoon K, Tatem K, Phadke A, Van der Meulen JH, Yu Q, Nagaraju K. Effects of Dantrolene Therapy on Disease Phenotype in Dystrophin Deficient mdx Mice. PLOS Currents Muscular Dystrophy. 2013 Nov 8. Edition 1. doi:10.1371/currents.md.e246cf493a7edb1669f42fb735936b46.
238. Pauly M, Daussin F, Burelle Y, Li T, Godin R, Fauconnier J, Koechlin-Ramonatxo C, Hugon G, Lacampagne A, Coisy-Quivy M, Liang F, Hussain S, Matecki S, Petrof BJ.

2012. AMPK activation stimulates autophagy and ameliorates muscular dystrophy in the mdx mouse diaphragm. Am J Pathol. 181(2): 583-92.

239. Jørgensen S.B., Treebak J.T., Viollet B., Schjerling P., Vaulont S., Wojtaszewski J.F., Richter E.A. 2007. Role of AMPKalpha2 in basal, training-, and AICAR-induced GLUT4, hexokinase II, and mitochondrial protein expression in mouse muscle. Am. J. Physiol. Endocrinol. Metab. 292: E331-E339.

240. Leick L., Fentz J., Biensø R.S., Knudsen J.G., Jeppesen J., Kiens B., Wojtaszewski J.F., Pilegaard H. 2010. PGC-1α is required for AICAR-induced expression of GLUT4 and mitochondrial proteins in mouse skeletal muscle. Am. J. Physiol. Endocrinol. Metab. 299: E456-E465.

241. Ciafaloni E, Fox DJ, Pandya S, Westfield CP, Puzhankara S, Romitti PA, Mathews KD, Miller TM, Matthews DJ, Miller LA, Cunniff C, Druschel CM, Moxley RT. 2009. Delayed diagnosis in Duchenne muscular dystrophy: data from the Muscular Dystrophy Surveillance Tracking and Research Network (MD STARnet) J Pediatr. 155: 380–385.

242. Fillmore N., Jacobs D.L., Mills D.B., Winder W.W., Hancock C.R. 2010. Chronic AMP-activated protein kinase activation and a high-fat diet have an additive effect on mitochondria in rat skeletal muscle. J. Appl. Physiol. 109: 511-520.

243. Buhl E.S., Jessen N., Pold R., Ledet T., Flyvbjerg A., Pedersen S.B., Pedersen O., Schmitz O., Lund S. 2002. Long-term AICAR administration reduces metabolic disturbances and lowers blood pressure in rats displaying features of the insulin resistance syndrome. Diabetes 51: 2199-2206.